MAGNETIC RESONANCE IMAGING IN RELAPSING-REMITTING MULTIPLE SCLEROSIS

DECLAN TARN CHARD

NMR Research Unit, Institute of Neurology, University College London,

Queen Square, London

Submitted to the University of London for the degree of

Doctor of Philosophy

ProQuest LLC
789 East Eisenhower Parkway
P.O. Box 1346
Ann Arbor, MI 48106-1346

ACKNOWLEDGEMENTS

The work presented in this thesis has relied upon many researchers; I have gained enormously from their wisdom, guidance and help, and am extremely grateful for this. In particular I thank David Miller, Alan Thompson and Gareth Barker whose encouragement, advice and support has been unfailing throughout. My fellow Fellows have been tolerant when I have been less than amiable company, and generous with their time and insight. I thank Colette Griffin, Gerard Davies, Waqar Rashid, Gordon Ingle, Peter Kapeller, Jaume Sastre-Garriga and Michela Tiberio in particular for their help with my work; and Simon Hickman, Peter Brex, Siobhan Leary and Nicholas Fox for constructive discussions. I am grateful to Geoffrey Parker and Mary McLean for sharing with me their invaluable technical expertise, and for patiently teaching me about the magnetic resonance imaging; and Martin King and Daniel Altmann for instructing me in the basics of statistical methodology. David MacManus and the radiographers have diligently acquired the data upon which this thesis is based, with a level of care that I hope has been matched by my use of it. I thank Katherine Mizskiel for kindly reviewing innumerable research scans; Raj Kapoor, who helped to initiate and sustain volunteer recruitment; the research volunteers who, despite considerable and regular inconvenience to themselves, have given up their time to help with this work; and the Multiple Sclerosis Society of Great Britain and Northern Ireland, and Schering AG, for funding me throughout my research. Finally, I thank my family and friends for their constancy.

ABSTRACT

The work presented in this thesis employed magnetic resonance imaging (MRI) techniques to determine the volume and metabolite profile of brain grey matter (GM) and white matter (WM) in people with clinically early relapsing-remitting multiple sclerosis (MS). Cross-sectional MRI and clinical data was obtained from 27 subjects with relapsing-remitting MS within 3 years of first symptom onset, and compared with MRI data from 29 normal control subjects. Subsets of these groups also provided longitudinal data over 18 months for volumetric analysis.

The principal observations were that: GM and WM atrophy may be observed early in the clinical course of the disease; WM atrophy was more apparent at baseline, but over the period of follow-up GM atrophy occurred more rapidly than that of WM; changes in metabolite concentrations were found in GM and WM suggesting neuronal and axonal damage, and WM glial activation and or proliferation; WM lesion loads explained a fraction of GM and WM atrophy and metabolite variability; clinical outcome related more closely to tissue metabolite changes (GM glutamate and glutamine, and normal-appearing WM inositol) than atrophy at this stage of the disease.

DECLARATION

For the studies described in sections 3 and 4 of this thesis, Colette Griffin and I recruited subjects; the T_1, T_2 and gadolinium-enhancing lesion loads were determined by Waqar Rashid, while I processed the other magnetic resonance data and performed the statistical analyses.

PUBLICATIONS ARISING FROM THIS THESIS

The following publications have arisen out of the work contained in this thesis, although for the purposes of the present work, much of the data has been re-analysed to allow more consistent presentation throughout.

DT Chard, MA McLean, GJM Parker, DG MacManus, DH Miller. Reproducibility of in vivo metabolite quantification with proton magnetic resonance spectroscopic imaging. J Magn Reson Imaging 2002;15:219-225.

DT Chard, CM Griffin, GJM Parker, R Kapoor, AJ Thompson, DH Miller. Brain atrophy in clinically early relapsing-remitting multiple sclerosis. Brain 2002;125:327-337.

DT Chard, GJM Parker, CM Griffin, AJ Thompson, DH Miller. The reproducibility and sensitivity of brain tissue volume measurements derived from an SPM-based segmentation methodology. J Magn Reson Imaging 2002;15:259-267.

DT Chard, CM Griffin, MA McLean, P Kapeller, R Kapoor, AJ Thompson, DH Miller. Brain metabolite changes in cortical grey and normal-appearing white matter in clinically early relapsing-remitting multiple sclerosis. Brain 2002; 125:2342-2352.

DT Chard, CM Griffin, W Rashid, GR Davies, DR Altmann, R Kapoor, GJ Barker, AJ Thompson, DH Miller. Progressive grey matter atrophy in clinically early relapsing-remitting multiple sclerosis. Mult Scler 2004; 10: 387-391.

ABBREVIATIONS

BBB = blood brain barrier

BP = brain parenchyma

BPF = brain parenchymal fraction

CDMS = clinically definite multiple sclerosis

CGM = cortical grey matter

CHESS = chemical shift selective saturation

Cho = choline containing compounds

CIS = clinically isolated syndrome

CNS = central nervous system

CPMS = clinically probable multiple sclerosis

Cr = creatine plus phosphocreatine

CSE = conventional spin echo

CV = coefficient of variation

EAE = experimental allergic encephalomyelitis

EDSS = expanded disability status scale

FID = free induction decay

FLAIR = fast fluid-attenuated inversion-recovery

FS = functional system

FSE = fast spin echo

FSPGR = fast spoiled gradient recalled

Gd = gadolinium

Glu = glutamate

Gln = glutamine

Glx = glutamate plus glutamine

GM = grey matter

GMF = grey matter fraction

GNDS = Guy's neurologic disability scale

^{1}H-MRS = proton magnetic resonance spectroscopy

^{1}H-MRSI = proton magnetic resonance spectroscopic imaging

HPT = nine hole peg test

ICC = intra-class correlation coefficient

IL = interleukin

InHC = inhomogeneity corrected

Ins = myo-inositol

IV = intravenous

LCModel = linear combination model (a software package)

LF = lesion fraction

LSDMS = laboratory supported definite multiple sclerosis

LSPMS = laboratory supported probable multiple sclerosis

MBP = myelin basic protein

MHC = major histocompatibility complex

MOG = myelin oligodendrocyte glycoprotein

MR = magnetic resonance

MRI = magnetic resonance imaging

MS = multiple sclerosis

MSFC = MS functional composite

MSIS-29 = MS impact scale (29 questions)

MSSS = multiple sclerosis severity score

MT = magnetisation transfer

NAA = *N*-acetyl-aspartate

NAAG = *N*-acetyl-aspartyl-glutamate

NAWM = normal-appearing white matter

NC = normal control

ND = not determined

NEX = number of excitations

NO = nitric oxide

OPC = oligodendrocyte precursor cell

PASAT = paced auditory serial addition test

PP = primary progressive

PPMS = primary progressive multiple sclerosis

ppm = parts per million

PRESS = point resolved spectroscopy

RC = reliability coefficient

RF = radio-frequency

RR = relapsing-remitting

RRMS = relapsing-remitting multiple sclerosis

SD = standard deviation

SE = standard error or spin echo

SP = secondary progressive

SPMS = secondary progressive multiple sclerosis

SPM99 = statistical parametric mapping version 99 (a software package)

STEAM = stimulated echo acquisition mode

TE = echo time

TI = total intra-cranial

TR = repetition time

tNAA = *N*-acetyl-aspartate plus N-acetyl-aspartyl-glutamate

TNF = tumour necrosis factor

TWT = Twenty-five foot timed walk test

VC = validity coefficient

VEP = visual evoked potential

WM = white matter

WMF = white matter fraction

2D = two-dimensional

3D = three-dimensional

TABLE OF CONTENTS

1 INTRODUCTION AND AIMS

Since its first recognition (Charcot, 1877), multiple sclerosis (MS) has predominantly been characterised as a multifocal inflammatory demyelinating disorder of central nervous system (CNS) white matter (WM). However, more recent histopathological work has begun to question this concept of MS, demonstrating that disease effects are not necessarily focal, nor restricted to the WM. Further, with the advent of magnetic resonance (MR) imaging (MRI), it has been possible to explore the *in vivo* relationship between evolving pathology and clinical outcomes; early work concentrated on the WM lesions, characterising the dynamics of their genesis and subsequent growth or resolution, and rather contrary to intuition, it has been shown that focal lesions do not readily account for a significant proportion of the clinical disease burden (McFarland *et al.*,2002). Building upon these observations, and concurrent with the development and refinement of MR techniques, attention has turned to consider both non-lesional tissues and pathological processes other than inflammation or demyelination. One aspect of this has been an exploration of neuronal and axonal damage that, while long recognised (Kornek and Lassmann, 1999), has only recently been the focus of concerted study.

The work contained in this thesis concentrates on two MR methodologies, tissue specific volume measures that enable an assessment of differential disease effects upon both WM and grey matter (GM), and proton magnetic resonance spectroscopy (^{1}H-MRS) that offers information on tissue metabolite concentrations, and to a degree insight in to cell specific disease effects.

There has been relatively limited work studying the earliest clinical stages of MS, although such studies have indicated that early changes in lesion loads may partially determine longer-term clinical outcomes (Brex *et al.*,2002) and that axonal damage in lesions may be more marked early in the course of the disease (Kuhlmann *et al.*,2002). Further, it has also been shown that clinical outcomes at two years after clinical onset can be used to define the longer term disease severity (Roxburgh *et al.*,2005). Given the potential impact early disease activity may have on the trajectory of subsequent disease progression, there is a clear need to obtain more information on the evolution of, and interplay between, pathological processes soon after disease onset. With this in mind, the work contained in this thesis focuses on observations made in subjects with MS within three years of first symptom onset, who were not or had not been treated with disease modifying agents.

This thesis begins by considering aspects of MS pathology and its clinical features, along with methods for assessing clinical outcomes; this is followed by an overview of MRI, and more specifically the role volumetric and spectroscopic measures have investigating aspects of *in vivo* pathology. It then moves on to the reliability of the MRI techniques used in work included in this thesis, before proceeding to explore clinically early MS disease effects.

2 BACKGROUND

2.1 MULTIPLE SCLEROSIS

2.1.1 CLINICAL PRESENTATION AND RECOGNISED PHENOTYPES

Charcot (Charcot, 1877) first clearly defined a clinical syndrome associated with *sclerose en plaques* and, it was apparent that just as the lesions could manifest themselves throughout the central nervous system (CNS), symptoms could similarly affect a wide range of neurological functions. While some symptoms are more common with MS than other disorders, for example optic neuritis, spinal cord and brainstem syndromes, none can be considered diagnostic on its own. Indeed this may simply reflect the clinical eloquence of lesions within the optic nerve, spinal cord, brainstem and cerebellum rather than a genuine predilection for these sites. While the most readily recognized features of the disease are those associated with sensory or motor neurological deficits, cognitive (Rao *et al.*,1991a; Rao *et al.*,1991b) impairment and psychiatric morbidity (Ron and Logsdail, 1989; Zorzon *et al.*,2001) contributes significantly to disability.

The clinical course of MS is equally variable ranging between forms that are progressive from clinical onset, occasionally leading to death within a few years, to a relatively benign form with little or no fixed disability several decades after the first clinical events. This clinical heterogeneity leads to difficulties with diagnosis and assigning prognoses. Defining the clinical course of MS has tended to be quite subjective, with a wide range of over-lapping terms applied. This heterogeneity was addressed by Lublin & Reingold (1996) (Table 2.1.1) when they undertook a survey of clinicians to reach consensus definitions of disease patterns. This was reached for

relapsing-remitting (RR), primary-progressive (PP), secondary-progressive (SP), progressive-relapsing (PR) patterns but not for relapsing-progressive (RP) MS. The latter was considered to overlap with the definitions of RRMS and SPMS, and could not be distinctly separated from them. They did not define what constitutes an attack, stating that this needs to be considered for individual studies, although both Poser *et al.* (1983) and McDonald *et al.* (2001) did.

Table 2.1.1a: Lublin & Reingold (1996) definitions of clinical course.

2.1.2 DIAGNOSTIC CRITERIA

Diagnostic criteria have been, and still are, based upon demonstrating lesion genesis disseminated in both time and place, although for those who present with symptom progression from onset without evidence of preceding episodic neurological deficits it has proven difficult to establish a diagnosis on clinical grounds alone. With the inclusion of information derived from MRI studies, cerebrospinal fluid (CSF) examination for oligoclonal bands, and visual evoked potentials (VEP), this has become more reliable. The diagnostic criteria have remained under review and have recently been updated (McDonald *et al.*,2001; Polman *et al.*,2005) to take greater account of MRI data.

In this work, the Poser *et al.* (1983) diagnostic criteria were employed (Table 2.1.1b). They define a relapse (also described as an attack, bout, episode, or exacerbation) based on symptoms lasting more than 24 hours with or without objective confirmation typical of the diagnosis, separated by a period of one month or more from a previous clinical event. Reliable historical information consistent with the diagnosis, for which no better explanation can be identified, is acceptable as evidence of a relapse. Remission is defined as a definite improvement in signs or symptoms for more than 24 hours. Clinical evidence of a lesion requires examination by a competent clinician; however, signs need not be persistent. Signs of simultaneously occurring separate lesions are acceptable, although optic neuritis spreading to involve the other eye within 15 days is not. The presence of oligoclonal bands on examination of the cerebrospinal fluid (CSF) adds laboratory support to the diagnosis. Visual evoked potentials and MRI findings are considered paraclinical

evidence. The Poser *et al.* criteria do not address those subjects with PPMS, although Thompson *et al.* (2000) have subsequently defined diagnostic criteria for this form of the disease and these have been incorporated in to the more recent McDonald *et al.* (2001) diagnostic criteria.

Table 2.1.1b: Poser *et al.* (1983) diagnostic criteria.

2.1.3 EPIDEMIOLOGY

Incidence and prevalence

A relatively recent survey of neurological disease centred on London estimated an incidence of 7 (95% confidence interval 4-11) cases per 100,000 of the population per year, with a lifetime prevalence of 2 (95% confidence interval of 2-3) cases per 1000 of the population (MacDonald *et al.*,2000). However, there is wide geographical variability in the prevalence of MS, both between and within continental regions, and latitudinal gradients have been identified (Compston, 1999), suggesting both environmental and genetic factors contribute towards susceptibility to MS. Gender differences, with a female to male ratio of about 2:1 (Confavreux *et al.*,2000; Prat and Antel, 2005), have also been observed.

Epidemics and infections

Whilst regional incidence and prevalence studies support the presence of environmental factors, some have argued that apparent epidemics of MS indicate an infective environmental agent (Kurtzke, 1993) and others have suggested that the change in prevalence represents an epidemic of recognition (Benedikz *et al.*,1994). To date a single potential infective trigger agent has not been clearly implicated, although it is recognized that viral infections (particularly *Herpesviridae* such as Epstein-Barr and more recently Human herpes virus 6) may predispose to the subsequent development of MS (Cermelli and Jacobson, 2000). It may transpire that an exogenous trigger actually consists of a suite of infective, or other, agents acting in concert.

Genetics

Pedigree studies have indicated that there is a genetic component to the disease although its influence is far from absolute. The age-adjusted risk for siblings of an affected individual is circa 3%, and circa 2% for both parents and children. In the United Kingdom and Canada, both countries where the prevalence of MS is high, monozygotic twins showed a much higher concordance rate when compared with dizygotic twins (circa 25% and 3% respectively) (Compston, 1999). Having established this, it has proven more difficult to identify particular genes, and this in part may reflect both disease heterogeneity and multifactorial genetic contributions. Association between a number of class II major histocompatibility complex alleles (DR15, DQ6 and to a lesser degree DR4) and MS have been identified but none are considered particularly strong.

Clinical phenotype distribution

The commonest initial presentation of MS is the RR form, recently estimated at 85% of cases (Confavreux *et al.*,2000). After a mean of 11 years of the 85% classified as having RRMS, 68% remain so classified, with 32% developing SPMS. During the relapsing remitting phase, relapses occur approximately once per year in untreated cases (Compston and Coles, 2002).

As noted above, some people with MS do not appear to have relapses at any stage but have syndromes that upon investigation are compatible with the diagnosis. It remains unclear whether PPMS is fundamentally different from SPMS, and there is some debate in the area (Thompson *et al.*,1997).

The relationship between relapses and progression is not as clear as may be expected. Confavreux *et al.* (2003; 2000) have found limited evidence to support a direct relationship, suggesting that relapses and long-term disease progression may be to a degree dissociated. In contrast, Brex *et al.* (2002) found a modest association between early lesion accumulation and clinical outcome 14 years after disease onset was observed.

2.1.4 *PATHOLOGY AND IMMUNOLOGY*

The presence of discoloured and atrophied lesions in the brain and spinal cord WM was noted in advance of the clinical phenotype being established (Carswell, 1838; Cruvellhier, 1842). It was Charcot who later described them as *sclerose en plaques* and clearly connected them with the clinical manifestations we now recognize (Charcot, 1877).

Microscopic examinations of these lesions revealed marked inflammation and demyelination, with *relative* sparing of axons associated with inflammation (Charcot, 1877). Demyelination was considered to be the pre-eminent cause of disability with subsequently limited consideration given to axonal and neuronal structures. With the recent development and application of further histopathological tools, a greater understanding of the extent and degree of neuronal and, in particular, axonal involvement has emerged along with insight into the pathological mechanisms leading to damage. Histopathological changes within normal-appearing WM (NAWM) (Allen and McKeown, 1979; Guseo and Jellinger, 1975) and in cortical GM (CGM)(Bo *et al.*,2000; Brownell and Hughes, 1962; Kidd *et al.*,1999; Peterson *et al.*,2001) matter have been observed, indicating that MS is neither as focal as initially thought nor is it restricted to the WM.

Focal white matter lesions

It remains unclear why changes in MS are quite so spatially heterogeneous. While there are widespread changes (discussed below), focal WM lesions are much more readily apparent, and it has yet to be shown what triggers their formation.

Is has been proposed that MS lesions can be divided in to four types dependent upon the pattern of inflammation, demyelination and remyelination, and oligodendrocyte characteristics, and that at a given time this is homogeneous within a given subject (Lucchinetti *et al.*,2000). Of these, patterns I and II are thought to relate to a T-cell or T-cell plus antibody response whilst patterns III and IV, have been described as reminiscent of virus or toxin induced damage with oligodendrocyte dystrophy. Interestingly, pattern III lesions have been predominantly found in subjects with a clinical course of less than 8 weeks, and pattern IV lesions have so far have been seen exclusively in PPMS. From this study, it was unclear if these patterns III and IV were maintained long-term, however the apparent change in frequency of lesion types in those with clinical manifestations of greater than 1 year to one dominated by pattern II lesions suggests that pattern III represents the initial response to either a viral or toxic trigger. Previous work has also noted marked heterogeneity in MS lesion characteristics related to the duration of clinical disease and lesion maturation (Gay *et al.*,1997). Lesions early in the clinical evolution of MS appear to show demyelination effected by resident microglia in association with a marked plasma cell and less marked T-cell response. Such early lesions do not exhibit clear evidence for a breakdown in the blood brain barrier (BBB), perhaps suggesting that microglial activation precedes this. It has also been suggested that demyelination may be preceded by apoptosis of oligodendrocytes, again in association with microglial activation (Barnett and Prineas, 2004). As lesions mature and the clinical course extends, a T-cell response becomes more evident (Gay *et al.*,1997). Taken together, these studies would appear to suggest that pathology at the earliest stages of

MS is not necessarily primarily inflammatory, but that it may evolve into a self-perpetuating T-cell mediated process. In this context it is interesting to note that axonal damage in WM lesions may be more marked early rather than later in the course of the disease (Kuhlmann *et al.*,2002).

Normal-appearing white matter

Macroscopically NAWM is not necessarily microscopically so. Studies have shown that demyelination (Guseo and Jellinger, 1975), astrogliosis (Allen and McKeown, 1979) and axonal loss (Evangelou *et al.*,2000) occurs in such tissues. Further, macroscopically normal-appearing tissues may not be so on MRI, and as such may still contain focal lesions (De Groot *et al.*,2001). The detection of lesions on MRI also depends upon the imaging methodology employed and thus normal-appearing on one MR sequence may not be so on another (see section 3.1.3). Given that even on MRI, despite a long disease duration, most brain tissue would be classified as normal-appearing (Kalkers *et al.*,2001), it is clear that to ignore subtle disease effects in such tissues may significantly underestimate the overall magnitude of disease effects.

MRI observations in the NAWM of subjects with established MS have noted abnormalities in magnetisation transfer (MT) (for example (Cercignani *et al.*,2001; Dehmeshki *et al.*,2003; Ge *et al.*,2002; Griffin *et al.*,2002a; Griffin *et al.*,2000; Leary *et al.*,1999b; Siger-Zajdel and Selmaj, 2001), diffusion (for example (Bammer *et al.*,2000; Cercignani *et al.*,2000; Ciccarelli *et al.*,2001; Filippi *et al.*,2000; Guo *et al.*,2002; Rovaris *et al.*,2002; Werring *et al.*,2001), T_1 and T_2 relaxation characteristics (Goodkin *et al.*,1998; Griffin *et al.*,2002b; Parry *et al.*,2002; Whittall

et al.,2002), and metabolite alterations (discussed in greater detail below), which appear consistent histopathological findings. Perhaps more importantly these changes might begin early in the clinical course of the disease; MT, volumetric and spectroscopic abnormalities have all been observed in subjects with CIS and clinically early MS (Brex *et al.*,2000a; Brex *et al.*,2001; Dalton *et al.*,2002; Dalton *et al.*,2004; Fernando *et al.*,2004; Fernando *et al.*,2005).

Grey matter

GM is not free from focal lesions (Bo *et al.*,2000; Brownell and Hughes, 1962; Kidd *et al.*,1999; Peterson *et al.*,2001), but they are more difficult to recognize, particularly with conventional MRI (Geurts *et al.*,2005). Indeed they may be found in the majority of MS subjects; Lumsden reports that 93% of 60 subjects studied had evidence of cortical involvement (Lumsden, 1970). Such lesions appear to be less inflammatory than those found in WM (Peterson *et al.*,2001), with limited lymphocytic infiltration (Bo *et al.*,2003) and complement activation (Brink *et al.*,2005).

Oligodendrocytes

Demyelination has long been established as significant component of MS pathology, and appears to involve a spatially heterogeneous inflammatory process mediated by T cells and perhaps autoantibodies. Significant oligodendrocyte populations have been observed in both acute and chronic lesions, particularly in periplaque regions (Chang *et al.*,2002; Solanky *et al.*,2001), suggesting a considerable potential for remyelination (Brusa *et al.*,2001; Prineas and Connell, 1979), however despite this remyelination may not be complete. It has been

suggested that remyelination failure represents a time-dependent decrease in the ability of demyelinated regions to support remyelination, combined with the limited rate at which oligodendrocyte precursor cells (OPC) migrate into them (Chari and Blakemore, 2002). Thus, while OPCs may present throughout chronic lesions, they may have missed a critical early phase in plaque evolution conducive to remyelination. The factors limiting remyelination remain uncertain (Hohlfeld, 2002).

The absolute functional significance of this is unclear, given that chronically demyelinated nerve fibres are still able to conduct signals, albeit at a reduced velocity (Felts *et al.*,1997). This is clearly seen when looking at recovery from optic neuritis, where functional recovery may be full despite persistent electrophysiological evidence of demyelination (Halliday *et al.*,1972).

In addition to their role in remyelination, oligodendrocytes may also play a part in the regeneration of axons following transection. It would appear that mature oligodendrocytes inhibit growth of axons in the adult CNS. However, there is evidence to suggest that oligodendrocytes are able to support axonal growth when there is relatively little tissue damage associated with axonal loss (Fawcett and Asher, 1999).

While axons may partly depend upon myelin for support (Yin *et al.*,1998), the reverse may also be true. Tsunada *et al.* (2003) employing a murine model of encephalomyelitis observe axonal injury preceding demyelination. From this, it may be speculated that dysfunction of either axons or myelin may establish a vicious cycle, with loss mutual support leading to the progressive degeneration of both.

Neurons and axons

Relatively recently, it has become clear that axonal and neuronal pathology has a significant part to play in the evolution of disability, with evidence coming from a number of histopathogical studies (Ferguson *et al.*,1997; Peterson *et al.*,2001; Trapp *et al.*,1998) revisiting an issue that had been overshadowed by the more overt presence of demyelination (Kornek and Lassmann, 1999). It has also been established in laboratory models of MS that axonal degeneration is present from the onset of the disease (Mancardi *et al.*,2000; Onuki *et al.*,2001).

It has been suggested that such axonal involvement is a bystander phenomenon associated primarily with inflammation and demyelination, and indeed this would be supported by the observations that axonal loss appears to be arrested in remyelinated lesions, but on-going in those that are chronically demyelinated (Kornek *et al.*,2000). However, in contrast, recent work has indicated that it may be the result of a more focussed immunological attack (Bitsch *et al.*,2000). In this work, it was suggested that axonal injury might be mediated directly by macrophages, microglia and, in particular CD8+ T-cells, the latter being supported by work by Medana *et al.* (2001). Further, whilst axonal loss was only found to correlate with the number of CD8+ T-cells, it was observed that there was considerable lesion heterogeneity indicating that other mechanisms may have a part to play. It has also been suggested that axonal degeneration in MS may, in part, be the result of immune targeting of neuronal proteolipid protein 1 (Garbern *et al.*,2002). Axonal damage has also been observed in the spinal cord remote from sites of focal demyelination and it

has been postulated that degeneration of myelin may be a secondary process leading to an inflammatory response (Bjartmar *et al.*,2001).

It has been shown that demyelination *per se* can lead to a reduced axonal diameter (Yin *et al.*,1998) and such denuded and atrophied axons may be more vulnerable to on-going inflammatory activity. Mediators of axonal damage may include nitric oxide and glutamate, both of which are also associated with inflammation. Nitric oxide (NO) has been found to cause conduction block (Redford *et al.*,1997) and also degeneration of electrically active axons (Smith *et al.*,2001). Disturbances of glutamate homeostasis and associated glutamate mediated excitotoxicity has also been proposed as another factor contributing towards axonal and oligodendrocyte damage, and it has been suggested that correction of this may prevent on-going axonal damage (Werner *et al.*,2001).

T-cells

Early observations noted infiltration of inflammatory cells in demyelinated lesions and thus a causative relationship was postulated. Subsequent studies indicated that this might be a T-cell mediated process with secondary microglial and macrophage activation. However, this may be common to a number of neuro-inflammatory processes, and as such may mark a general response to neural tissue damage rather than a disease specific finding (Neumann, 2001). Further, microglial and astrocytic activation may result directly from neuronal damage; through both cytokines and microglial antigen presentation in association with MHC class II, these are able to promote T-cell participation (Neumann, 2001), and the T-cell response may be a secondary event (Gay *et al.*,1997).

It remains unclear if demyelination is driven directly by inflammation or if this represents a response to another as yet undefined process. Both CD4+ and, to a greater degree, CD8+ T-cells have been detected in MS lesions (Babbe *et al.*,2000; Gay *et al.*,1997) suggesting a role in the pathological process. CD4+ T-cells (activated by antigen presentation in association with MHC class II complexes on resident microglia) may have a role to play in directing an inflammatory response. CD8+ cytotoxic T-cells (activated by antigen presentation in association with MHC class I complexes), derived from a limited number of cell lines suggesting antigenic specificity (Babbe *et al.*,2000), appear to predominate over CD4+ T-cells in active lesions (Gay *et al.*,1997), however no consistent role in pathogenesis has been defined.

Further, the direct relationship between demyelination and inflammation in MS has been called into question by the observation that demyelination can occur in the apparent absence any inflammatory process and outside focal lesions (Guseo and Jellinger, 1975); and that inflammation can occur in unmyelinated regions such as the retina (Shaw *et al.*,1987). It would also appear that inflammation might also in part aid tissue repair rather than simply cause damage (Kappos and Duda, 2002).

Evidence from MRI would appear to support the concept that most lesions, as seen on T_2-weighted images, exhibit breakdown in the BBB at an early stage in their development (Ciccarelli *et al.*,1999; McFarland *et al.*,2002). However this does not establish causality; other work has suggested that MR changes may occur before overt Gd-enhancement (an MR marker of breakdown in the BBB (Bruck *et al.*,1997;

Goodkin *et al.*,1998; Katz *et al.*,1993), and that the spatial probability distributions of Gd-enhancing and T_2 lesions need not entirely coincide (Lee *et al.*,1999).

B-cells and auto-antibodies

The presence of oligoclonal intrathecal immunoglobulin synthesis in MS has been known about for some time, and the bands appear to be directed against a range of antigens (Cross *et al.*,2001). Some are directed against myelin antigens such as myelin basic protein (MBP) and myelin oligodendrocyte glycoprotein (MOG), although these are not specific to MS (Karni *et al.*,1999). Further, studies using the main animal model of MS, experimental allergic encephalomyelitis (EAE), indicate that the passive transfer of B-cells or antibodies is not able to induce demyelination (Cross *et al.*,2001). This contrasts with the passive transfer of sensitized T-cells or active immunization with myelin derived proteins that are able to do so. This suggests that auto-antibodies may not have a direct role in initiating pathology although they may play a significant part in the regulation and localization of inflammation, for example it has been suggested that those directed against MBP may actually promote remyelination (Rodriguez *et al.*,1996) while anti-MOG antibodies may promote demyelination (Linington and Lassmann, 1987).

Astrocytes

The role of astrocytes in the pathology of MS remains unclear. Astrocytes react to a variety of CNS insults and resultant glial scars consist predominately of meshworks of astrocyte processes (Fawcett and Asher, 1999). In MS, astroglial proliferation appears widespread, having been observed in both focal WM lesions and NAWM (Allen and McKeown, 1979); it has yet to be clearly established if it has

a beneficial or detrimental effect upon clinical outcomes. It has been suggested that over-expression of cytokines by astrocytes, in particular glial maturation factor, may promote immune activation in the nervous system (Zaheer *et al.*,2002). This in turn may be mediated by microglia, which when stimulated express MHC class II antigens.

From present evidence, axonal regeneration seems to occur in a predominantly astrocytic environment, particularly at sites of focal damage. This environment may promote and inhibit axonal growth dependent on a variety of interacting factors, although the exact nature of these is far from clear (Fawcett and Asher, 1999). Astrocytes may also promote oligodendrocyte survival, possibly through cell surface interactions (laminin on astrocytes and integrin on oligodendrocytes) or humoral factors (Corley *et al.*,2001), and this in turn may have a role promoting timely remyelination.

Microglia

Microglia act as the CNS's resident macrophages and antigen presenting cells, and are rapidly and stereotypically activated in many CNS disease processes (Kreutzberg, 1996). After activation they proliferate and migrate to the site of injury while becoming morphologically more macrophage-like and expressing increasing levels of MHC class I and II antigens. They may both promote damage and repair, and their role in MS remains unclear.

Complement

Complement would appear to have a role mediating cellular damage in MS. It is activated by both antibodies and via the classical pathway by myelin itself

(possibly through MOG) (Vanguri et al.) and has been localized to WM lesions (Compston *et al.*,1989; Lucchinetti *et al.*,2000) but less consistently to those in the GM (Brink *et al.*,2005; Schwab and McGeer, 2002). The relative importance of its contribution to tissue damage has yet to be fully established.

2.1.5 PATHOPHYSIOLOGY

Symptoms experienced by people with MS can be broadly divided into positive and negative, and these may wax and wane or be irreversible (Smith and McDonald, 1999). Negative symptoms include anaesthesia and paralysis and are the result of conduction delay and block. Positive symptoms include paraesthesia and neuralgia, which may be associated with mechanical action on regions of demyelination (as in Lhermitte's sign (Al-Araji and Oger, 2005)), and are due to axonal hyper-excitability and spontaneous discharges.

Many axons in the nervous system are not myelinated but still readily able to convey signals. However, myelination speeds up conduction velocities and thus offers advantages when information needs to be transmitted rapidly. Conduction in myelinated axons differs from that of unmyelinated fibres, which rely upon a continuous wave of depolarisation, in that only discrete sections of the axon membrane (the nodes of Ranvier) between regions of myelination need to depolarise for an action potential to be conducted, a process known as saltatory conduction. The changes in membrane potential associated with the passage of an action potential rely upon the controlled influx of Na^+ ions into the axon. The Na channels through which they pass are concentrated at the nodes of Ranvier in myelinated fibres and are more evenly distributed in unmyelinated fibres.

Negative symptoms

Negative symptoms are the result of conduction block and signal attenuation, and this in turn may be due to a variety of transient and longer-term factors. Acutely, the loss of myelin stops saltatory conduction, leaving remote islands of Na^+ channels

that are unable to support action potential propagation. With time, Na^+ channels may redistribute themselves more evenly over the axonal membrane so restoring signal conduction, albeit at a reduced velocity (Smith and McDonald, 1999). Such demyelinated axons also appear sensitive to the effects of NO, which may lead to further transient conduction block (Kapoor *et al.*,1999), and well-recognised temperature sensitivity (Uhthoff's symptom (Selhorst and Saul, 1995)). In addition humoral factors such as cytokines or antibodies may also act as neuro-electric blocking factors (Smith and McDonald, 1999), although exactly which components are involved remains unclear.

Positive symptoms

Positive symptoms are the result of axonal hyper-excitability, with persistent and excessive activity. This may be spontaneous, or associated with mechanical (Lhermitte's phenomenon and phosphenes on eye-movement (Davis *et al.*,1976)) and possibly molecular factors such as glutamate-mediated excitation.

Relapses, remissions and persistent disability

An acute symptomatic event need not be associated with demyelination alone (Barnett and Prineas, 2004), and similarly recovery from such episodes need not imply that remyelination has occurred (Brusa *et al.*,2001). Thus, a relapse and subsequent remission may represent a variety of pathological events. Irreversible disability may follow a relapse or may be a slowly progressive feature of the disease. While it seems reasonable to assume that such unrecoverable functional deficits reflect the unrecoverable loss of signal transmission, and thus by implication the final loss of an axon or entire neuron, the pathways leading to this may differ dependent

upon their association with relapses. Axonal damage (Ferguson *et al.*,1997) and transection (Trapp *et al.*,1998) have been observed in acute white matter lesions, the latter offering a clear link between incomplete recovery from an acute relapse and inflammatory activity. Progressive changes may be mediated by: (i) less marked but either more persistent or more widespread inflammation; (ii) other processes either initiated by acute inflammation but not dependent upon its persistence; or (iii) processes which are either independent or at least semi-independent of focal inflammation. The possibility of such semi-independence is suggested by some of the work previously considered (section 2.1.3) and from clinical work by Confavreux *et al.* (2000) who, in a study exploring the relationships between acute relapses and longer-term disability, found no clear link between these clinical parameters.

2.1.6 *MEASURES OF CLINICAL OUTCOME*

Assessing disability in MS is difficult. The effects of MS are widespread, and to fully assess its effects would require an extensive battery of specific tests. Further, it is difficult to effectively design and implement tests that assess either a single function or the integrity of any single component of the nervous system. Thus, measures currently employed in MS are a compromise between specificity to a particular function and global sensitivity to disease effects.

At present the main measures of disability used in clinical studies are the expanded disability status scale (EDSS) (Kurtzke, 1983), and more recently, the MS functional composite score (MSFC) (Cutter *et al.*,1999; Fischer *et al.*,1999).

The expanded disability status scale

The EDSS is a twenty-point scale from 0.0 to 10.0. It is based upon a combination of functional systems (FS) scores and in its mid-levels estimates ambulation (see Appendix). It is a non-linear scale with clinical impairment without disability represented by the first five points, subsequent increasing stages of disability, and ultimately death due to MS. It has been suggested that after a reaching a score of 4, progressive changes rather than those associated with relapses, account for further deterioration (Confavreux *et al.*,2003; Confavreux *et al.*,2000). The non-linear progression through the EDSS scale makes it different to compare the relative disease severity in subjects with differing disease durations, and to address this the multiple sclerosis severity scale (MSSS) was developed (Roxburgh *et al.*,2005).

The MS functional composite (MSFC) score

The MSFC is derived from the results of two 25 foot timed walk tests (TWT) (Cutter *et al.*,1999), four nine hole peg tests (HPT) (two trials for each hand) (Goodkin *et al.*,1988), and a paced serial addition test (PASAT) with 3 second stimulus intervals (Gronwell, 1977). The average of the two TWT and reciprocal average of the four HPT are calculated. The preferred method for calculating the MSFC uses the study cohort to create Z-scores for all three measures (Fischer *et al.*,1999). To calculate a Z-score, the mean and standard deviation (SD) of a given parameter are first calculated using data from all subjects in the cohort. The average cohort parameter value is then deducted from a given subjects results, and this difference is then divided by the whole cohorts parameter SD. Thus for the PASAT:

$$Z_{PASAT} = \frac{CohortMean_{PASAT} - Subject_{PASAT}}{CohortSD_{PASAT}}$$

Similarly, Z-scores are calculated for the TWT (Z_{TWT}) and reciprocal average of the HPT ($Z_{1/HPT}$). The MSFC is then calculated as:

$$MSFC = \frac{Z_{1/9HPT} - Z_{25TWT} + Z_{PASAT}}{3}$$

Relative merits of the expanded disability status scale and multiple sclerosis functional composite scores

The EDSS has a number of limitations related to its intrinsically non-linear nature and limited sensitivity to change (Hobart *et al.*,2000) and the MSFC was designed to address some of these issues. While the EDSS is weighted towards lower limb function, the MSFC was specifically designed to include upper limb and

cognitive function in the score. In addition the components of the MSFC measure rather than classify function. There is evidence to suggest the inclusion of arm and cognitive function measures in the MSFC adds relevant information to such global scores of disability in MS (Kalkers *et al.*,2001), although the MSFC is not perfect and there is an argument in favour of using the components of the measure rather than the composite. Further, for a given EDSS score, clinicians will immediately have some conception of a given subject's level of disability, i.e. if they require a walking aid or not, while the MSFC does not offer such readily accessible clinical information.

Neither the EDSS nor MSFC directly assesses the subject's perceptions of disability, which will be central to their perceived well being and so the success or failure of a given treatment. The Guy's neurologic disability scale (GNDS) is patient centred, and it would appear that on this scale, subject's perceptions of disability correlate strongly with both the EDSS and MSFC (Hoogervorst *et al.*,2001). The GNDS still potentially retains some bias toward a clinician's belief about the importance of symptoms, and more recently the MS impact scale (MSIS-29) has been developed using a more rigorous psychometric methodology (Hobart *et al.*,2001). Its clinical utility has yet to be established.

2.2 *MAGNETIC RESONANCE IMAGING*

2.2.1 PHYSICS

MRI exploits the properties of subatomic particles in magnetic fields and their interactions with electromagnetic radiation. In the present work, the particle of interest is the hydrogen nucleus (^{1}H), although other nuclei may be studied with MRI. Fortunately, ^{1}H is ubiquitous in the human body, predominantly in the form of water, but also in observable amounts in a number of other molecules.

There are four main properties of materials (tissues) that are used by MRI to determine structural and constituent information: T_1 and T_2 relaxation times, proton densities (PD) and chemical shifts. These will be discussed in the following section.

Electromagnetic properties of ^{1}H nuclei

^{1}H nuclei consist of single protons that exhibit a property known as nuclear spin. Nuclear spin can be thought of as a rotation about the centre of the particle which, if the particle is charged, creates a current loop which in turn produces a magnetic moment parallel to the axis of rotation. This is known as a magnetic dipole moment. Particles exhibiting this property are often referred to simply as spins.

In the presence of an external magnetic field (B_0), spins will align themselves either parallel or anti-parallel to B_0. These two orientations are linked to nuclear energy states: parallel orientation is a lower energy state than anti-parallel. Thus for a given spin, there will be a magnetic component parallel to B_0, which by convention is designated the z-axis; if the spins are disturbed from equilibrium, there will also be a component in the xy-plane. If a 90° pulse (a radio frequency [RF] pulse generated by

the MR scanner) is applied, the spins magnetic moments can be fully tipped from the z-axis into the xy-plane.

Another property of spins is that they precess around B_0, and if they are in the xy-plane this gives rise to an oscillating magnetic field in the xy-plane. The rate at which this field oscillates is described by the Larmor equation:

$$\omega = \gamma B_0$$

where ω is the angular precessional frequency expressed in radians per second or Hz, and γ is the gyromagnetic ratio, which a constant for a given nucleus [$\gamma(^1H)$=42.6 MHz/Tesla], and B_0 is the external magnetic field strength in Tesla.

MRI relies upon the absorption and emission of energy by spins in the form of electromagnetic radiation. The frequency at which spins both absorb and radiate energy is defined by the Larmor equation, and is given by ω (in units of radian per second) or $2\pi\omega$ (in units of Hz). For an MRI scanner operating at 1.5 Tesla, the frequency for ^1H will be about 64 MHz, i.e. in the RF range of the electromagnetic spectrum.

Bulk magnetisation and Bloch equations

MRI does not look at single spins in isolation; observations are made on many spins simultaneously. Under such circumstances the bulk magnetic field (M) induced in a test material is actually observed and its behaviour under the influence of external magnetic fields and electromagnetic radiation is described by the Bloch equations. Assuming that B_0 is parallel to the z-axis and RF pulses are applied in the xy-plane, the evolution of the components of the bulk magnetic field at a time t can be described by:

$$\frac{dM_z(t)}{dt} = \gamma[M_x(t)B_y(t) - M_y(t)B_x(t)] - \frac{M_z(t) - M_0}{T_1}$$

$$\frac{dM_x(t)}{dt} = \gamma[M_y(t)B_z(t) - M_z(t)B_y(t)] - \frac{M_x(t)}{T_2}$$

$$\frac{dM_y(t)}{dt} = \gamma[M_z(t)B_x(t) - M_x(t)B_z(t)] - \frac{M_y(t)}{T_2}$$

where M_x, M_y and M_z are orthogonal components of M, and B_x, B_y and B_z are orthogonal components of B, the magnetic field (comprising both the main magnetic field, along z, and the fields in x and y associated with RF pulses). M_0 (the steady state bulk magnetic field) is proportional to B_0 and this relationship is described by:

$$M_0 = \chi B_0$$

where χ is the magnetic susceptibility of a material. There are two other components to these equations, the T_1 (longitudinal or spin-lattice) and T_2 (spin-spin) relaxation times. MRI makes use of differences in these properties between materials to provide contrast in structural images.

T_1 relaxation

T_1 differs between materials, dependent of the rate at which excited spins can radiate energy into their surrounding molecular lattice (hence another name for T_1 relaxation being spin-lattice relaxation). The strength of M_z at a time t after the application of a 90° RF pulse along (by convention) the x-axis is given by the equation:

$$M_z(t) = M_0(1 - e^{-t/T_1})$$

T_2 relaxation

In a material exposed to an external field B_0 spins will all precess at approximately the same frequency, but any component of the net magnetisation in the xy-plane will be zero if the spins are not in phase with each other. If they are brought into phase an oscillating magnetic field in the xy-plane will be seen. In a perfectly homogeneous magnetic field, spins would always remain in phase, however the magnetic field experienced by individual spins will depend not only on B_0 but also surrounding spins distorting local field homogeneity. This will slightly alter the precessional frequency of individual spins, and will lead to dephasing with time. This in turn will result in the decay of M_{xy}; following the application of a 90° RF pulse this is described by the equation:

$$M_{xy}(t) = M_{xy}(0)e^{-t/T_2}$$

T_2 is the transverse relaxation time, also known as the spin-spin relaxation time. This value will be correct in a perfectly homogeneous B_0 field but current technology cannot generate such fields. External B_0 field inhomogeneity will result in dephasing, leading to a reduction (shortening) of the apparent T_2, and this value is denoted by T_2*. As with T_1, T_2 also varies between materials.

Proton density

Another factor influencing the potential MR signal is the number of mobile protons or proton density (PD) in a given volume of tissue. For example, CSF contains more mobile protons than either GM or WM, and so the maximum potential signal is greater for CSF than brain tissue. This has the effect of scaling the signal

intensities predicted by the Block equations, and as illustrated below, this will alter apparent tissue contrasts.

Chemical shift

Spins in a given molecule will experience a slightly different external field to the main B_0 field, due to shielding of the nucleus by its electron cloud. This alteration in the apparent external field experienced by a given spin will alter its precessional frequency slightly, producing a frequency offset known as chemical shift. Many biological molecules contain a number of MR visible spins which are part of chemically distinct groups (such as methyl or hydroxyl groups), all of which will experience slightly different external fields due to the molecular electron cloud patterns. This (in addition to J-coupling [described below]) will lead to a spectrum of frequencies being generated by such molecules. This spectrum provides a fingerprint for the molecule, and in ^{1}H-MRS this is the basis of identifying metabolites and quantifying metabolite concentrations. Nuclear shielding can be summarised by the equation:

$$B_i = B_0(1-\sigma_i)$$

where B_i is the external field experienced by spin i, where the nucleus has a nuclear shielding term of σ_i. The shift in resonance frequency from a reference frequency (by convention relative to a very heavily shielded compound known a TMS (tetramethylsilane) is given in parts per million (ppm), a measure that is independent of B_0. In these units, protons in water resonate at 4.7ppm, lipid protons at about 0.9-1.2ppm, and most metabolites somewhere in between.

Spins in molecules may also experience J-coupling, which occurs when spins interact via chemical bonds. This further alters their precessional frequency, splitting spectral lines into multiplets. Small frequency differences between multiplets lead to phase shifts that may cause their signals may cancel out, leading to changes in apparent T_2 relaxation times. Such effects may be observed for many molecules currently studied using ^{1}H-MRS, although the relative importance of these differ (Govindaraju *et al.*,2000).

2.2.2 *STRUCTURAL IMAGING*

Inducing repeated T_1 and T_2 relaxation

In order to determine T_1 and T_2 characteristics, the spins in the material must be repeatedly excited (i.e. magnetisation tipped into the transverse plane), and as noted briefly above, this is achieved using RF pulses. Recording the signal (voltage) in the coil immediately after an appropriate RF pulse has been applied reveals an oscillating decay curve, diminishing at a rate determined by the T_2* relaxation time. This is known as the free induction decay (FID) curve (see Figure 2.2.2a) and although it is not of great use in itself, using further RF pulses to induce echoes (effectively replicates of the FID) is.

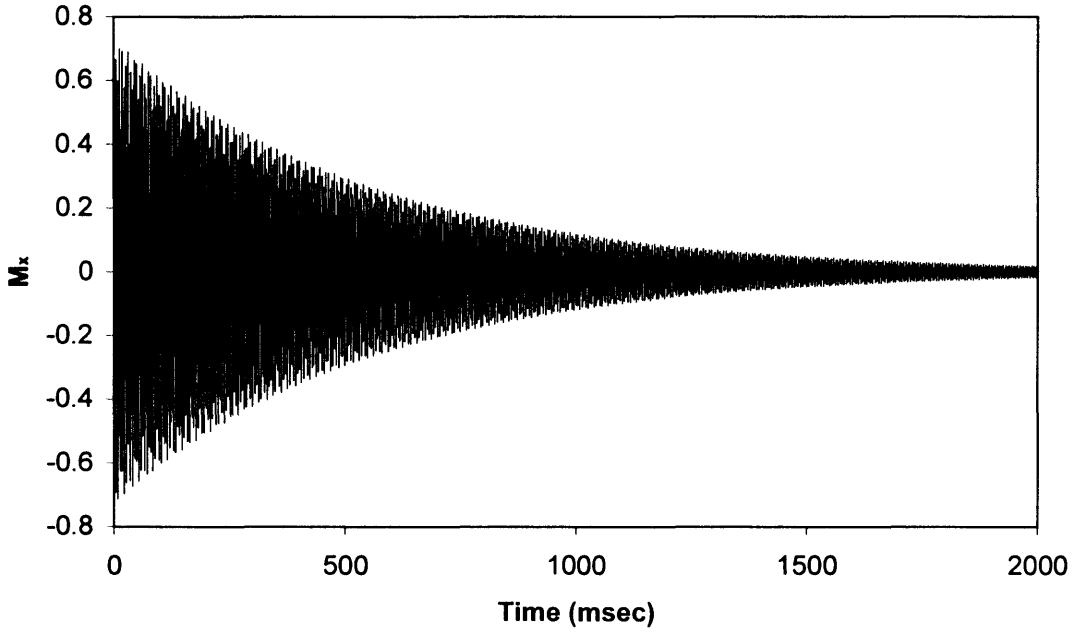

Figure 2.2.2a: Simulated free induction decay curve using average white matter relaxation values in a perfectly homogeneous 0.001 Tesla external field. Signal intensity is estimated relative to fully relaxed water maximum values.

Radiofrequency pulses

Using RF pulses of a particular amplitude and duration, it is possible to effectively tip M_z through any given angle: a 90° pulse will tip M_0 into the xy-plane; a 180° pulse will invert M_z. We are only able to detect a signal when there is net magnetisation in the xy-plane, and we rely upon tipping M_z into M_{xy} to determine the T_1 and T_2 characteristics of a material. A 180° pulse will not only invert M_z, but also effectively reverses the direction of precession experienced by individual spins. This is useful as it allows the generation of spin echoes by rephasing spins after they have experienced T_2* decay. By reversing the direction of precession but not the rate, dephasing related to B_0 inhomogeneities is unwound, resulting in a crescendo-decrescendo RF signal, known as a spin echo, that resembles mirror images of an FID back-to-back.

Echo and repetition times

Echo and repetition times (TE and TR) refer to scan acquisition parameters and by varying these values we are able to weight images based on the T_1 or T_2 characteristics of a material. The TR is the time interval between 90° RF in a series of excitations. As noted above there will be an FID immediately after this, although it is difficult to observe for technical reasons and instead imaging relies upon inducing spin echoes by applying further 180° pulses at given times after the initial 90° pulse. This combination of RF pulses, along with the pattern of magnetic field gradients applied to encode spatial information in an image (see below), is known as a pulse sequence. Different pulse sequences can be used to probe different aspects of the MR signal, and provide different tradeoffs between image contrast, signal to

noise, scan time and other considerations. Some examples are given in Figure 2.2.2b). The time at which a spin echo is induced after the 90° pulse is known as the TE. Given that T_1 and T_2 decay occurs at different rates, by selecting appropriate combinations of TR and TE the resultant images can be weighted towards the T_1 or T_2 characteristics of a given tissue. Sequences with short TR and TE are T_1-weighted while those with long TR and TE are T_2-weighted, although it must be remembered that all sequences also have some degree of proton density weighting.

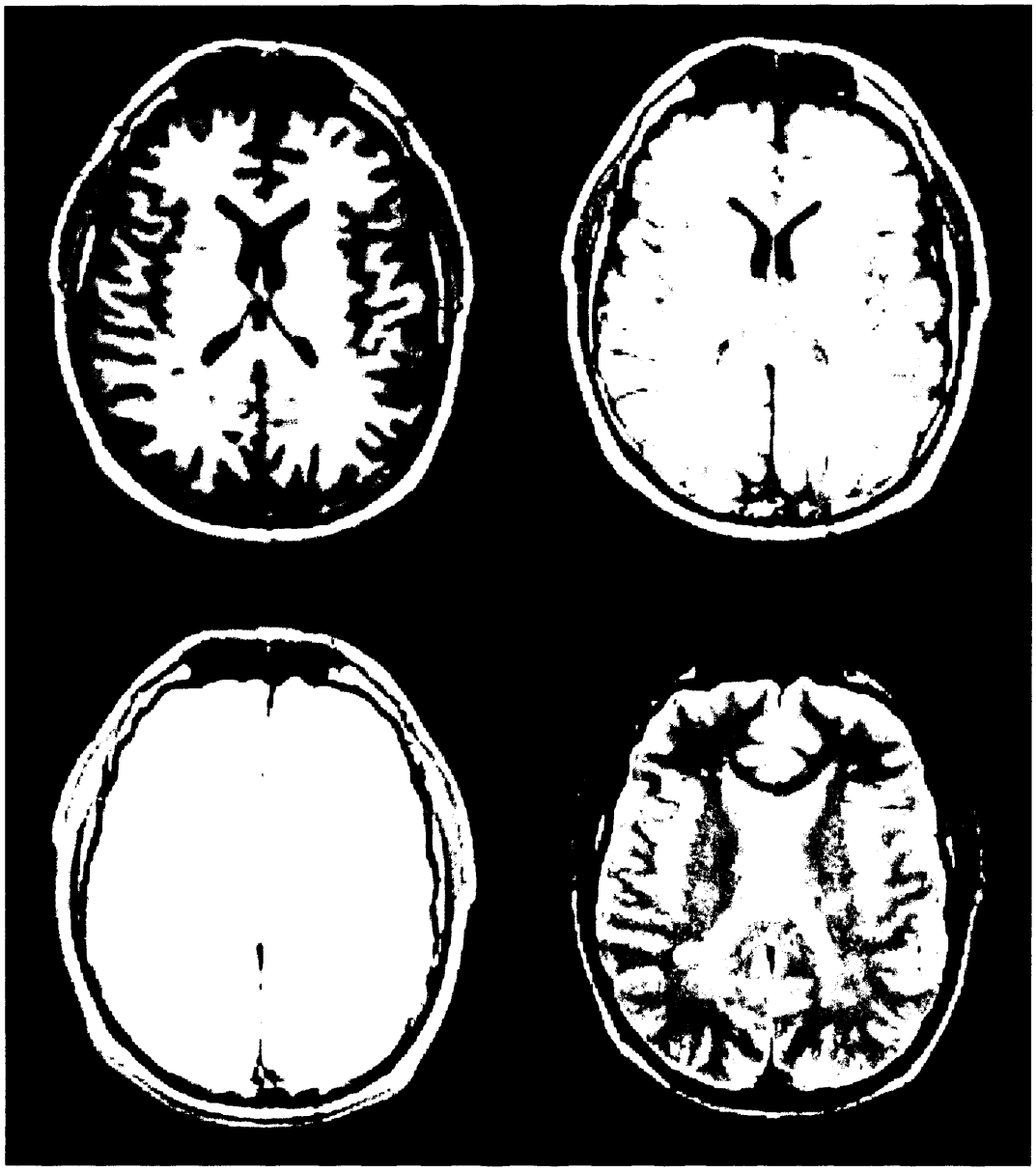

Figure 2.2.2b: Images from a subject with MS acquired using a variety of sequences. From the top left clockwise: an inversion-prepared 3D fast spoiled gradient recall (FSPGR); 2D T_1-weighted spin echo (SE); 2D T_2-weighted fast spin echo (FSE); and 2D PD-weighted FSE. The slice thickness is 1.5 mm for the 3D FSPGR and 5 mm for the other images.

Inversion preparation

While T_1, T_2 and PD characteristics offer a reasonable degree of tissue differentiation there are situations where that nulling of signal from a particular tissue or fluid may be useful. In such a situation inversion prepared (also known as inversion recovery) sequences may be used. Rather than tipping M_z through 90°, an initial 180° RF pulse is used to invert M_z. M_z will recover its equilibrium state at a rate determined by T_1 and will pass though a point where there is no net longitudinal magnetisation, the null point. If a 90° pulse followed by a further 180° pulse is applied at this time (known as the inversion time [TI]) to generate a spin echo, M_z will be zero and there will be no resultant signal. As tissue T_1 values differ, signal from a particular tissue may be suppressed (selecting TI equal to $\ln(2 \times T_1)$), while retaining at least some signal from other tissues. In neuroimaging, this technique is most frequently used to null CSF (when it is known as FLAIR (fluid attenuation by inversion recovery) or fat (when it is known as STIR (short TI inversion recovery), although it could equally be used to null GM or WM. Inversion recovery prepared sequences can also be used simply to enhance T1 contrast between tissues, choosing a TI that affects all the tissues but nulls none.

Spatial localisation

In order to generate either a structural image or localised measurement within a material, location in three dimensions has to be established: varying the frequency at which spins resonate, by applying magnetic field gradients, allows this.

By convention test materials are divided in to slices orthogonal to the z-axis, and slice selection is achieved by adding a gradient to the B_0 field. This gradient

makes the precessional frequency of spins proportional to their position along the z-axis, and by applying RF pulses within a defined frequency range, only those spins lying within a slab corresponding to these frequencies will be excited. The thickness of this slab depends upon the range of frequencies included in the RF pulse: the wider the range (bandwidth) the thicker the slice. It should be noted that this will also be dependent upon the magnitude of the B_0 gradient, thusfor a given RF bandwidth large B_0 gradients will allow thinner slices than small gradients.

Having defined the slice to be acquired, position along the y-axis (usually the vertical axis) may be established using a phase-encoding gradient. This takes the form of a transient magnetic gradient applied along the y-axis that briefly alters that precessional frequency of spins such that they are systematically dephased by an amount denoting their relative position along the axis.

Position along the x-axis is determined by applying a frequency-encoding magnetic gradient during collection of a spin echo. This alters the frequency of the collected signal dependent upon location along the x-axis of the precessing spins, thus relative frequencies indicate position along the x-axis.

Image reconstruction

To extract the spatially encoded information from a spin echo Fourier transforms are employed to translate the time-domain signal into the frequency-domain. This yields the signal intensities at particular frequencies. In two-dimensional (2D) imaging, these define the x and y positions with a given slice, and the image is reconstructed as grid of intensities.

Three-dimensional (3D) imaging is a modification of this, with the slice-selection gradient and RF pulse exciting the whole structure to be imaged, and then two phase-encoding gradients applied in the z and y directions, leaving frequency encoding to account for the x position as before. High-resolution 3D imaging has advantages over 2D imaging when reconstructing complex structures, although the former is generally limited to T_1-weighted acquisitions due to lengthy scan times required for PD and T_2-weighting.

Fast imaging techniques

So far we have considered conventional MRI techniques to derive images. There are a number ways in which the process may be hastened, although there is a trade-off between speed and signal-to-noise ratio. Methods include acquiring multiple echoes during one TR, reducing the RF pulse flip angles to allow reduced TR without incurring heavy T1 weighting, and acquiring data more selectively. While such techniques yield images faster, they seek to do so with similar contrast to their conventional equivalents, and thus the previous discussion covers those issues needed to understand their practical application.

2.2.3 *PROTON MAGNETIC RESONANCE SPECTROSCOPIC IMAGING*

Spectra

While structural imaging relies upon a strong signal from water, MR techniques may also look for signals from other molecules, and ^{1}H-MRS does exactly this. As noted above individual protons within a given molecule may have differing chemical shifts and thus a range resonant frequencies may be observed from a single molecule. In a given tissue, many different types of molecule contribute towards the seen signal, and Fourier transformation (now detecting inherent, rather than magnetic field gradient induced, frequency differences) reveals a range of overlapping peaks known as a spectrum (Figure 2.2.2c). The pattern of these signals act as a molecular fingerprint and, as with structural imaging, the intensity of the derived signal is proportional to molecular concentration. Metabolite peak locations may be reported both in Hz or parts per million (ppm). The former value depends on the B_0 field strength, while the latter is the ratio between the peak location frequency and that of a reference frequency, and is independent of the B_0; the latter is generally reported.

Water suppression

The signal from water dominates spectra (Figure 2.2.3a even after water suppression) and it is difficult to digitise the small amplitude signals from other molecules without some suppression of the water signal. In order to achieve this as series of chemical shift selective saturation (CHESS) pulses are employed to systematically stimulate and dephase water resonance signals. A single CHESS pulse

can reduce the magnitude of the water signal by a factor of 100, and with multiple pulses able to achieve suppression by a factor of 1000.

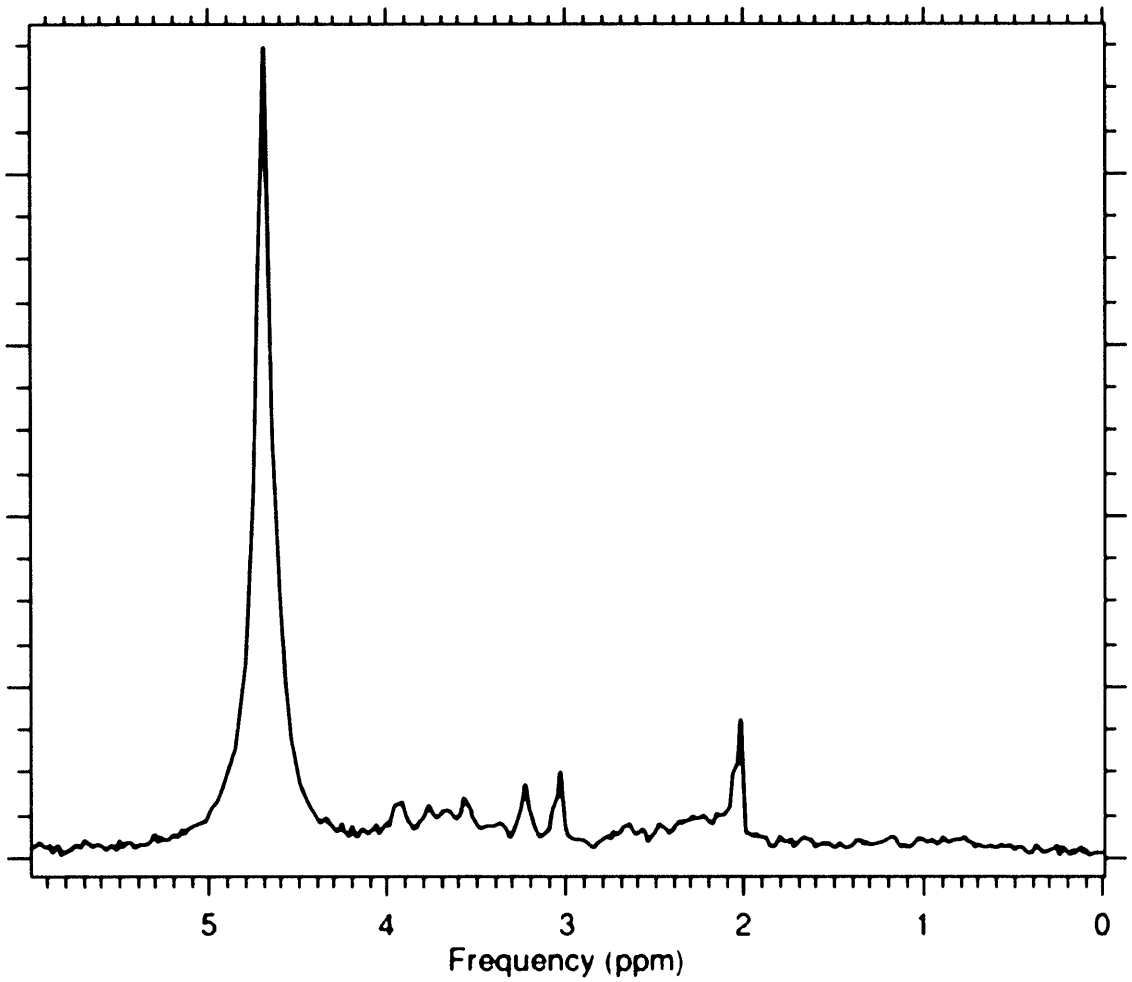

Figure 2.2.3a: A frequency-domain representation of a spectrum after CHESS water suppression; from left to right the main peaks are water (c 4.7 ppm), Ins (c 3.5 ppm), Cho (c 3.2 ppm), Cr (c 3.0 ppm), Glx (c 2.5 to 2.1 ppm) and NAA (c 2.0 ppm). See Figure 2.3.2a for an enlargement of the spectral region containing the main metabolite peaks.

Spatial localisation

There are two commonly used methods used to localise the volume of interest for *in vivo* ^{1}H spectroscopy examinations on clinical MR scanners, stimulated echo acquisition mode (STEAM) and point resolved spectroscopic (PRESS) localisation. Both rely upon using three slice-selective gradients, one along each axis, and three RF pulses. Only those spins at the intersection of all three planes defined by the slice-selection gradients are excited by all the pulses to yield a usable echo. PRESS sequences use one 90° and two 180° pulses while STEAM makes use of three 90° pulses. This allows the STEAM pulse sequence to be shorter than PRESS, enabling shorter TE at the expense of around 50% of the potentially available signal. For this reason, many studies now employ PRESS rather than STEAM.

^{1}H-MRS imaging (^{1}H-MRSI) extends this methodology by allowing spatial localisation within the volume of interest. This is achieved with phase-encoding in either one, two or three dimensions. Given that the frequency distribution of the detected signal contains chemical shift information, frequency-encoding cannot be used. The phase-encoded spatial information is extracted using Fourier transforms (FT), as for conventional structural imaging, while a further FT detects the spectral (frequency) information.

Outer volume suppression

While volume selection using PRESS or STEAM limits signal contamination from surrounding volumes it does not totally eliminate it. Signal from surrounding tissues can still contribute to the derived spectra and this can be a particular problem when the adjacent tissues contain significant amounts of ^{1}H-MRS visible lipids. Such

peaks can dominate spectra making quantification of metabolites less reliable. Outer volume suppression (OVS) complements volume selection by actively suppressing the signal from the outside the excitation volume. This is achieved in a similar way to CHESS water suppression with volume selective stimulation followed by dephasing.

2.3 *REVIEW OF SPECIFIC MAGNETIC RESONANCE METHODOLOGIES EMPLOYED*

2.3.1 *STRUCTURAL IMAGING, TISSUE SEGMENTATION AND VOLUME MEASUREMENTS*

There are four main issues to consider when selecting an acquisition for tissue volume estimation, these are: image acquisition times, contrast and resolution, and the segmentation technique to be used (discussed in the next section). Sequences must provide enough information to accurately and precisely define boundaries. The overall limiting factor is the SNR, and to maintain this while increasing image resolution at a given magnetic field strength requires a corresponding increase in scan times. This may be compensated for by the use of fast acquisition techniques, which typically have a greater efficiency (a greater SNR per unit time) than more conventional ones. It is desirable to keep acquisition times short, not simply for the comfort of the subject, but also to reduce the chances of the subject moving during the scan. Further, in those people with neurological disease, involuntary movement may lead to greater image degradation than would be observed in healthy control subjects, and so minimising scan times will help to limit any associated differentials in image quality.

Direct comparisons of the reliability of tissue segmentations derived from images of differing resolutions has not been extensively investigated, but for lesions in MS it appears that the higher the resolution the higher the precision of volume estimates (Filippi *et al.*,1997a; Molyneux *et al.*,1998b).

Tissue segmentation also requires adequate image contrast to distinguish each type reliably. It would appear that for whole brain segmentation T_1-weighting (perhaps further improved with inversion recovery preparation) offers better contrast between brain and CSF than T_2/PD-weighting, and this is reflected in higher precisions (Leigh *et al.*,2002). Differentiation of GM and WM is more difficult, although segmentation may be driven by both single (for example Ashburner *et al.* (2000)) and multi-contrast acquisitions (for example Alfano *et al.* (1997)). T_2 and PD-weighted images in general require longer scan times than T_1-weighted images. This is due to the longer TR of such sequences which cannot be fully compensated for by the use of fast imaging techniques without loss of image quality (Mittal *et al.*,1999). Given this, on balance it appears that T_1-weighted 3D sequences are to be preferred for tissue volume estimation (Miller *et al.*,2002), offering a reasonable balance between resolution, contrast and scan acquisition times (voxels of 1 mm^3 with whole brain coverage can be acquired in under 10 minutes).

The reliability of volume determination is fundamentally limited by the quality of the images acquired and scan processing needs to be optimised to maximally realise this potential. A variety of approaches have been employed and all rely upon being able to partition volumes, either by directly identifying boundaries or by classifying individual voxels. While there is a wide range of techniques available to segment images (Miller *et al.*,2002), there have been few direct comparisons of techniques allowing an objective assessment of their relative merits (Leigh *et al.*,2002). Automated methodologies are generally more time-efficient than manual

or semi-automated procedures, particularly when applied to high-resolution images, and are less open to operator bias.

Image non-uniformity associated with B_1 field inhomogeneity tends to lead to reductions in apparent tissue signal intensities, in particular in the brainstem and cerebellum when imaged using standard head-coils. This has lead to the development of a variety of correction strategies, some based upon phantom studies and others estimating bias fields directly from the images to be segmented. Which approach is optimal has yet to be clearly established and, as with segmentation techniques, there has been little work directly comparing inhomogeneity correction strategies (Arnold *et al.*,2001).

Tissue volumes may be estimated either as absolute values or as fractions of an invariant volume. Absolute measures may be significantly influenced by random inter-subject variability and scanner scaling effects that may ablate sensitivity to age, gender and disease effects. The intracranial volume is an invariant measure that allows for random scanner scaling effects, yielding fractional volume estimates which are more temporally stable than their absolute equivalents (for example (Whitwell *et al.*,2001)). Such fractional measures have firmly established themselves in the study of atrophy in MS (Miller *et al.*,2002).

2.3.2 *PROTON MAGNETIC RESONANCE IMAGING AND METABOLITE CONCENTRATION QUANTIFICATION*

As noted in section 2.2.3 spectra may be acquired as single voxels or as part of spectroscopic volumes, as in ^{1}H-MRSI. However, in terms of time to acquire a voxel, the latter is much more time efficient i.e. for a given voxel size and SNR, acquiring multiple voxels as a ^{1}H-MRSI grid is faster than acquiring the same voxels separately. However, homogenously shimming the spectroscopic volume becomes more difficult the larger it is, leading to poorer line widths in the resulting spectra. In ^{1}H-MRSI. voxels at the edge of the volume may also not be fully excited, leading to lower signal intensity and problems with quantification, although this problem can be alleviated by exciting a region larger than that from which useable information is desired, and by using smaller voxels i.e. more phase-encode steps.

Disease associated effects upon metabolite T_1 and T_2 characteristics also need to be considered, particularly with relatively long TE and short TR sequences. For a hypothetical metabolite with a T_1 of 1.5 s (at the upper limit that estimated for Cr, Cho, Ins, Glx and NAA at 3T or less) and T_2 of 150 ms (at the lower limit of that estimated for Cr, Cho and NAA at 3T or less (Mlynarik *et al.*,2001)) quantified using a sequence with a TE of 30 ms and TR of 3 s (as employed in this work), a 10% change in signal would require a circa 35% change in either T_1 or T_2; a 5% change in signal would require a circa 15% change in T_1 or a greater than 20% change in T_2. For metabolites with shorter T_1 and longer T_2, the percentage changes required will be correspondingly larger, thus these estimates represent lower limits for the

percentage T_1 or T_2 change required. For sequences with longer TE and shorter TR, the percentage changes required will be smaller.

Having obtained spectra, it remains to quantify metabolite concentrations from them. Most techniques make use of frequency-domain spectra, and the present discussion will be limited to this, although it is possible to use the time-domain data directly (Vanhamme *et al.*,2001). The two approaches should ultimately be equivalent although the former is intuitively more readily appreciated.

Given that the area of a frequency-domain peak is related to the number of spins contributing towards it, it is possible to use peak area or height as an estimate of a metabolites concentration. While NAA, creatine (Cr) and choline (Cho) may be quantified in this way, metabolites which show multiplet rather than singlet peaks, or short TE acquisitions with more complex spectral patterns benefit from more sophisticated analyses techniques. Early studies tended to report peak areas or heights as ratios to apparently stable metabolites such as Cr. However, Cr concentrations may be altered in disease states (Rooney *et al.*,1997; Suhy *et al.*,2000), and changes with age (discussed below), and as such, the reporting of ratios makes pathological interpretation even more difficult. In order to avoid this, calibrated absolute quantification techniques have been developed. An example of such a method is the Linear Combination Model (LCModel) developed by Provencher (Provencher, 1993). It is a phantom calibrated absolute quantification technique that makes use of previously acquired model spectra from a range of metabolites that it combines using linear scaling to estimate metabolite concentrations. Processing also estimates a spline fitted baseline, to account for

residual water signals and broad peaks not included in the metabolite basis sets, such as lipids.

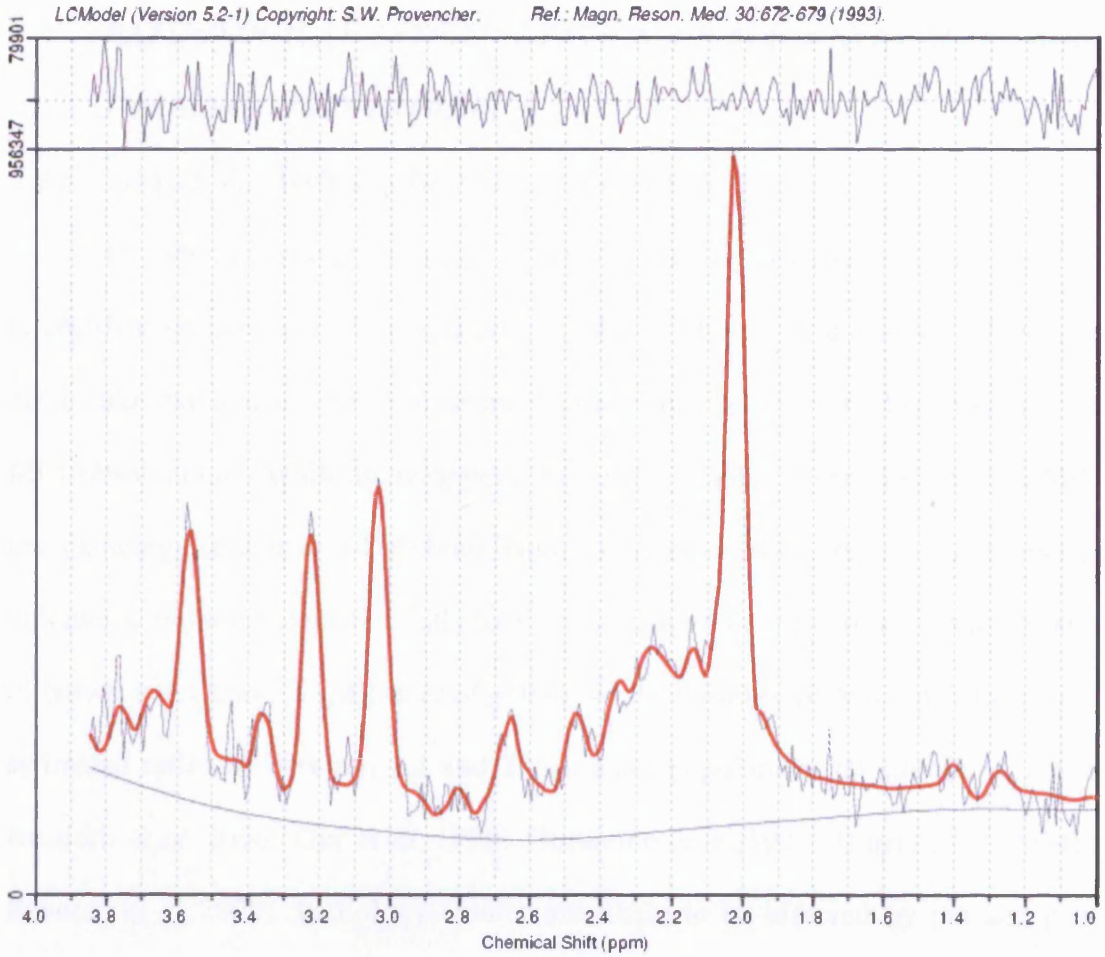

Figure 2.3.2a: Typical output from LCModel. The fitted spectrum (in red) overlays the observed spectrum, below which is the spline fitted baseline. The residual difference between the observed and fitted spectrum is shown above.

2.4 PATHOLOGICAL INTERPRETATION OF MAGNETIC RESONANCE IMAGING OBSERVATIONS

2.4.1 TISSUE VOLUMES IN NORMAL CONTROL SUBJECTS

In order to assess abnormal brain volumes or atrophy, we first need to establish what is normal. Understanding of this is limited by a absence of either a clear gold standard *in vivo* or post mortem measurements with which to calibrate MRI observations. While there appears to be reasonable agreement between MRI and pathology studies on whole brain volumes, assessment of grey and white matter volumes is more problematic. Pathology studies suggest a grey to white matter ratio of between 1.1 and 1.5 (Miller *et al.*,1980), while a variety of MRI measures have estimated ratios of between 1.2 and 2.0 in adult populations (Blatter *et al.*,1995; Brunetti *et al.*,2000; Gur *et al.*,1999; Guttmann *et al.*,1998; Harris *et al.*,1994b; Resnick *et al.*,2000). Pathology studies are likely to be affected by pre and post mortem tissue degeneration, and tissue fixation artefacts that need not homogeneously affect tissues (Messert *et al.*,1972; Miller *et al.*,1980; Yates *et al.*,1975); MRI studies are significantly influenced by differences in scan acquisition and segmentation methodologies. Therefore neither can be considered as offering completely accurate tissue-specific reference values. Given these difficulties establishing validated tissue volumes in quite large regions, it may be expected that smaller structures will be even more problematic.

When looking at the effects of age, gender and disease effects, there are some further issues that need to be addressed: cross-sectional versus longitudinal data;

biological variability; adjustments for intra-cranial volumes; measurement reproducibility; and statistical modelling. Considering these further:

i. Many MRI studies, and by definition all post mortem studies, are cross-sectional and so may be influenced by secular trends i.e. differences between generations of people (Miller and Corsellis, 1977). Longitudinal studies should be less vulnerable to confounding by such trends;

ii. The variability inherent in tissues may differ - one region or tissue may show quite marked inter-subject variability while another may not;

iii. Correction for intra-cranial volumes has been found to reduce the inter-subject variability in brain tissue volumes, yielding measurements apparently more sensitive to age, gender and disease effects. However, the amount of inter-subject variability controlled for by this correction may differ between the tissues or brain regions, so leaving proportionally different amounts of residual variability;

iv. The reproducibility of tissue specific and regional measurements may differ, leading to methodologically related differences in data variability;

v. These factors may in turn influence the apparent magnitude and statistical significance of age, gender and disease effects upon tissue specific or regional volumes. Results derived from modelling of such data should be considered in this context.

It appears that, on average, women have smaller brain volumes than men (the average brain volume being approximately 1400 ml in adult males and approximately 1235 ml in females (estimated using a tissue density figure from

(Miller *et al.*,1980) and brain weights from (Pakkenberg and Gundersen, 1997)), and that this difference is predominantly due to smaller white matter volumes in women with, to a lesser degree, larger grey matter volumes in men (Good *et al.*,2001; Gur *et al.*,1999; Pakkenberg and Gundersen, 1997; Passe *et al.*,1997; Reiss *et al.*,1996; Resnick *et al.*,2000).

In adults, present evidence suggests that ageing effects both grey and white matter at an overall rate of tissue loss of about 0.2 to 0.3% per year (Blatter *et al.*,1995; Brunetti *et al.*,2000; Good *et al.*,2001; Gur *et al.*,1999; Guttmann *et al.*,1998; Harris *et al.*,1994b; Jernigan *et al.*,2001; Lim *et al.*,1992; Meier-Ruge *et al.*,1992; Miller *et al.*,1980; Pakkenberg and Gundersen, 1997; Passe *et al.*,1997; Pfefferbaum *et al.*,1994; Raz *et al.*,1997; Resnick *et al.*,2000). Whether this occurs simultaneously, or whether one tissue predominates over the other for certain periods remains open to debate. A significant number of studies attribute age-related brain atrophy predominantly to grey matter volume loss (Blatter *et al.*,1995; Brunetti *et al.*,2000; Good *et al.*,2001; Gur *et al.*,1999; Lim *et al.*,1992; Passe *et al.*,1997; Pfefferbaum *et al.*,1994; Raz *et al.*,1997). However, a number of studies have suggested that white matter atrophy may be more prominent than grey matter atrophy, most noticeably in those aged 70 and over (Guttmann *et al.*,1998; Jernigan *et al.*,2001; Meier-Ruge *et al.*,1992; Miller *et al.*,1980). A general decline in brain tissue volumes in adults appears to be reflected by increasing ventricular volumes (Blatter *et al.*,1995; Coffey *et al.*,1998; Good *et al.*,2001; Guttmann *et al.*,1998; Jernigan *et al.*,2001; Pfefferbaum *et al.*,1994; Resnick *et al.*,2000) although this may not be prominent in younger adults (Gur *et al.*,1999). These findings suggest that

assumptions of linear changes in brain volume with ageing may not be ideal, particularly in subjects below the age of 20, when brain maturation may still be occurring (Pfefferbaum *et al.*,1994; Reiss *et al.*,1996), and those over the age of 70.

Ageing also appears to show regional variability over and above tissue specific differences (Coffey *et al.*,1992; Good *et al.*,2001; Jernigan *et al.*,2001; Raz *et al.*,1997; Resnick *et al.*,2000), although studies differ in their localisation of this. Significant age-gender interactions have also been observed (Blatter *et al.*,1995; Coffey *et al.*,1998; Good *et al.*,2001; Gur *et al.*,1991; Oguro *et al.*,1998; Xu *et al.*,2000), although the magnitude of this effect may vary between brain regions (Coffey *et al.*,1998; Gur *et al.*,1991; Raz *et al.*,1997; Xu *et al.*,2000). It is also important to note that tissue signal intensity characteristics may also alter with age (Coffey *et al.*,1992; Jernigan *et al.*,2001), and this may influence tissue segmentation, leading to erroneous results.

2.4.2 PATHOLOGICAL SUBSTRATES OF BRAIN TISSUE ATROPHY

Volumetric brain measurements on their own cannot define the intrinsic characteristics of the tissue being quantified (i.e. its cellular composition); this is the realm of other MRI measurements and histopathology studies. However, for a given tissue, they can help to quantify the extent and, in combination with measurements of composition, the magnitude of disease effects.

Studies in normal controls highlight the difficulties associated with interpretation of brain tissue volume measurements. In a post mortem study of previously healthy controls, an age related 9.5% reduction in neuron numbers was mirrored by a 12.4% reduction in neocortical volume and 28.0% reduction in white matter volume (Pakkenberg and Gundersen, 1997). Similarly, a gender related difference in neuron numbers of 15.5% was mirrored by a 14.9% difference in neocortical volume and an 18.1% difference in WM volume. The disparity between neocortical and white matter atrophy suggests that, particularly in white matter, additional factors contribute towards volume loss, and it would appear that glial cell loss may also be a significant factor, particularly in those over 70 years of age (Meier-Ruge *et al.*,1992). However, as noted above, these observations may be influenced by pre and post mortem effects; in particular tissue oedema which may mask underlying tissue atrophy (Messert *et al.*,1972; Yates *et al.*,1975).

In MS studies, it seems reasonable to assume that, with certain caveats, brain tissue atrophy marks neuronal and axonal loss (Miller *et al.*,2002). However, other factors may also influence apparent tissue volume loss and this need not be consistent between tissues. Inflammation associated with oedema and demyelination

is more marked in white matter than grey matter (discussed above) and so may be expected to have more obvious effects upon white matter rather than grey matter volume measures. Oedema may transiently mask atrophy, while demyelination may both directly lead to volume loss and also result in secondary axonal atrophy (Yin *et al.*, 1998).

2.4.3 *PATHOLOGICAL SUBSTRATES OF FOCAL BRAIN LESIONS*

The effects of MS appear to be heterogeneous with relatively focal changes observed both on histopathology and MR examinations. Focal changes are more readily apparent on T_2-weighted MRI than direct inspection of pathology specimens (De Groot *et al.*,2001), while lesion changes are variably visible on MRI.

Image contrast and resolution both appear to alter the discernable lesion load. Considering image contrast first, fast fluid-attenuated inversion-recovery (FLAIR) sequences appear to detect slightly more lesions that T_2-weighted FSE sequences (Tubridy *et al.*,1999). FLAIR acquisitions appear to be significantly more sensitive than T_2-FSE to cortical and subcortical lesions (Bakshi *et al.*,2001; Tubridy *et al.*,1999), although they may be less sensitive to posterior fossa lesions (Tubridy *et al.*,1999) which may negate increased sensitivity elsewhere. Lesions are usually seen as hyper-intensities on such sequences, although as an interesting aside, regional hypo-intensity particularly in the basal ganglia and thalamus has been observed and attributed to iron deposition (Bakshi *et al.*,2000). Focal changes are generally less conspicuous on T_1-weighed images, and are seen as hypo-intensities. T_1 lesions appear to represent a subset of T_2 lesions, and as such ratios between the two may offer an indication of the degree of tissue damage within lesions (McFarland *et al.*,2002).

Focal enhancement on T_1-weighted imaging post intravenous (IV) administration of gadolinium (Gd) is generally accepted as a marker of breakdown in the BBB associated with acute inflammation (Bruck *et al.*,1997; Katz *et al.*,1993). Sensitivity to such changes appears greater when using triple dose Gd (0.3 mmol/kg)

rather than single dose, with about a 70% increase in enhancing lesion counts (Filippi *et al.*,1995; Silver *et al.*,1997). Further, such lesions tend to enhance for less than a month (Silver *et al.*,1999; Tortorella *et al.*,1999), and so the frequency of scanning may affect the adequacy of estimates (Lai *et al.*,1996). Such lesions are more frequently seen on T_2 rather than un-enhanced T_1-weighted images, and they tend to persist on the former while resolving on the latter (Paolillo *et al.*,1999; van Walderveen *et al.*,1999b). Further, enhancing lesion loads tend to correlate more strongly with changing T_2 rather than T_1 lesion loads (van Walderveen *et al.*,1999b). Considered together, this would suggest that T_2, and to a lesser degree, T_1 lesion loads represent accumulated focal inflammation. However, this view is challenged by the observation that Gd-enhancing lesions and T_2 lesions do not show the same spatial probability distributions (Lee *et al.*,1999). While this discrepancy may indeed indicate that T_2 lesions need not show Gd-enhancement at any stage, the possibility of regional variability in the duration of enhancement needs to be explored.

Returning to the issue of image resolution, it has been noted that decreasing slice thickness may improve lesion identification by reducing partial volume effects (Filippi *et al.*,1998c; Molyneux *et al.*,1998b), although this may have little effect on the relationship between lesion loads and clinical outcomes (Rovaris *et al.*,1998b).

T_2 and T_1 lesions may have differing pathological weighting and thus specificity. While both may be influenced by extracellular oedema, demyelination and axonal loss, T_1 hypo-intense lesions tend to be weighted towards axonal loss in chronically affected MS lesions rather than acute inflammatory activity (De Groot *et al.*,2001; van Waesberghe *et al.*,1999; van Walderveen *et al.*,1998a; van Walderveen

et al.,1998b) while new T_2-weighted lesions would appear to be, in part, related to acute inflammatory changes (Lee *et al.*,1998), although an appreciable proportion of acute lesions display T_1 hypointensity that resolves over several months (Minneboo *et al.*,2005). Correlations between disability, as assessed by EDSS, and lesion loads appear to be greater for T_1 rather than T_2 lesion loads (McFarland *et al.*,2002).

2.4.4 TISSUE METABOLITE CONCENTRATIONS IN NORMAL CONTROL SUBJECTS

It is difficult to directly compare studies estimating tissue specific metabolite concentrations due to significant differences in the methodologies used to identify tissues and quantify metabolites. Further, there are considerable differences in data presentation, with results given as ratios to Cr or Cho, in institutional units, or mmol/l. Given this, only broad qualitative comparisons can be made. There are a reasonable number of studies looking at the relative concentrations of Cr, Cho and NAA in GM and WM, with somewhat fewer measuring Ins and Glx (see Table 2.4.4a). Overlying tissue specific differences there may also be regional differences within given tissue types. While a number of studies have looked for regional effects without allowing for potential tissue specific differences, one study did (Wiedermann *et al.*,2001), producing results that suggest higher concentrations of Cr, NAA and Ins, and lower concentrations of Cho when comparing frontal and parietal lobe GM. Histopathology studies exploring tissue specific metabolite concentrations have been limited: Petroff and colleagues (1989) found that the anterolateral temporal lobe GM contained more Cr, NAA and Glu than the underlying WM, although such differences were not observed in other GM regions.

Study	GM to WM metabolite ratio				
	Cho	Cr	Glx	Ins	NAA
Soher *et al.* 1996	0.9	1.2	ND	ND	0.9
Chang *et al.* 1996	1.0	1.2	ND	1.0	1.2
Wang *et al.* 1998	1.2	1.9	ND	ND	1.5
Pan *et al.* 1998	0.9	1.4	ND	ND	0.8
Pfefferbaum *et al.* 1999	0.8	2.0	ND	ND	1.3
Noworolski *et al.* 1999	0.8	1.4	ND	ND	1.3
Chang *et al.* 1999	1.4	1.3	1.6	1.2	1.2
Saunders *et al.* 1999	0.7	1.2	ND	1.1	1.1
Lundbom *et al.* 1999	0.8	1.3	ND	ND	0.7
McLean *et al.* 2000	0.9	1.7	2.4	1.6	1.2
Wiedermann *et al.* 2001	0.5	1.1	ND	0.9	0.9
Schuff *et al.* 2001	1.7	1.8	ND	ND	1.6

Table 2.4.4a: Grey to white matter metabolite ratios.

Age and gender effects may also be present. However, it should be recalled that the resolution of ^{1}H-MRS techniques are limited and so the volumes sampled are generally composites of WM, GM and other tissues, along with variable amounts of CSF. Factors affecting the regional distribution of these tissues, such as age and gender (see section 2.1.4), may confound results by altering the contents of apparently tissue specific voxels.

Acknowledging these limitations, there seems to be a relatively consistent trend towards increasing Cr and Cho with age in WM, while age effects on Ins, NAA and Glx are more mixed (Leary *et al.*,2000; Pfefferbaum *et al.*,1999; Schuff *et al.*,2001; Soher *et al.*,1996).

It has been suggested that increasing Cho and Cr may mirror decreasing brain water contents with age (Chang *et al.*,1996), and such hydration effects may offset age-related changes in other metabolites associated with cell loss. Gender differences have not been extensively explored but may also be present (Grachev and Apkarian, 2000).

2.4.5 *PATHOLOGICAL SUBSTRATES OF ALTERATIONS IN TISSUE METABOLITE CONCENTRATIONS*

While measurement of metabolite concentrations does provide some useful insight in cell densities and cellular metabolic activity, disentangling these two components have proven difficult. By combining information from a variety of concurrently estimated metabolite concentrations, we can begin to consider the interplay between metabolic turnover and cellular density, although it is presently not possible to derive pure estimates of either.

Creatine

The Cr peaks (main peak 3.0 ppm) in ^{1}H-MRSI include contributions from both creatine and phosphocreatine (Miller, 1991). Phosphocreatine serves as a high-energy phosphate donor, and through creatine kinase (CK) activity maintains adenosine-triphosphate (ATP) concentrations (Wyss and Kaddurah-Daouk, 2000). Cr concentration in the brain appears to be linked to CK activity and thus energy metabolism. Concentrations seem to be higher in GM than WM, mirroring ATP turnover (Wyss and Kaddurah-Daouk, 2000). Given this, Cr appears to mark energy flux in the brain, and this will be a function of both cellular density and metabolic activity.

Choline

The Cho peak (main peak 3.2 ppm) consists predominantly of phosphoryl-choline (PC) and glycero-phosphoryl-choline (GPC), although phosphoryl-ethanolamine (PE) and glycero-phosphoryl-ethanolamine (GPE), and in certain disease conditions, free choline may also contribute towards the measured signal

(Bluml *et al.*,1999). These choline containing compounds are mostly precursors or degradation products of cell membrane phosphatidyl-choline, which does not directly contribute significantly to the Cho peak due to its immobility. ^{1}H-MRSI observable Cho appears to mark membrane turnover, of which there will be elements related to normal cellular function and cellular degradation (Boulanger *et al.*,2000). Concentrations vary dependent on the degree and activity of myelination and demyelination (Bluml *et al.*,1999). In MS, increases have been directly linked to glial proliferation (Bitsch *et al.*,1999).

Inositol

The Ins peak (main peak 3.6 ppm) marks myo-inositol, which is synthesised from recycling of inositol-phospholipids and *de novo* from glucose-6-phosphate. Free inositol appears to have a role in intra-cellular osmoregulation, and in the synthesis of second messengers (Lubrich *et al.*,2000). It is particularly concentrated in glial cells when compared with neurons (Brand *et al.*,1993; Glanville *et al.*,1989) and appear to be higher in astrocytes when compared with oligodendrocytes (Urenjak *et al.*,1993) or oligodendrocyte type 2 astrocyte (O2A) progenitors (Griffin *et al.*,2002c). In MS a combined ^{1}H-MRS and histopathological study has shown it to be a marker of glial proliferation (Bitsch *et al.*,1999).

N-acetyl-aspartate

The tNAA peaks (main peak 2.0 ppm) comprise both N-acetyl-aspartate (NAA) and N-acetyl-aspartyl-glutamate (NAAG). NAA is predominantly localized to neurons in the adult CNS (Simmons *et al.*,1991), although it may also be found in mature oligodendrocytes (Bhakoo and Pearce, 2000) and O2A progenitors (Urenjak

et al.,1992). Its function remains unclear. It is synthesised primarily in neurons (Baslow, 2000), although its almost complete absence is compatible with neuronal survival (Martin *et al.*,2001). There is evidence to suggest that it may be related to myelin formation or maintenance or both (Chakraborty *et al.*,2001), but this remains to be clarified. NAAG is synthesised from NAA, and appears to have a role as neurotransmitter (Neale *et al.*,2000). Changes in NAA levels may be transient and related to mitochondrial metabolic dysfunction (Demougeot *et al.*,2001; Mader *et al.*,2000; Narayana *et al.*,1998) although it has been confirmed as a marker of axonal density in MS lesions (Bitsch *et al.*,1999), mature WM tracts (Bjartmar *et al.*,2002), and the spinal cord (Bjartmar *et al.*,2000).

Glutamate and glutamine

Glutamine is synthesised in astrocytes predominantly from cycling of glutamate, a major excitatory neurotransmitter, and this process appears to be tightly linked to glucose metabolism (Rothman *et al.*,1999). Thus, like Cr, alterations in apparent Glx concentrations may be related to neuronal and glial cellular density and metabolic activity.

2.5 *FACTORS INFLUENCING DATA PROCESSING AND INTERPRETATION*

In order to effectively and realistically interpret the results of measurements, it is necessary to know something of the characteristics of the measurement techniques employed. We need to know that a measure is a valid representation of the property we wish to assess, that the measurement technique is reliable (precise, reproducible) and, preferably, that it is accurate. These concerns apply equally to the MRI and clinical measures, and this should be recalled when interpreting results.

Measurement error may be decomposed into a bias or systematic error, the difference between the true value and that estimated by the measurement technique, and subject error, the random variability due to errors in data acquisition and entry. This may be summarised as:

$$X_i = T_i + b + E_i$$

where X_i is the observed measure in subject i, T_i is the true value in subject i, b is the bias in the measurement, and E_i is the subject error (an estimate of precision) (Armstrong *et al.*,1992). Some authors use the term accuracy to include both b and E_i, while others restrict its use to b alone.

Precision

The precision of a measure refers to observation variability about a true value as assessed using that measure. In clinical studies, this usually involves repeated measures in a group of subjects. Variability in the resultant measures will then relate both to inter-subject factors such as age and gender effects, and intra-subject factors

such as random biological variability in the parameter being estimated and measurement errors.

Reliability (reproducibility) may be presented in a variety of ways. It may be given as within-subject (intra-subject) standard deviations (SD) (Bland and Altman, 1996c); as repeatability, which is the 95% limit for the difference between two replicate measures, calculated as $\sqrt{2} \times 1.96 \times$ within-subject SD (Bland and Altman, 1996c); as a coefficient of variation (CV), a dimensionless estimate of variability calculated as the within-subject SD divided mean parameter values (Bland and Altman, 1996b); and as a reliability coefficient (RC), defined as the ratio of between-subject variances to total variance (also known as the intra-class correlation coefficient [ICC]) (Bland and Altman, 1996a).

The concept of partitioning variability to within and between-subject components may be extended to further refine estimates of the sources of this variability. Data from appropriately designed experiments, interrogated using variance components analysis (Tedeschi *et al.*,1996), allows this. For example within-subject measurement variability of an MR measure may involve both random repositioning and intrinsic measurement errors. By repeating measures with and without repositioning in the same subjects, the relative magnitude of these effects may be ascertained.

Sensitivity and power

Related to the precision of a measure is its sensitivity to change with time and differences between groups. Using estimates of measurement error, an estimate of the cohort sizes required to be able to detect a defined difference with a defined

probability may be made. In order to be able to detect a difference d at a $P<0.05$ level 90% of the time, the size of the cohort required, n, may be approximated by:

$$n = \left(2 \times SD_w^{\ 2}\right) \times \left(\frac{3.24}{d}\right)^2$$

where SD_w represents within-subject SD (Bland, 1987). Such an estimate may be useful when interpreting results from various measurement techniques.

Bias and calibration

The bias of a measurement refers to its systematic relationship to a true value. This may be observable when a gold standard technique is available, or unobservable when one is not. Given the absence of such standards, many MRI measures may be considered at best methodologically accurate, i.e. yield consistent results when applied to the same sample when independently implemented. This means that absolute values derived from various techniques may not be considered equivalent, and while conclusions from previous studies may be used to inform interpretation of data, raw results should not be directly compared.

In order to improve methodological accuracy, measures may be calibrated using samples with known characteristics. Such calibration experiments serve two purposes: they enable some degree of objective *in vitro* accuracy to be established; and as part of quality assurance, they allow the temporal stability of measurements to be assessed and fluctuations adjusted for. Such experiments are critical in longitudinal studies, particularly when there is an alteration in the scanner hardware and or software due to component failure, preventative maintenance, or an upgrade.

Differential measurement error

Measurement errors may not be the same in two groups, and if not treated appropriately this may lead to both ablation of genuine differences and the introduction of artefactual differences. Differential subject errors will tend to obscure relationships, while differential biases may have mixed effects. Biases may also be related to a confounding factor, for example estimates of brain tissue volumes may be altered systematically by the presence of focal lesions. Careful consideration should be given to the potential for such effects and their impact upon any conclusions drawn from a study.

Validation

Validation of a measure ideally employs a gold standard against which the technique under investigation is compared. However, in many instances MRI measures are the only way to assess a parameter *in vivo*, offering no absolute measure of the property they purport to quantify. In such circumstances, validity may still be explored; under certain circumstances it has been shown that the square root of the RC estimates the correlation between the observed measure and the true value of the parameter, and so in the absence of a gold standard, an estimate of the validity of the measure may still be obtained (Armstrong *et al.*,1992). This parameter is referred to as the validity coefficient (VC).

However, establishing how closely observations relate to a true measure when there is no gold standard, does not tell what is represented by the true measure. In this situation, construct validity needs to be considered. This takes evidence from other sources, and constructs hypotheses that can be tested to confirm that the

measure assesses what it is supposed to. Taking as an example the validation of the EDSS by Hobart *et al.* (2000), they postulated that if this was a measure of disability then correlations with other measures of disability would be high while those with measures of handicap would be low, that such correlations will be predictably ranked, and that there should be no correlations with age.

Measurement purity

MR parameters may be influenced by a variety of factors, and thus when considering their validity we need to be very clear what we expect them to measure, and where the measurement ends and interpretation of the results begin. For example, a valid measure of brain tissue volume measures may not be directly assumed to be an equally valid measure of brain neuronal populations, although it may be interpreted in such terms.

Attenuation

Random errors will tend to attenuate the strength of relationships between parameters and thus limit the maximum strength of observable associations. An estimate of this attenuation may be obtained by from the reliabilities (Armstrong *et al.*,1992). Thus:

$$\beta_O = \beta_T \sqrt{\rho_{TX_1} \rho_{TX_2}}$$

where β_O is the observed correlation between two measurements X_1 and X_2, β_T is the true correlation, and ρ_{TX_1} and ρ_{TX_2} are the reliability coefficients of the measurements. For example an inter-rater ICC for EDSS has been estimated at 0.78 (Hobart *et al.*,2000), while for T_2 lesion loads, an intra-rater ICC of 1.00 has been

estimated (Molyneux *et al.*,1998a). Assuming a perfect relationship between EDSS and T_2 lesion load, it may be expected that the maximum observable correlation would be attenuated to around 0.78.

Confounding factors

Factors that may spuriously influence our results are termed confounders. For example, we may wish to look for gender effects (strictly speaking we should say sex effects, although it is rare for sex to be objectively confirmed in studies not directly addressing sex-specific features) in a given parameter. However, if we do not consider age, and there is a significant age imbalance between males and females, apparent gender effects may be confounded by age and so be incorrectly quantified.

Data models

Given this, the complexity of the data should dictate the complexity of the models used to extract information from them. A frequently employed technique is multiple linear regression, a subset of general linear modelling. This allows the simultaneous assessment of a variety of factors, both continuous covariates such as age, and categorical variables such as gender or disease type. Such models may be constructed in a variety of ways, and there are no clearly established methods for defining what is and is not optimal (Freund and Wilson, 1998). Prior information, be this from logical deduction or evidence from other studies, combined with clear definitions of the questions to be answered, should be used to inform initial model design. Models may subsequently be refined, as dictated by initial findings, to yield results robust to confounding factors.

It could be argued that such data modelling lacks objectivity and that simple statistics such as a t-test should be consistently employed. However, such an approach is still effectively modelling the data, albeit using a very simple model, and as such is just as open to accusations of subjectivity, and perhaps more open to questions of confounding. Given this, a pragmatic approach to data modelling would counsel the use of the simplest model that adequately explains non-random variability.

Data interpretation

It is sobering to recall that P stands for probability in statistical tests and values of 1 or 0 (absolute certainty) are generally not seen. Results may be wrong, indeed the conventionally accepted significance level of $P<0.05$ accepts that 1 in 20 times the conclusions drawn from a single test will be incorrect. Further, in a given study, as the number of statistical comparisons undertaken increases, so does the likelihood that there will be a result spuriously reaching significance; if 10 independent comparisons are undertaken, the probability of one or more falsely significant results is 0.40, with 20 comparisons it is 0.64 (Bland, 1987). This counsels a cautious approach to interpretation of derived results, with multiple sources being drawn upon to increase confidence.

3 MEASUREMENT CHARACTERISTICS

3.1 MAGNETIC RESONANCE DATA ACQUIRED AND PROCESSING TECHNIQUES EMPLOYED

All scans included in this work were acquired using General Electric Signa 1.5 T systems (General Electric Medical Systems, Milwaukee, WI, USA) and a standard quadrature head coil.

3.1.1 STRUCTURAL IMAGING, TISSUE SEGMENTATION AND VOLUME MEASUREMENTS

Scan acquisition

Volumetric imaging utilised an inversion recovery prepared three-dimensional fast spoiled gradient recalled (3D FSPGR) scan (TR 13.3 ms, TE 4.2 ms, inversion time 450 ms, matrix 160 * 256 interpolated to a matrix of 192 * 256, field of view 225 * 300 mm, final in plane resolution 1.2 mm by 1.2 mm, with 124 1.5 mm slices covering the whole brain). All data-sets were orientated with the axes of the imaging volume coincidental to the axes of the scanner gradients. Axial reconstructions were used for all processing and analyses.

During a separate scanning sessions, dual echo fast spin echo (FSE) sequences (TR 2000 ms, effective TE 19/95 ms, NEX 2, in plane resolution 0.9 mm by 0.9 mm with 28 x 5 mm slices covering the whole brain) and T_1-weighted spin echo sequences (TR 540 ms, TE 20 ms, NEX 1, in plane resolution 0.9 mm by 0.9 mm with 28 x 5 mm slices covering the whole brain) were acquired in all subjects. In MS subjects only, the latter was also acquired 20 minutes post IV Gd administration (0.3 mmol per kg body weight of Magnevist [Schering AG, Berlin, Germany]). The

FSE was used to confirm the presence of lesions identified on the 3D FSPGR and derived T_2 lesion loads, while the T_1-weighted images were used to determine T_1-hypointense and Gd-enhancing lesion loads.

Tissue segmentation

The 3D FSPGR were automatically segmented into images representing the probability of any given voxel containing GM, WM, cerebrospinal fluid (CSF) and other tissues using SPM99 (Wellcome Department of Cognitive Neurology, Institute of Neurology, Queen Square, London) (Ashburner and Friston, 2000) with, unless otherwise specified, maximum image inhomogeneity correction applied. The SPM99 segmentation methodology employed a mixed model cluster analysis incorporating tissue intensity information and tissue spatial distribution prior probabilities in the form of the Montreal Neurological Institute ICBM152 template (Montreal Neurological Institute, Montreal, Quebec, Canada) and iteratively optimising tissue definition while correcting for image non-uniformity (Sled *et al.*,1998).

Lesion segmentation

In MS subjects, lesions were segmented from the 3D FSPGR using a semi-automatic local thresholding technique, part of the DispImage image display package (Plummer, Department of Medical Physics & Bioengineering, University College London Hospitals NHS Trust, London, UK) (Plummer, 1992). Lesions were seen as hypo-intensities on this sequence; their presence was confirmed by reference to the proton-density PD weighted FSE images, where they appeared as hyper-intensities. Lesions were also segmented using the same technique applied to the proton-density weighted FSE images and T_1-weighted pre- and post-gadolinium enhanced images,

which provided T_2, T_1 hypo-intense and Gd-enhancing total lesion volumes (loads) respectively.

Volume determination

The spinal cord cut-off location, used to exclude cord from the brain tissue volume estimations, was determined visually on the 3D FSPGR image as the most rostral slice not containing cerebellum. The outputs from SPM99 and 3D FSPGR lesion segmentations were processed using in-house software, which took account of the user specified cord cut-off level, to quantify tissue volumes. The lesion mask over-rode all SPM99 tissue classifications; otherwise a voxel was classified as GM, WM, CSF or other tissue dependent on which mask had the greatest probability (maximum likelihood) at that location. This generated mutually exclusive masks for each tissue i.e. a given voxel was partitioned to one mask only. Results were assessed as fractions of total intra-cranial (TI) volume as determined by adding the GM, WM, lesion and CSF volumes. Brain parenchymal fraction (BPF) was calculated as GM, WM plus lesion volume divided by TI volume. White matter fraction (WMF) was calculated as WM plus lesion volumes (virtually all lesions were located in the WM) divided by TI volume. The grey matter fraction (GMF) was calculated as the GM volume divided by the TI volume. The lesion fraction (LF) was calculated as the lesion volume over the TI volume.

3.1.2 *PROTON MAGNETIC RESONANCE SPECTROSCOPIC IMAGING AND METABOLITE QUANTIFICATION*

Scan acquisition

For all spectroscopic examinations, a 3D FSPGR (see section 3.1.1) was acquired first and used to localise the spectroscopic volume. The plane of the excitation volume for ^{1}H-MRSI scan acquisition was pure axial (orthogonal to the scanner axes), and was immediately superior to the roof of the lateral ventricles. The ^{1}H-MRSI scans were acquired using a point resolved spectroscopic (PRESS) localization scheme (TE 30 ms, TR 3000 ms, NEX 1, 24 * 24 phase encodes over a 300 * 300 mm field of view, slice thickness 15 mm, spectral width 2500 Hz, 2048 complex points), with outer-volume suppression bands contiguous with the edges of the PRESS selected volume in all three dimensions. The anterior to posterior and left to right dimensions of the outer-volume suppression bands matched those of the PRESS selected volume, which varied from subject to subject. Automated pre-scanning optimised the shim, water suppression, and set both transmitter and receiver gains (Webb *et al.*,1994).

Metabolite quantification

Spectroscopy pre-processing was performed using SAGE 7.0 (General Electric Medical Systems, Milwaukee, Wisconsin, USA). Grids of voxels with individual voxel dimensions 12.5 mm * 12.5 mm * 15.0 mm (2.3 mL) were automatically extracted and passed to LCModel (version 5.2) (Provencher, 1993) for metabolite quantification in mmol/L. Metabolite concentrations estimated were: choline containing compounds (Cho); creatine and phosphocreatine (Cr), myo-

inositol (Ins), N-acetyl-aspartate (NAA) plus N-acetyl-aspartyl-glutamate (together designated tNAA), and glutamate plus glutamine (Glx). GM, NAWM, cerebrospinal fluid (CSF) and lesion masks were derived from the 3D FSPGR images as described in section 3.1.1. These masks were used to quantify the tissue contents for each ^{1}H-MRSI voxel. ^{1}H-MRSI voxels were excluded from further analysis if they were not entirely within the PRESS excitation volume.

3.2 *WHOLE BRAIN, GREY AND WHITE MATTER VOLUME ESTIMATES*

Introduction

Understanding the components of measurement variability, and factors contributing to this, enable more realistic interpretation of results. With this in mind, the study described here was designed to: estimate the reliability of the brain tissue volume measures employed in this thesis; decompose the elements of inter- subject variability in terms of previously observed age and gender effects; consider the potential for differential measurement error associated with focal white matter lesions; and consider the validity of these measures as estimates of brain tissue volumes. Previous work has suggested that image non-uniformity corrections are of benefit when assessing tissue volumes (Arnold *et al.*,2001) and that adjustments for intra-cranial volumes reduce inter-subject variability (Blatter *et al.*,1995; Mathalon *et al.*,1993; Whitwell *et al.*,2001). This study also explored the effects an image non-uniformity correction has upon the resultant tissue segmentations and their reliability, and whether adjustment for intra-cranial volume does or does not improve sensitivity to known age and gender effects.

In the absence of gold standards for *in vivo* brain tissue volumes, validity was assessed in terms of consistency with observations from previous MRI and histopathology work.

Materials and methods

Subjects

The data came from a cohort of 29 normal control subjects (16 females and 13 males, mean age 36.6 years at first scan, median 33.5, range 23.2 to 55.2) with no

history of neurological disease or other medical conditions. A subset of the subjects underwent multiple scans to assess the method's reproducibility and this is described in detail below. This project had approval from the ethics committee of the National Hospital for Neurology and Neurosurgery, Queen Square, London, UK. All subjects gave informed consent.

Scan Acquisition

3D FSPGR scans, as described in section 3.1.1, were acquired in all subjects.

Segmentation and volume determination

The 3D FSPGR images were processed as outlined in section 3.1.1, except when assessing the effects of image inhomogeneity correction (see below), when images were processed with and without this adjustment.

Inhomogeneity correction

SPM99 includes an option to include a step that attempts to correct for the effect of B_1-field non-uniformity, which may otherwise lead to artefactual image intensity gradients. The method employed aims to correct for low spatial frequency image non-uniformity by estimating tissue specific intensity profiles (peaks) and iteratively estimating a non-uniformity field correction that effectively minimizes peak width (Ashburner and Friston, 2000). The effect of this correction was tested on 8 normal control subjects (5 males and 3 females) who had three scans, each pair separated by an average of 191 days (median 193, range 141 to 215 days). RC and CV were calculated for all parameters derived from these images with and without the correction.

Effect of delayed re-scanning

The delay in scanning meant that there was a chance that genuine volume changes could have occurred over this time, for example due to ageing (see section 2.4.1) or hydration effects (Walters *et al.*,2001). In order to estimate an upper limit for the reproducibility of the measurements, three subjects underwent three scans on the same day, with repositioning between scans; images from this subgroup were processed with inhomogeneity correction.

Susceptibility to focal white matter abnormalities

In a single subject, the effects of artificially added white matter lesions upon segmentation were assessed. Using tools within the DispImage image display package (Plummer, Department of Medical Physics & Bioengineering, University College London Hospitals NHS Trust, London, UK) (Plummer, 1992), a series of ovoid regions within white matter, each circa 0.25 ml in volume, extending over multiple slices, were set to a fixed intensity to simulate the presence of lesions. Two main characteristics of white matter lesions may influence segmentation: total lesion volume and lesion intensity. Variable lesion volumes were simulated by adding greater numbers of artificial lesions to the test image. The total lesion volume ranged from 3 to 24 ml and the intensity was set to that estimated to be halfway between white matter and CSF. Lesion intensity effects were assessed using a fixed total lesion volume of 12 ml. Five intensity levels were tested: that of CSF; that of white matter; and three evenly spaced intervals in between.

The artificial lesion mask generated using DispImage was employed to define which voxels lay within lesion regions. Lesion intensity and volume effects were assessed with and without this reclassification of such lesion regions as white matter.

Statistical analyses

RC and CV were estimated as outlined in section 2.5, using variance estimates from restricted estimate of maximum likelihood (REML) variance components models (Scheffe, 1959; Tedeschi *et al.*,1996). The model included subject as a random factor with all other variability partitioned to the error term.

The effects of age and gender on TI, BP, GM, WM, BPF, GMF and WMF volumes in normal control subjects were investigated using multiple linear regression models with gender as a categorical (fixed) factor, age (in days) as a continuous covariate, and an age-gender interaction term.

Results

The RC were generally in excess of 90% and this is reflected in correspondingly low CV (Table 3.2a and Figure 3.2a), suggesting that measurement errors contribute little to observed tissue variability. The image non-uniformity correction had little discernable effect upon RC and CV, although inspection of the resultant segmentations revealed clearly sharper tissue differentiation in the cerebellum, basal ganglia and thalamus (Figure 3.2b, 3.2c and 3.2d) when the correction was applied. Image non-uniformity correction also tended to increase the average TI volumes, and increase the volume of GM at the expense of WM (Table 3.2b).

At a $P<0.05$ level, WM and BP volumes differed significantly between genders but the other absolute volume measures did not. BPF did not significantly differ with gender, whilst both GMF and WMF did (Tables 3.2c, 3.2d and 3.2e).

Statistical modelling of this cross-sectional data revealed that overall BPF and GMF decreased significantly with age, whereas BP and GM volumes only reached borderline significance (Tables 3.2d and 3.2e, and Figure 3.2e). Excluding interactions between age and gender, the parameter estimate for yearly change in BPF was -0.002, -0.3% proportional to the mean value in the cohort (95% confidence interval [CI] -0.003 to -0.001, $P<0.001$, model R^2 0.599); for GMF was -0.002, -0.3% (CI -0.003 to -0.001, $P<0.001$, model R^2 0.512); for WMF was -0.001, -0.1% (CI -0.001 to 0.000, $P=0.172$, model R^2 0.183); for TI volume was 0.4, 0.0% (CI -3.9 to 4.8, $P=0.840$, model R^2 0.430); for BP volume was-2.7, -0.2% (CI -5.8 to 0.3, $P=0.079$, model R^2 0.545); for GM volume -2.2, -0.3% (CI -4.2 to -0.2, $P=0.031$, model R^2 0.499); and for WM volume was -0.5, -0.1% (CI -1.9 to 0.8, $P=0.477$, model R^2 0.498). Interactions between gender and age were significant for WM, and WMF, and of borderline significance for GMF (Tables 3.2d and 3.2e).

The effects of artificial WM lesions appear limited when set in the context of age related changes in fractional tissue volumes (Figures 3.2f, and 3.2g compared with 3.2e). Further, volumes corrected for lesion misclassification show only modest deviations from lesion free values, despite lesion intensities set to that of CSF and lesion volumes greater than 20 ml.

Re-scan delay (days)	InHC	Reliability coefficients, coefficients of variation (%) and within-subject SD						
		Absolute volume				Fractional volumes		
		TI	BP	GM	WM	BPF	GMF	WMF
190[a]	Yes	0.993, 1.2, 16.7	0.991, 1.1, 12.6	0.986, 1.3, 9.9	0.991, 1.1, 4.4	0.936, 1.0, 0.007	0.934, 1.1, 0.006	0.925, 1.2, 0.003
190[a]	No	0.993, 1.3, 16.8	0.994, 0.9, 10.0	0.990, 1.1, 7.9	0.993, 1.0, 4.2	0.939, 0.9, 0.007	0.958, 0.8, 0.005	0.868, 1.3, 0.004
0[b]	Yes	0.998, 0.2, 3.5	0.997, 0.2, 3.1	0.966, 0.6, 5.2	0.990, 0.9, 3.7	0.963, 0.2, 0.002	0.896, 0.6, 0.003	0.975, 0.8, 0.002

Table 3.2a: Reliability coefficients, coefficients of variation and within-subject SD for absolute and fractional tissue volumes quantified using tissue segmentations from SPM99 with and without image inhomogeneity correction (InHC) applied to data from 8 subjects imaged on 3 occasions a mean of 191 days apart, and with image inhomogeneity correction applied to data from 3 subjects imaged 3 times on the same day. [a] 8 subjects; [b] 3 subjects .

Image InHC	Absolute volume (ml)				Fraction		
	TI	BP	GM	WM	BPF	GMF	WMF
Yes	1360.5, 1319.1, 1170.9 to 1759.7	1135.7, 1098.9, 1017.4 to 1379.8	748.4, 716.0, 682.6 to 906.8	387.2, 382.9, 334.3 to 473.0	0.84, 0.84, 0.78 to 0.87	0.55, 0.55, 0.52 to 0.58	0.29, 0.29, 0.27 to 0.30
No	1341.3, 1296.6, 1156.4 to 1733.0	1137.8, 1099.5, 1020.7 to 1390.5	730.7, 698.8, 668.2 to 889.9	407.1, 400.7, 352.1 to 500.6	0.85, 0.85, 0.80 to 0.88	0.55, 0.55, 0.51 to 0.58	0.30, 0.30, 0.29 to 0.32

Table 3.2b: Mean, median, and range of absolute and fractional tissue volumes from baseline scans in 8 subjects with and without image inhomogeneity correction (InHC).

Gender	Tissue volume (ml)				Tissue fraction		
	TI	BP	GM	WM	BPF	GMF	WMF
Male	1441.0, 1404.3, 1284.3 to 1759.8	1208.1, 1186.9, 1065.7 to 1379.8	794.2, 804.6, 714.3 to 906.8	413.9, 407.5, 337.6 to 478.5	0.84, 0.85, 0.78 to 0.87	0.55, 0.55, 0.52 to 0.57	0.29, 0.28, 0.26 to 0.32
Female	1264.2, 1262.8, 1109.8 to 1389.5	1060.6, 1056.7, 916.7 to 1169.4	710.4, 710.8, 614.6 to 795.8	350.1, 349.6, 301.7 to 404.7	0.84, 0.85, 0.78 to 0.87	0.56, 0.57, 0.51 to 0.60	0.28, 0.28, 0.25 to 0.30

Table 3.2c: Mean, median and range of absolute and fractional tissue volumes by gender in normal control subjects estimated from inhomogeneity corrected images. Results are from 13 males (mean age at scanning 36.3 years, median 32.3, range 27.2 to 52.7) and 16 females (mean age at scanning 36.9 years, median 33.5, range 23.2 to 55.2).

Measure	Factor			
	Gender	Age - males	Age - females	Age*gender
BPF	0.009 (1.1%), -0.050 to 0.068, 0.754	-0.002 (-0.3%), -0.003 to -0.001, 0.002	-0.002 (-0.3%), -0.003 to -0.001, <0.001	0.789
GMF	0.072 (12.9%), 0.017 to 0.126, 0.013	-0.001 (-0.1%), -0.002 to 0.000, 0.173	-0.002 (-0.4%), -0.003 to -0.002, <0.001	0.030
WMF	-0.063 (22.2%), -0.105 to -0.020, 0.005	-0.001 (-0.5%), -0.002 to -0.000, 0.006	0.000 (0.0%), -0.001 to 0.001, 0.735	0.015

Table 3.2d: Parameter estimates (% compared to the mean value for all subjects), 95% confidence limits and P values for the effects of gender, age (estimated to the nearest day but presented as change per year) on absolute tissue volumes. Gender parameters compare females with males. Age*gender gives the estimates significance of the difference in age effects between genders. Model R^2: BPF 0.600; GMF 0.597; WMF 0.359.

Measure	Factor			
	Gender	Age - males	Age - females	Age*gender
TI	-325.5 (24.1%), -667.2 to 16.2, 0.061	-2.2 (-0.2%), -9.4 to 5.1, 0.546	1.9 (0.2%), -3.6 to 7.4, 0.479	0.365
GM	-96.4 (-12.8%), -256.6 to 63.7, 0.226	-2.5 (-0.3), -5.9 to 0.9, 0.147	-2.1 (-0.3), -4.7 to 0.5, 0.106	0.034
WM	-178.3(46.7%), -277.3 to -79.2, 0.001	-2.5 (-0.7%), -4.6 to -0.4, 0.022	0.7 (0.2%), -0.9 to 2.2, 0.400	0.021

Table 3.2e: Parameter estimates (% compared to the mean value for all subjects), 95% confidence limits and P values for the effects of gender, age (estimated to the nearest day but presented as change per year) on fractional tissue volumes. Gender parameters compare females with males. Age*gender gives the estimates significance of the difference in age effects between genders. Model R^2: TI 0.449; BP 0.568; GM 0.500; WM 0.596.

Discussion

Reliability

The reliability figures suggest that over 90% of variability in tissue volumes obtained from non-uniformity corrected images is attributable to inter-subject factors. This is reflected in the correspondingly low CV values.

The use of a non-uniformity correction appears to have a limited effect upon the reliability of tissue segmentations, although inspection of the resultant images suggests greater clarity in the definition of cerebellum, basal ganglia and thalami, with a consequent increase in GM tissue volumes. However, anecdotal evidence would suggest that its most marked effect is a reduction in gross segmentation errors, particularly in the presence of significant tissue abnormality (Figure 3.2h). This is a rather extreme example of segmentation failure, and even when processed with the inhomogeneity correction would be deemed unsuitable due to the significant residual non-brain material included in the grey matter segments. The use of such a correction is supported by previous work looking at the effects upon tissue segmentation, although direct comparisons between techniques have been limited and do not necessarily address the effects they may have upon derived measures (Arnold *et al.*,2001).

RC and CV figures do not appear to be greatly influenced by the delay between scans, although the CV are consistently lower in the group scanned on a single day when compared with those scanned over a year. The difference in CV may be explained by biological factors such as age related changes and hydration effects (Walters *et al.*,2001), and scanner scaling effects.

Age and gender effects upon tissue volumes

The cross-sectional age trends revealed in this study indicate that while, in absolute terms, volume variation with age only reached borderline significance for BP and GM, as fractions of total intra-cranial volumes all measures were clearly significant. More specifically, BPF fell with age and, in the age range studied; this was predominantly due to GM rather than WM tissue loss. These are consistent with previous work (see section 2.4.1).

Looking at the gender effects seen, WM but not GM volumes differed significantly between males and females, in agreement with previous findings, but after correction for intra-cranial volume the proportions of GM and WM were both found to be significantly different (Tables 3.2d and 3.2e). These are consistent with previous work (see section 2.4.1).

Interactions between age and gender (differences in the degree of tissue loss with age between genders) appeared to be significant for WM (both as an absolute and fractional measure) and GMF. The numbers in each group are small and counsel caution when interpreting these results, but they do suggest that age and gender interact, and this is also consistent with previous work (see section 2.4.1).

Fractional tissue volumes

Significant additional trends were detected in the fractional volume data over and above those found in the absolute volume results. Several studies have made use of an adjustment for intra-cranial volume when assessing trends in the normal healthy population (Blatter *et al.*,1995; Mathalon *et al.*,1993; Whitwell *et al.*,2001) and the effects of disease states such as Alzheimer's dementia and multiple sclerosis

(Brunetti *et al.*,2000; Jenkins *et al.*,2000; Liu *et al.*,1999; Rudick *et al.*,1999), supporting the utility of such a strategy.

Bias associated with focal white matter abnormalities

While acknowledging the imperfections of the model used to simulate white matter lesions, which fail to fully simulate lesion intensity, morphology and location heterogeneity, the results do suggest that volumes derived from SPM99 segmentations are relatively insensitive to the presence of white matter lesions. This can be seen by comparing Figures 3.2f and 3.2g with Figure 3.2e, which are all plotted on the same scale. Formal correction for lesion tissue misclassification marginally reduces their effect, although the utility of this correction would appear limited in subjects with small lesion volumes. Focal white matter lesions in MS subjects on this 3D FSPGR sequence tend to have intensities similar to GM, circa 75% of the way between the intensity of CSF and WM. For the estimates of volumes effects, a lesion intensity of 50% was used, and so the effects of increasing lesion volume in MS subjects may be less marked than indicated by these simulations.

Tissue volume estimates compared with literature values

Literature values on BP volumes suggest the average volume in males is circa 1400 ml and females 1240 ml (see section 2.4.1). Estimates from this study suggest tissue volumes of 1208 and 1060 ml respectively, which equates to 0.86 and 0.85 times less tissue. As noted previously, we cannot rely upon post-mortem data to provide accurate measures of *in vivo* tissue volumes, and so the best that we may expect is a constant ratio between observations. In this regard the tissue volumes show good consistency between genders.

The absolute GM volumes were estimated to be 1.9 and 2.0 times that of the WM volumes in males and females respectively (Table 3.2c). Post mortem studies have estimated this ratio to be between 1.1 and 1.5 dependent on age and previous MRI studies have found it to range from 1.2 to 2.0, also varying with age (see section 2.4.1). Previous work has suggested that imaging parameters may significantly effect tissue volumes (Blatter *et al.*,1995; Harris *et al.*,1994a), it is therefore difficult to say which values are correct in absolute terms.

Validity

Considering the present results in the context of previous work, it would appear that the use of image non-uniformity correction and adjustment for intra-cranial volumes are reasonable when assessing tissue volumes both in cross-sectional and longitudinal work, and should be employed. The derived fractional volume measures show high reliability, which implies high validity (estimated VC > 0.95 for all fractional measures). Validity is also supported by consistency between estimates of tissue volumes, age and gender effects derived from this work and literature values. Qualitative assessment of the effects focal WM lesions have upon these fractional estimates suggests a modest influence, with a tendency to underestimate the degree of disease associated GM atrophy and to overestimate the degree of WM atrophy. This limited differential measurement error should be recalled when considering results comparing groups with differing volumes of focal WM abnormalities.

Conclusions

This work suggests that fractional tissue volumes estimated from non-uniformity corrected tissue segmentations generated by SPM99 are both reliable and at least as valid as other MRI measures of brain tissue volumes in normal control and MS subjects.

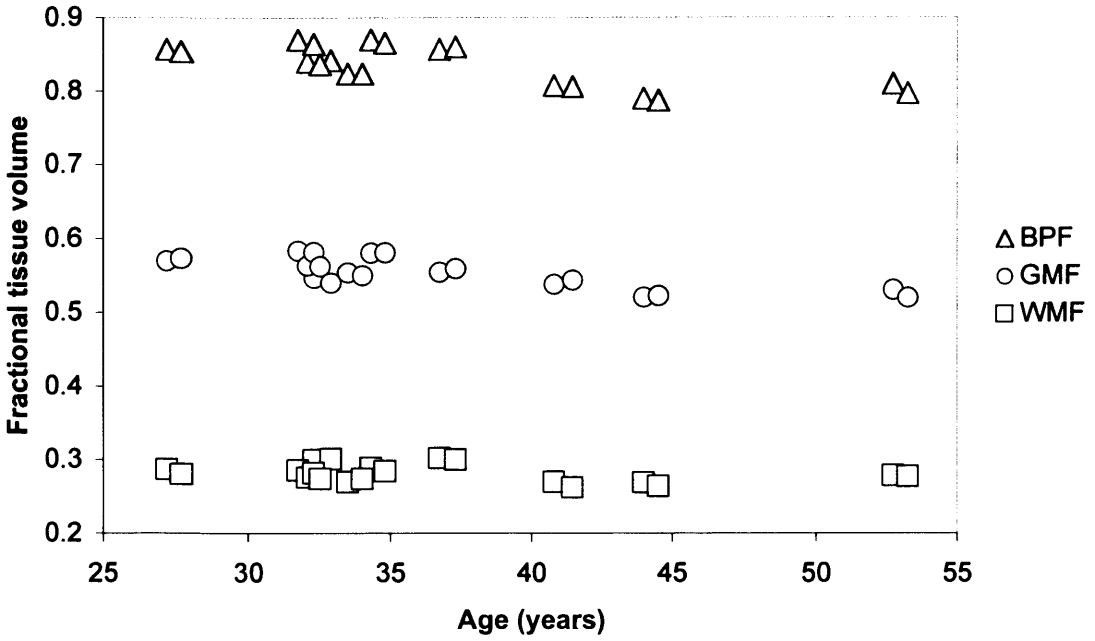

Figure 3.2a: Fractional tissue volumes from paired scans in 10 normal control subjects.

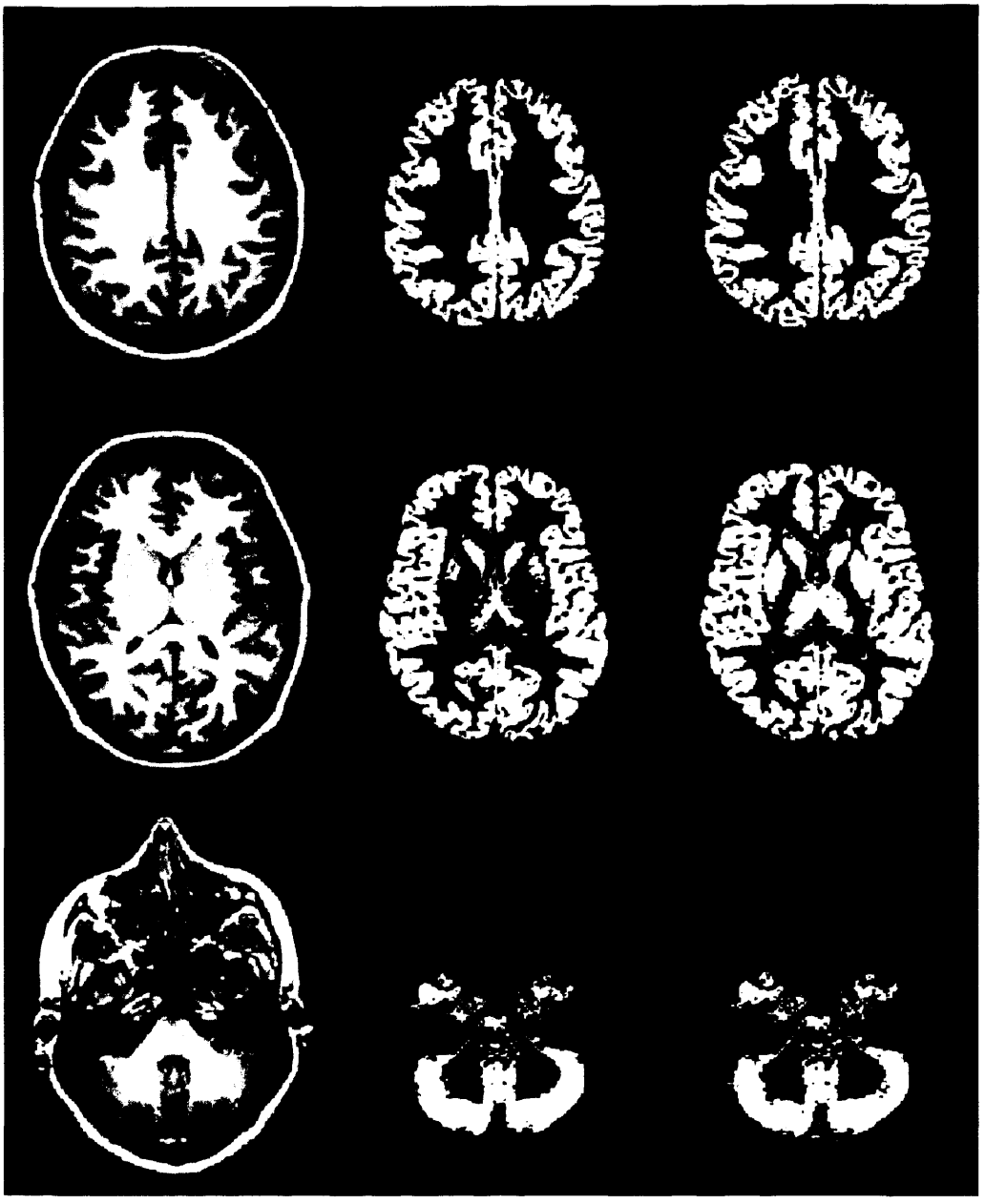

Figure 3.2b: Slices from a 3D FSPGR along with corresponding grey matter segmentation images from SPM99, with and without image non-uniformity correction. From left to right: the original images; grey matter segmentation without non-uniformity correction; grey matter segmentation with non-uniformity correction.

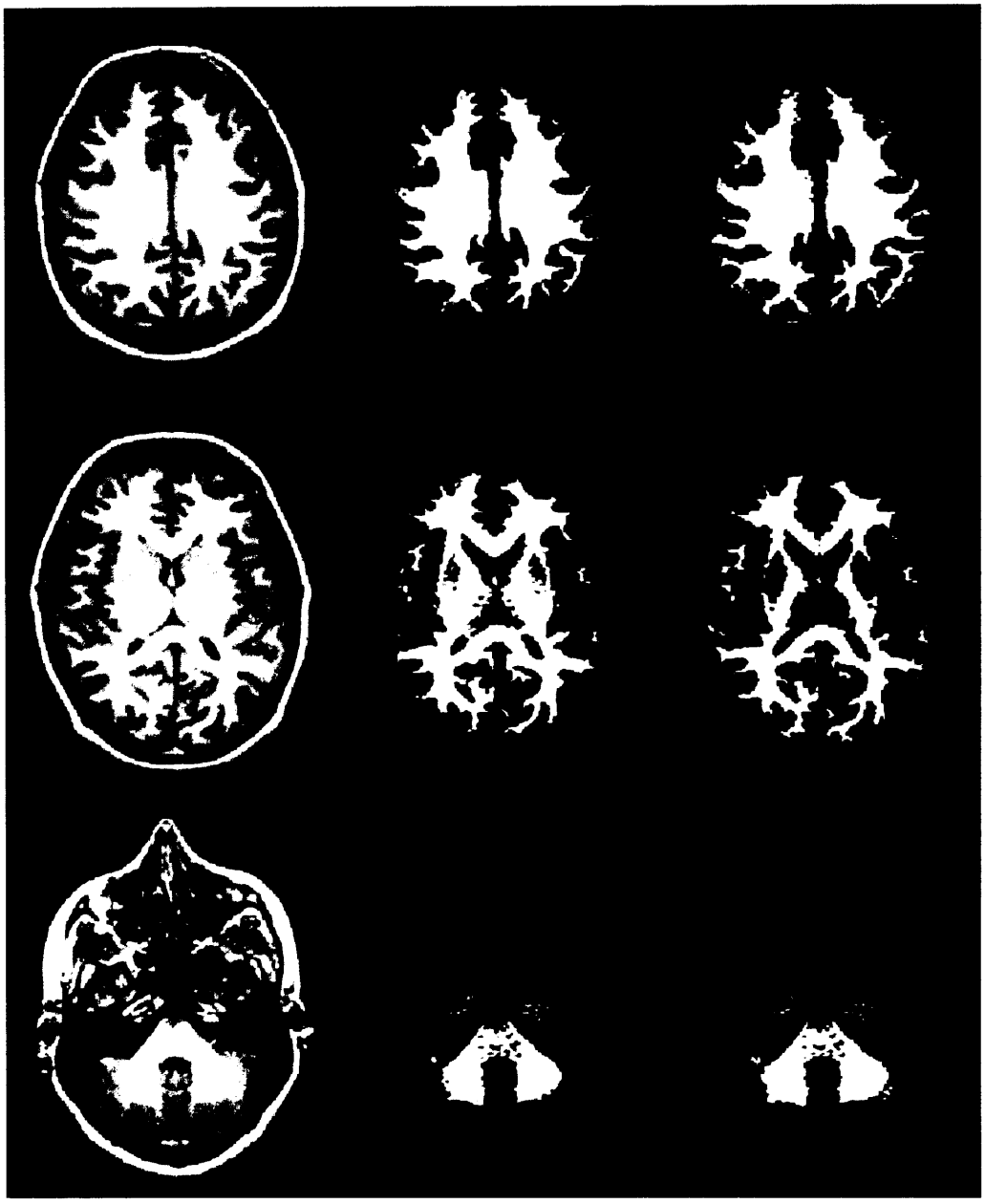

Figure 3.2c: Slices from a 3D FSPGR along with corresponding white matter segmentation images from SPM99, with and without image non-uniformity correction. From left to right: the original images; white matter segmentation without non-uniformity correction; white matter segmentation with non-uniformity correction.

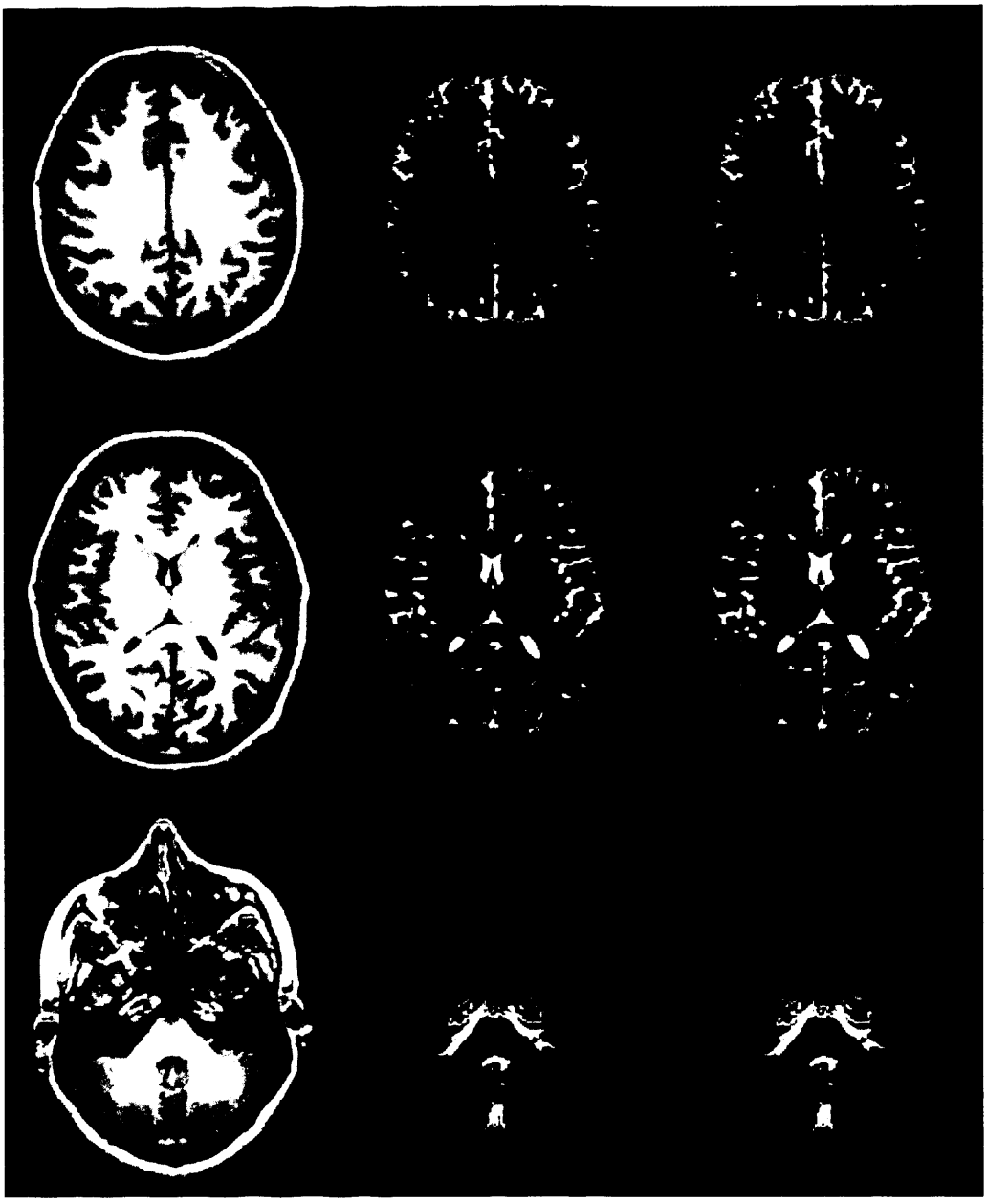

Figure 3.2d: Slices from a 3D FSPGR along with corresponding CSF segmentation images from SPM99, with and without image non-uniformity correction. From left to right: the original images; CSF segmentation without non-uniformity correction; CSF segmentation with non-uniformity correction.

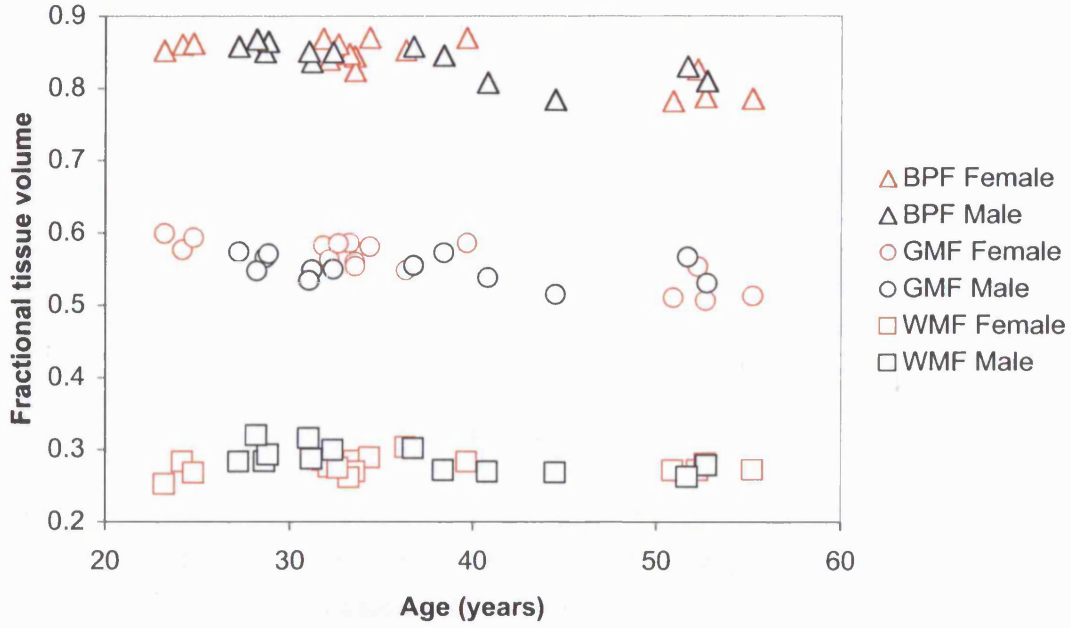

Figure 3.2e: Fractional tissue volumes by age and gender in 29 normal control subjects.

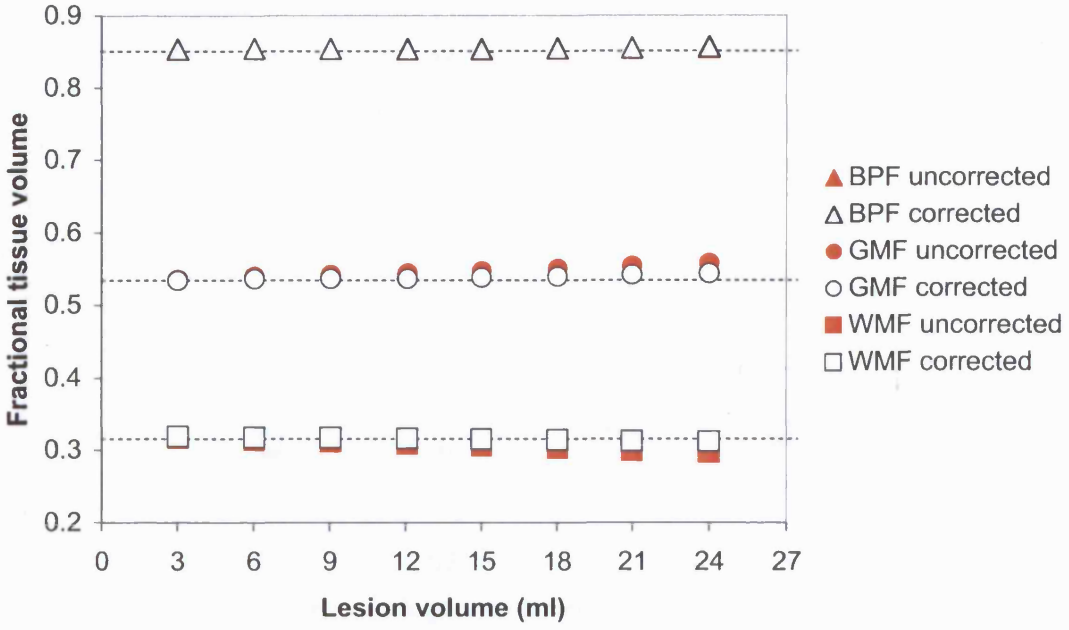

Figure 3.2f: Effects of WM lesions on fractional tissue volume estimates, with values corrected and uncorrected for lesion misclassification. Lesion intensity set to that halfway between WM and CSF. Dashed horizontal lines represent values from the original lesion free images.

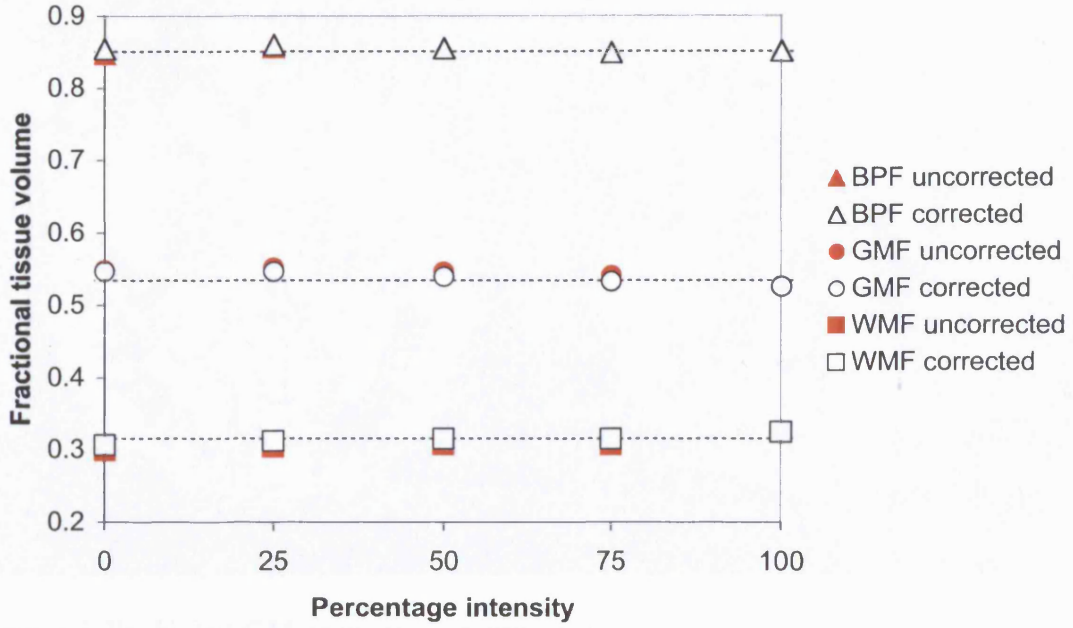

Figure 3.2g: Effects of WM lesion intensity on fractional tissue volume estimates, with values corrected and uncorrected for lesion misclassification. Lesion volume set to a constant total volume of 12.1 ml. Intensity of WM is 100% and CSF is 0%. That of GM and focal WM lesions in MS tends to be circa 75% on this scale. Dashed horizontal lines represent values from the original lesion free images.

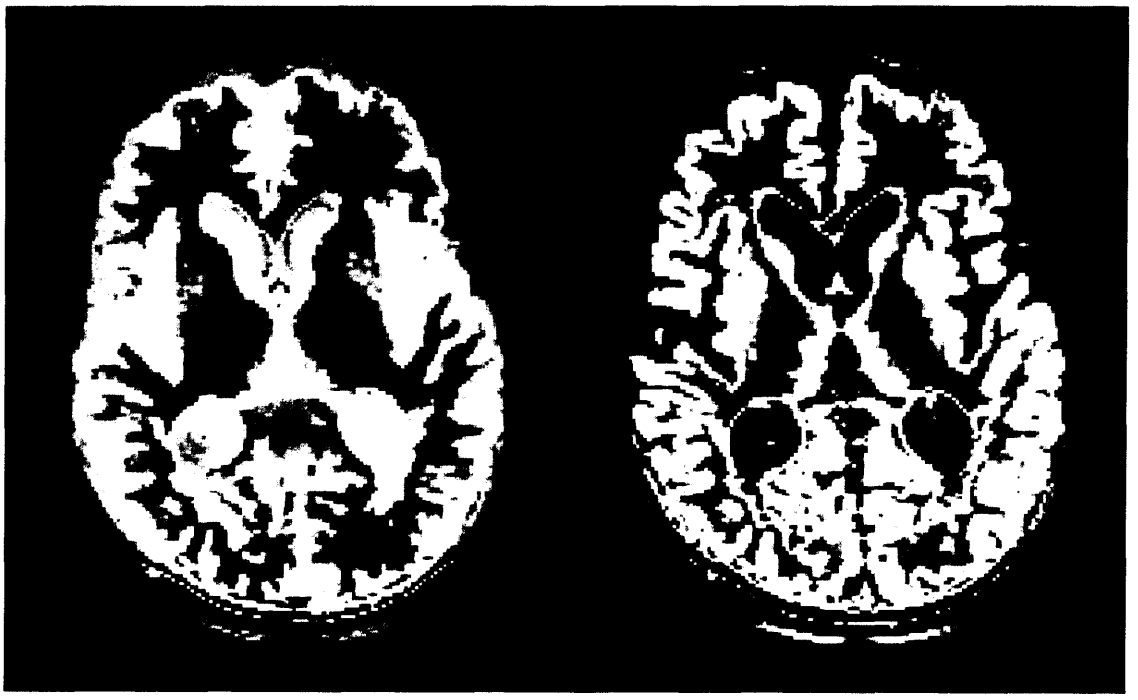

Figure 3.2h: Failed GM segmentation images from a subject with MS (3D FSPGR lesion volume circa 66 ml). The image on the left was processed without and on the right with inhomogeneity correction. Original data courtesy of Gordon Ingle.

3.3 *FOCAL WHITE MATTER LESION VOLUME ESTIMATES*

Introduction

In this work in addition the usual T_1, T_2 and Gd-enhancing lesion loads, lesions were also contoured on the 3D FSPGR. The former have previously been assessed and their reliability and validity considered (discussed below), while the characteristics of the latter have not been extensively explored.

Lesion contouring measurement error may be attributable to a number of factors such as the contouring method used, inter and intra-observer variability, subject repositioning in serial studies and scan acquisition parameters such as resolution and contrast weighting. Processing may be further broken down to lesion identification and contouring.

It would appear that semi-automated techniques offer greater reproducibility when compared with manual ones (Molyneux *et al.*,1998a). Inter-observer factors are potentially as important as intra-observer factors (for example on T_2-weighted SE [5mm slice thickness] processed at two centres, intra-observer CV 5.1 and 3.1% compared with inter-observer 8.3 and 7.1% (Filippi *et al.*,1998b)). Formal operator training may reduce the intra-observer component of measurement variability (Rovaris *et al.*,1999). Using thinner imaging slices (3 mm instead of 5 mm) improves reproducibility (Filippi *et al.*,1997a; Filippi *et al.*,1998d; Molyneux *et al.*,1998b), although this need not translate into significantly increased sensitivity to change (Rovaris *et al.*,1998b). This may relate to a large effect on a small error translating into little change in relative sources of variability i.e. measurement errors are already a small component of measurement variability even on images with slice thicknesses

of 5mm (Molyneux *et al.*,1998a). Subject repositioning also appears to be a significant component of measurement variability (Filippi *et al.*,1997a; Rovaris *et al.*,1998a); as is magnetic field strength, with higher main field strengths being associated with lower CVs (Filippi *et al.*,1997b).

Reproducibility appears to be affected by image contrast mechanisms. Fast fluid-attenuated inversion-recovery (FLAIR) images seem to yield more reproducible lesion measures than T_2-weighted conventional spin echo images (intra-observer CV 2.6 and 3.1% respectively; inter-observer CV 2.9 and 7.1% respectively) (Filippi *et al.*,1998b). Differences may be less marked between conventional T_1 and T_2-weighted images (Rovaris *et al.*,1999).

Many reproducibility studies have made use of marked scans (i.e. scans on which the position and approximate extent are marked on a printed copy by a single observer) to reduce the effect of inter-observer lesion identification variability on subsequent volume measurement. This may be expected to improve the apparent reliability of such measures by eliminating identification errors (Filippi *et al.*,1998a).

Methods

Subjects

Data came from 27 RR MS subjects (mean age 34.9 years, median 33.7, range 24.1 to 48.4).

Scan acquisition and processing

All subjects had 3D FSPGR, PD/T_2-weighted dual echo FSE and T_1-weighted SE sequences acquired (see section 3.1.1). These were processed using a semi-automated contouring technique based upon tools with DispImage (see section

3.1.1). In all subjects the T_1, T_2 and Gd-enhancing lesion loads were determined by the same observer (WR). In eight of the subjects, the 3D FSPGR lesion loads were determined on two occasions separated by seven days by a different observer (DC) using unmarked scans.

Statistical analyses

Treating estimates of lesion loads as random samples of all possible estimates, regardless of the observer, CV and RC were estimated from all parameters, yielding intra-observer values for the 3D FSPGR and inter-observer values for the T_1 and T_2 lesion loads. Spearman correlations between lesion loads from differing images were also estimated.

Results

Total lesion loads derived from the 3D FSPGR images were closer to those derived from a T_2-weighted rather than T_1-weighted sequence (Table 3.3a). Spearman correlation coefficients between lesion loads were as follows: 3D FSPGR and T_2 lesion load 0.98 (CI 0.96 to 0.99, P<0.001); 3D FSPGR and T_1 lesion load 0.90 (CI 0.78 to 0.95, P<0.001); 3D FSPGR and Gd-enhancing lesion loads 0.19 (CI –0.21 to 0.54, P=0.337); T_2 and T_1 lesion loads 0.90 (CI 0.79 to 0.96, P<0.001); T_2 and Gd-enhancing 0.26 (CI –0.15 to 0.59, P=0.337); T_1 and Gd-enhancing 0.46 (CI 0.08 to 0.72, P=0.017). For the 3D FSPGR the RC was 0.994, CV 7.2% and within-subject SD 0.6 ml.

	Lesion parameter (ml)			
	3D FSPGR	T_2	T_1	Gd-enhancing
Mean	7.7	9.0	2.0	0.6
Median	4.1	4.8	0.8	0.2
Range	0.5 to 39.9	1.1 to 40.8	0.0 to 9.9	0.0 to 4.3

Table 3.3a: Lesion loads derived from differing scan sequences in 27 MS subjects.

Discussion

These results suggest that lesion contouring on the 3D FSPGR images is reliable, and yields lesion loads similar to those derived from T_2-weighted images, the current standard for lesion identification. The reliability figures compare well with those of T_2-weighted lesions (intra-observer CV 4.2% and RC 0.998 for T_2 lesion loads determined on *marked* scans (Molyneux *et al.*,1998a), compared with intra-observer CV of 7.2% and RC 0.994 for 3D FSPGR lesion loads determined on *unmarked* scans).

The high correlation between lesion loads derived from the 3D FSPGR and T_2-weighted images suggests that they are effectively measuring the same underlying parameter, although with slightly differing biases. Previous work reached similar conclusions when comparing conventional 2D T_2-weighted images with magnetisation-prepared rapid-acquisition gradient-echo (MP-RAGE) images, but also concluded that the former may better identify GM lesions while the latter may better detect WM changes (Shah *et al.*,1992).

Correlations between the T_1 and both 3D FSPGR and T_2-weighted lesion loads are also high, although slightly lower than those observed between 3D FSPGR and T_2 lesion loads. This discrepancy may be partly accounted for by differential sensitivities to underlying pathology and measurement errors (see section 2.4.3).

The lower correlations observed between the Gd-enhancing lesion loads and other lesion parameters would suggest that Gd-enhancing lesion loads are marking a different underlying parameter, which from present evidence would appear to be breakdown of the BBB (see section 2.4.3).

Conclusions

This work suggests that MS lesion identification on 3D FSPGR images using a semi-automated contouring technique is reliable as lesion identification on T_2-weighted images.

3.4 TISSUE SPECIFIC METABOLITE CONCENTRATION QUANTIFICATION

Introduction

As noted in section 3.2, a robust awareness of methodological limitations along with normal factors that may influence observations is required to realistically interpret results derived from ^{1}H-MRSI observations. In the case of metabolite quantification, as with brain tissue volume estimates, a variety of factors both methodological and biological need to be considered. This work aimed to assess the reliability of metabolite quantification on a voxel by voxel basis, both within and between scanners; assess the reliability and validity of tissue specific metabolite concentration estimates; and explore potential tissue specific age and gender effects in normal control subjects. As with tissue volume estimates the effects of focal lesions in MS needs to be considered, however unlike tissue volume estimates an artificial simulation of the effects lesions may have upon quantifications has not been possible; this will be considered in the discussion.

Methods

Subjects

The data came from a cohort of 29 normal control subjects (16 females and 13 males, mean age 36.6 years at first scan, median 33.5, range 23.2 to 55.2) with no history of neurological disease or other medical conditions. A subset of the subjects underwent multiple scans to assess the method's reliability and this is described in detail below. This project had approval from the ethics committee of the National

Hospital for Neurology and Neurosurgery, Queen Square, London, UK. All subjects gave informed consent.

Scan acquisition

Scans were acquired as outlined in section 3.1.2. Three subjects underwent scanning on two identically specified scanners (see section 3.1) to assess quantification dependence upon individual scanner factors.

Metabolite and tissue quantification

Voxel metabolite concentrations and tissue contents were estimated as outlined in section 3.1.2.

Tissue specific metabolite quantification

LCModel estimates the certainty of metabolite quantifications in terms of a percentage SD (%SD) i.e. it provides an estimate of confidence limits for a metabolite concentration derived from a given voxel. In order to allow for the inherently different quantification errors associated with different metabolites, voxels were retained if LCModel estimates of the quantification error were less than 23% for Cho, 9% for Cr, 78% for Ins, 6% for NAA and 24% for Glx. If errors for one of these metabolites exceeded this limit then all metabolite data from the voxel was discarded. These figures were estimated as the upper 95% limit (mean + (2 × %SD)) of the quantification error for metabolites derived from a combined cohort of the 29 control subjects and the 27 MS subjects included in the work presented in section 4.3.

Voxels were retained if they contained > 80% GM plus NAWM and, in subjects with MS, <1% lesion. Voxels were classified as CGM or NAWM if they

contained > 60% of a given tissue type. From 1712 NC voxels acquired, 918 voxels remained after exclusion of those that were incompletely excited, 819 remained after excluding those that exceeded the allowed quantification errors. Of these 469 WM and 84 GM voxels were extracted. In a given subject, average tissue contents and metabolite concentrations for a particular voxel type were estimated from the extracted voxels.

Voxel by voxel reliability

Voxel by voxel reliability was estimated both within and between scanners. For the single scanner study, one subject underwent three sessions of scanning, each separated by 2 days. At each session, three ^{1}H-MRSI scans were acquired without subject repositioning. For the dual scanner study, single scans were acquired in three subjects using two machines, in sessions separated by an average of 60 days (56, 62 and 63 days in each subject respectively).

Tissue specific reliability

Tissue specific reliability was assessed using data from eight normal control subjects (5 males and 3 females) who had three scans, each pair separated by an average of 191 days (median 193, range 141 to 215 days). On one occasion a single subject, while producing useable WM voxels, yielded no suitable GM voxels.

Statistical analyses

RC and CV were estimated as outlined in section 2.5, using variance estimates from restricted estimate of maximum likelihood (REML) variance components models (Scheffe, 1959; Tedeschi *et al.*,1996). The single scanner model included voxel and sessions as random factors with all other variability partitioned to

the error term. The dual scanner study model included subject and voxel as random factors. Differences in tissue specific metabolite concentrations were assessed using Wilcoxon signed rank tests. The effects of age and gender on tissue specific metabolite concentrations were assessed using models that included age as a continuous covariate, gender as a fixed factor, voxel tissue contents (GM contents of WM voxels and vice versa), CSF contamination and BP volumes.

Results

The reliability results suggest that on a voxel by voxel basis, more than 50% of measurement variability for all metabolite concentrations estimated may be attributable to factors other than measurement error (Tables 3.4a and 3.4b). Mean LCModel estimates of quantification error (%SD) from the single scanner data were: Cho 8.9, Cr 7.4, Glx 18.3, Ins 11.0, and tNAA 4.2. GM voxels on average contain 71% GM, 16% WM and 12% CSF, while WM voxels on average contain 19% GM, 80% WM and 1% CSF.

Tissue specific metabolite concentrations appear different for all metabolites except for tNAA, with the most marked differences being for Glx and least obvious being for Cho (Table 3.4c). Wilcoxon signed rank tests confirm that these differences are significant at a $P<0.05$ level.

Estimates of WM metabolite concentrations were derived from an average of 16 voxels per subject, and are generally more reliable than those of individual voxels, regardless of the duration of follow-up (Table 3.4d). GM metabolite concentrations are derived from an average of 3 voxels per subject, and while tending to be more reliable than results from individual voxels, the differential is less clear than that

observed for WM. With longer follow-up tissue specific reliability appears to decrease for GM but not WM measurements.

Age and gender effects were assessed allowing for voxel tissue contents, CSF contamination and BP volume. The latter factor was included to account for the potential effects of age related atrophy leading to increasing albeit subtle partial volume effects not reflected in voxel tissue and CSF contents. Gender effects were found to be significant at a $P<0.05$ level for GM Cho (-0.291 females compared with males, CI -0.579 to -0.003, P=0.048), and WM Glx (-1.007, CI -1.743 to -0.271, P=0.009), and of borderline significance ($P<0.06$) for GM and WM Cr (-0.788, CI -1.601 to 0.026, P=0.057; -0.509, 95% CI -1.022 to 0.004, P=0.052 respectively), and WM Ins (-0.422, 95% CI -0.843 to 0.000, P=0.050). Age effects were not significant for any metabolites although age effects may also be subsumed by age-related reductions in BP volumes. BP volumes were found to significantly influence the results of GM Cho, Cr and Ins, and WM Cr. WM contamination of GM voxels did not significantly influence results, while GM contamination of WM voxels did for Cr and Glx. CSF contamination was significant factor in the models of WM Ins and Glx concentrations.

Metabolite	Variance components			RC, CV, (%) and within-voxel SD
	Voxel	Session	Error	
Cho	0.068	0.001	0.019	0.771, 11.9, 0.142
Cr	0.680	0.000	0.204	0.769, 9.5, 0.452
Glx	4.744	0.066	1.842	0.713, 15.2, 1.381
Ins	0.392	0.000	0.398	0.496, 18.4, 0.631
tNAA	1.075	0.000	0.255	0.808, 5.7, 0.505

Table 3.4a: Variance components with reliability coefficients (RC), coefficients of variation (CV) and within-subject within-session SD estimated from the single scanner data.

Metabolite	Variance components			RC, CV (%) and within-subject SD
	Voxel	Subject	Error	
Cho	0.047	0.003	0.014	0.782, 10.2, 0.118
Cr	0.475	0.016	0.325	0.602, 12.3, 0.570
Glx	3.978	0.571	1.477	0.755, 13.8, 1.215
Ins	0.296	0.064	0.261	0.580, 14.7, 0.511
tNAA	0.397	0.452	0.512	0.624, 8.9, 0.716

Table 3.4b: Variance components with reliability coefficients (RC), coefficients of variation (CV) and within-subject SD estimated from the dual scanner data.

Tissue	Metabolite				
	Cho	Cr	Glx	Ins	tNAA
GM - male	1.197, 1.169, 0.94 to 1.56	6.235, 6.200, 5.45 to 7.34	12.556, 12.808, 9.86 to 15.46	4.461, 4.225, 3.79 to 5.48	8.746, 8.801, 7.92 to 9.79
WM - male	1.229, 1.199, 1.05 to 1.50	4.767, 4.784, 4.12 to 5.46	7.833, 7.858, 6.93 to 8.90	3.812, 3.611, 2.99 to 4.66	8.772, 9.010, 7.65 to 9.50
GM - female	1.128, 1.114, 0.78 to 1.59	6.378, 6.371, 5.15 to 7.80	12.043, 11.909, 10.56 to 13.50	4.544, 4.467, 3.83 to 5.42	9.082, 8.689, 8.01 to 11.55
WM - female	1.330, 1.282, 1.00 to 1.75	4.954, 4.791, 4.11 to 6.39	7.637, 7.833, 6.64 to 8.54	3.523, 3.467, 3.10 to 4.32	8.845, 8.725, 7.61 to 10.28

Table 3.4c: tissue specific metabolite concentrations in mmol/l by gender. Mean, median and range values are given.

Follow-up	Reliability coefficients, coefficients of variation (%) and within-subject SD				
	GM Cho	GM Cr	GM Ins	GM tNAA	GM Glx
6 months	0.810, 8.8, 0.105	0.557, 8.2, 0.523	0.147, 9.8, 0.457	0.401, 10.3, 0.920	0.000, 13.5, 1.585
12 months	0.147, 18.4, 0.207	0.000, 15.0, 0.903	0.000, 14.0, 0.619	0.000, 12.9, 1.113	0.000, 15.6, 1.758
	WM Cho	WM Cr	WM Ins	WM tNAA	WM Glx
6 months	0.680, 9.3, 0.117	0.497, 8.0, 0.397	0.562, 7.6, 0.291	0.478, 5.7, 0.509	0.362, 6.6, 0.507
12 months	0.666, 8.8, 0.109	0.391, 8.0, 0.389	0.477, 9.6, 0.354	0.274, 6.4, 0.564	0.203, 7.1, 0.534

Table 3.4d: Reliability coefficients, coefficients of variation and within-subject SD for GM and WM metabolite quantifications using data from 8 subjects imaged on 3 occasions a mean of 191 days apart. Values are presented for both six and 12 month follow-up.

Discussion

Reliability

The reliability figures suggest that on average more than 50% of variability in tissue metabolite concentrations is related to factors other than measurement error. However the figures are not as high as that observed for tissue volume measures (see section 3.2) and this is mirrored by correspondingly higher CV. Reliability does not appear to markedly differ within or between scanners, suggesting that measurement error, in particular bias, is not markedly dependent upon the scanner used.

Tissue specific metabolite estimates appear more reliable than those derived from single voxels (as reflected in CV and intra-subject SD measures, but not RC as discussed below). This is more clearly seen for WM when compared with GM results, and may be explained by a number of factors. Firstly, the WM results are derived from more voxels per subject (on average 16 compared with 3 for GM). Secondly, WM metabolite concentrations may be more homogeneous than GM, thus differences in voxel location may have less of an effect upon apparent tissue metabolite concentrations. Thirdly, the anatomical complexity of GM means that GM voxels are more likely to be contaminated with CSF and WM than WM voxels are to be with CSF and GM. This effect may be subtle and difficult to observe directly, particularly in GM voxels where GM-CSF boundaries will be less distinct than WM-CSF boundaries, and this may explain why a direct effect of CSF contamination is only observed in WM (Ins and Glx) while BP volumes are more consistently related to GM rather than WM metabolite concentration estimates. Finally, WM metabolite concentrations may be more stable with time. This latter

hypothesis is supported by the observation that WM reliability is less influenced by the follow-up period than is the case for GM. It seems unlikely that scanner related measurement error would differentially affect WM and GM, leaving differences in the natural temporal variability of metabolites as the more likely explanation for this finding.

Age and gender effects upon tissue specific metabolite concentrations

Age effects were not found to be a significant factor in determining any of the tissue specific metabolite concentrations studied. However, BP volume in particular, and voxel contents to a lesser degree, may vary with age and as such be subsuming age related effects. Indeed, if these factors are removed from the models, age effects are significant for GM Ins, WM Cr, Cho and Ins, and to a borderline degree GM Cho (data not shown). In MS, brain atrophy may result both from normal ageing and disease effects thus partially decoupling relationships between age and BP volume. Given this, it would seem prudent to include both age and BP volumes in models exploring disease effects. In contrast to the tissue volume results, age and gender interactions were not detected when included in the model.

Bias associated with focal white matter abnormalities

Lesions may influence tissue specific metabolite concentrations in two main ways. Firstly, they can contaminate voxels otherwise classified as WM or GM, and due to genuine alterations in metabolite concentrations in lesion tissues alter the apparent concentration of metabolites in a given tissue. Secondly, MS lesions are associated with macromolecular peaks at <2ppm (Davie *et al.*,1994; Mader *et al.*,2001; Narayana *et al.*,1998). These may alter peak fitting and thus influence the

quantification of other metabolites. However, work by McLean *et al.* suggests that LCModel estimates of metabolite concentrations are little affected by additional unaccounted for peaks, although reliability may be improved by metabolite nulling (McLean *et al.*,2002).

Tissue specific metabolite concentration estimates compared with literature values

Comparing values obtained in this work with others is complicated by the relative paucity of such data from other studies. While several have explored this, many have quantified metabolites in arbitrary units or relative to Cr or Cho, making it difficult to make direct comparisons. In the context of those presenting tissue specific metabolite concentrations in mmol/l, the present values are not unreasonable (see section 2.4.4).

Validity

The validity coefficients for voxel by voxel metabolite concentrations range from 0.70 for Ins to 0.90 for tNAA (estimated from the single scanner data presented in Table 3.4d). Sub-selection of tissue specific voxels, while reducing CV, appears also to reduce RC. If RC alone were considered, we would conclude that the technique employed is not a valid measure of tissue specific metabolite concentrations. However, this observation is artefactual given that significant elements of inter-voxel variability may be explained by differences in their tissue contents (Tables 3.4a, 3.4b and 3.4c). Sub-selection of voxels will reduce inter-voxel variability while not necessarily equally reducing measurement errors. A reduced RC in these circumstances paradoxically would appear not to refute validity.

Validity is also supported by the observation of significant tissue specific differences in metabolite concentrations consistent with previous findings. Age and gender effects are less well characterised and presently cannot be used to reliably support validity, although the present observations do not seem out of line with general themes observed in the literature (see section 2.4.4).

Conclusions

When compared with brain tissue volume measurements, tissue specific metabolite estimates derived from the technique employed in this work appear less reliable and valid, although they are still reliable enough to the detect biologically plausible differences in tissue specific metabolite concentrations in limited cohorts.

4 ASSESSMENT OF EARLY DISEASE EFFECTS IN MULTIPLE SCLEROSIS

4.1 INTRODUCTION

MS Cohort

This work made use of data from 27 subjects with relapsing-remitting MS, as defined using standard criteria (Poser *et al.*,1983) (section 2.1.2). The group consisted of 20 females and 7 males; mean age 34.9 years when first scanned, median 33.7, range 24.1 to 48.4. All subjects were recruited within three years of first symptom onset (mean disease duration from first symptom onset 1.8 years, median 1.7 years, range 0.5 to 2.8 years). The mean EDSS score at their baseline assessments was 1.2 (median 1.0, range 0.0 to 3.0). Subjects were clinically assessed as outlined in section 2.1.6 and MR imaging performed at six monthly intervals. Each collection of MR data was divided into two sessions. Conventional T_1 (Gd-enhanced and non-enhanced) and T_2/PD-weighted images were acquired (section 3.1.1) in a separate session from the volumetric (section 3.1.1) and ^{1}H-MRSI (section 3.1.2) data. It is the latter data that form the core of this thesis.

In addition, diffusion tensor, magnetisation transfer, T_1-relaxation, spinal cord T_1-weighted (Gd-enhanced and non-enhanced), and spinal cord volumetric imaging were also undertaken. It is intended that subjects be followed-up over three years.

4.2 *CROSS-SECTIONAL ESTIMATES OF BRAIN TISSUE ATROPHY*

Introduction

There has been considerable work on quantifying the severity and extent of brain tissue damage in MS using MRI and relating this to clinical outcome. This has included the use of brain atrophy techniques that have been employed in relapsing-remitting and progressive clinical subtypes of MS (Miller *et al.*,2002). These studies have shown that atrophy occurs at a significantly faster rate in MS subjects compared with a normal healthy population.

It has not been clear how early in the course of MS atrophy appears and whether it affects both WM and GM. In addition, atrophy measures and estimates of T_1 or T_2 lesion loads are only weakly correlated in established MS (Bermel *et al.*,2003), if at all (De Stefano *et al.*,2002; Gasperini *et al.*,2002; Ge *et al.*,2000; Losseff *et al.*,1996), and a recent review of the association between Gd-enhancing lesion loads and atrophy revealed a similarly limited relationship (Zivadinov and Zorzon, 2002). Whether this atrophy is the result of earlier lesion-induced damage, raising the possibility that it is more directly related to lesion measures in the early stages of MS, remains to be determined.

Methods

Subjects

NC data came from a cohort of 29 subjects (16 females and 13 males, mean age 36.6 years at first scan, median 33.5, range 23.2 to 55.2) with no history of neurological disease or other medical conditions (section 2.1.8).

RRMS data came from a cohort of 27 subjects (20 females and 7 males; mean age 34.9 years when first scanned, median 33.7, range 24.1 to 48.4). The patients were required to have a disease duration of less than 3 years when recruited for the study. At time of scanning, mean delay from first symptom onset was 1.8 years (median 1.7, range 0.5 to 2.8). Their mean EDSS score was 1.2 (median 1.0, range 0.0 to 3.0). None of the MS subjects had received beta-interferon or glatiramer acetate at any stage prior to scanning, nor had they been treated with corticosteroids within the previous month. The project had approval from the ethics committee of the National Hospital for Neurology and Neurosurgery, Queen Square, London, UK. All subjects gave informed consent.

Scan acquisition

Data from four scans were included in the study. The first was a 3D FSPGR; the second was a dual fast spin echo (FSE) sequence; the third and fourth were pre- and 20 minutes post-gadolinium enhanced (0.3 mmol per kg body weight of Magnevist (Schering AG, Berlin, Germany)) T_1-weighted spin echo sequences. These sequences are described in section 3.1.1.

The second, third and fourth scans were acquired during the same scanning session; the first (3D FSPGR) scan was acquired during an earlier separate session. Sessions were separated by a mean of 9 days (median 7, range 2 to 60 days), during which time subjects did not report any additional clinical events.

Image analysis

Tissue and lesion segmentation was performed as described in section 3.1.1.

Clinical assessments

MS subjects underwent examination to estimate their EDSS (Kurtzke, 1983), TWT (Cutter *et al.*,1999), HPT (Goodkin *et al.*,1988), and PASAT (3 second stimulus interval) (Gronwell, 1977) scores. The average of two trials for the TWT and average of four trials of the HPT (averaged as reciprocals of the mean times from two trials for each hand) (Fischer *et al.*,1999) were calculated and, along with the PASAT and MSFC scores (calculated using the preferred method (Fischer *et al.*,1999)), were used in further analyses.

Statistical analyses

Statistical analyses were performed using SPSS 10.0 (SPSS Inc., Chicago, Illinois, USA). The associations between EDSS and tissue fractional volumes, lesion volumes, age and disease duration were investigated using Spearman correlations. MS disease effects were assessed using multiple linear regression models with age as a continuous covariate, gender and subject type (MS or normal control) as categorical factors, and an age-gender interaction term. For MS subjects, the relative effects on fractional tissue volumes of T_2, T_1 and Gd-enhancing lesion volumes, and disease duration on fractional tissue volumes were assessed using Spearman correlations. 3D FSPGR lesion volumes were not investigated because they were used to correct fractional volumes and were therefore not independent of the other measures. Two-tailed significance values were estimated for correlations. A P-value <0.05 was regarded as significant. In MS subjects, associations with T_2 lesion load and disease duration were also explored using multiple linear regression, with both factors included as continuous covariates. During initial analysis, age and gender

effects were not found to be significant in MS subjects and so were not included in the models.

Results

Lesion volumes

In the MS subjects the mean total lesion volumes were: 3D FSPGR hypo-intense lesion volume 7.7 ml (median 4.1, range 0.5 to 39.9 ml); T_2 lesion volumes (contoured on the PD-weighted FSE sequence) 9.0 ml (median 4.8, range 1.1 to 40.8 ml); T_1 hypo-intense lesion volume (on the pre-contrast T_1 weighted SE sequence) 2.0 ml (median 0.2, range 0.0 to 9.9 ml) and GD enhancing lesion volume 0.6 ml (median 0.2, range 0.0 to 4.3 ml).

Correlations between lesion volumes, brain tissue fractions and clinical parameters

None of the lesion volume measurements were correlated with age or disease duration. PASAT correlated modestly with age (r_s=-0.404, CI –0.686 to –0.017, P=0.037) but otherwise EDSS, HPT, TWT and MSFC did not; these parameters did not significantly correlate with disease duration. 3D FSPGR lesion volume correlated with TWT (r_s=0.39, CI -0.00 to 0.68, P=0.045); T_2 lesion load correlated with EDSS (r_s=0.39, CI –0.00 to 0.67, P=0.047), HPT (estimated as the reciprocal average) (r_s=0.38, CI –0.01 to 0.67, P=0.050) and MSFC (r_s=-0.43, CI 0.05 to 0.70, P=0.024); WMF with HPT (r_s=-0.44, CI –0.71 to –0.06, P=0.023). Other correlations were not significant.

Fractional tissue volumes: absolute disease and disease duration effects

MS disease effects were found to be significant for both GM and WM. Estimated disease effects allowing for age and gender were: -0.032 (CI –0.047 to

–0.018) for BPF (-3.9% compared with controls at age 35.8 years [the mean age of both MS and normal control cohorts] P<0.001, R^2=0.354); -0.016 (CI –0.029 to –0.003) for GMF (-2.9%, P=0.014, R^2=0.326); and -0.016 (CI –0.024 to –0.008) for WMF (-5.7%, P<0.001, R^2=0.335) (Table 4.2a). Disease duration did not significantly correlate with any fractional tissue volumes directly. However, when modelled with T_2 lesion load, both were significant factors for GMF (-0.013 [CI -0.024 to –0.001] per year, P=0.035; and T_2 -0.002 per ml [CI -0.003 to -0.001], P<0.001, R^2=0.569), while only T_2 lesion load significantly contributed towards BPF estimates (-0.002 per ml, [CI –0.003 to –0.001], P<0.001, R^2=0.595) and neither was significant for WMF.

Fractional tissue volumes: comparative lesion volume effects

Table 4.2b shows the correlations of tissue fraction measures with lesion volumes in MS subjects. BPF and GMF were both strongly correlated with T_2 and moderately with T_1 hypo-intense lesion volumes, but not with T_1 post-gadolinium enhancing lesion volumes. WMF was not correlated with any lesion volume measure. Figure 4.2a shows tissue fractions plotted against T_2 lesion loads.

Discussion

Many previous studies have detected brain tissue atrophy in MS (reviewed in (Miller *et al.*,2002)), but relatively few had looked specifically for GM changes when this study was performed (Cifelli *et al.*,2002; Ge *et al.*,2001; Liu *et al.*,1999), or for atrophy in people with clinically early MS. This study reveals significant brain atrophy, affecting both white and grey matter, in a cohort of clinically definite MS subjects with clinical disease duration of 1.8 years. Subsequent work has confirmed

this observation (Quarantelli *et al.*,2003; Sanfilipo *et al.*,2005; Sastre-Garriga *et al.*,2004; Tedeschi *et al.*,2005).

Brain tissue fraction findings in MS

After allowing for age and gender effects, BPF was significantly reduced in the MS group, with a greater proportional reduction in WMF (mean c. –5.7%) than GMF (mean c. -2.9%). In controls, age related changes were more apparent for GMF (mean -0.3% per year) than WMF (mean -0.1% per year). Therefore, atrophy early in the clinical course of MS does not appear to represent a simple acceleration of the usual age related changes.

The reduction in BPF in the present early relapsing-remitting MS study accords with previous reports of subjects with CIS (Brex *et al.*,2000a) and studies assessing atrophy in subjects within 5 years of clinical disease onset (Zivadinov *et al.*,2001). It therefore seems reasonable to conclude that brain atrophy occurs in the early stages of MS.

There had been little previous work investigating white matter and grey matter separately for the presence of atrophy in MS. Liu *et al.* (Liu *et al.*,1999) in a mixed cohort of 40 RR and SP MS subjects (median disease duration 7 years) found significant WM atrophy (-11.9%, $p<0.001$) but no discernable effect upon GM. No significant difference was observed between RR and SP cohorts. This is concordant with work by Ge *et al.* (Ge *et al.*,2001) concluded that in a cohort of 30 RRMS subjects with a mean disease duration of 3.8 years, loss of brain tissue was mainly confined to WM (-6.4%). While no overall disease effect was observed on %GM (as a fraction of intra-cranial volume) a correlation with T_2 lesion load was seen (r_s=-

0.52, P<0.005). No association between T_2 lesion load and %WM was seen. However, subsequently, Quarantelli *et al.* (2003) have also detected GM (-7.1%, p<0.001), although without WM atrophy, in a cohort of 50 RRMS subjects (mean clinical disease duration 9.9 years) and an association between GM (r_s=-0.43, p<0.001) but not WM atrophy and T_2 lesion loads; De Stefano *et al.* (2003) have observed neocortical atrophy in people with RRMS and disease durations less than 5 years; Sastre-Garriga *et al.* (2004) in a cohort of 43 PPMS compared with 45 normal control subject found both GM (GMF –3.5%) and WM (WMF –6.2%) atrophy, using the same technique employed in the present work; while Tedeschi *et al.* (2005) and Sanfilipo *et al.* (2005) also both found atrophy in GM and WM (although Sanfilipo *et al.* did not find WM atrophy to be significant). Work assessing thalamic volumes, normalised for intracranial volumes, in 14 subjects with SPMS (median disease duration 18.5 years) has also found a ~17% decrease in volume when compared with age and gender matched normal control subjects (Cifelli *et al.*,2002); and in 14 subjects with RRMS a ~25% decrease (Wylezinska *et al.*,2003).

Relationship between brain tissue fractions and lesion measures

There was no correlation between the enhancing lesion loads and measures of atrophy. Enhancing lesions are correlated with active inflammation on pathological studies (Bruck *et al.*,1997; Katz *et al.*,1993); however, only a small proportion of lesions will display inflammation at a single time point. A realistic evaluation of the relationship between this MR marker of inflammation and atrophy would require an assessment of serial data obtained from multiple enhancing scans obtained at frequent intervals (noting that new lesions enhance on average for only one month)

(Harris *et al.*,1991; Thompson *et al.*,1991). There is little of such data available in patients with early disease; data from cohorts with longer disease durations has revealed only modest correlations (Coles *et al.*,1999; Saindane *et al.*,2000; Simon *et al.*,1999).

Inspection of figure 4.2a reveals a readily apparent relationship between T_2 lesion volumes and both BPF and GMF, but not WMF. Assessment of correlations (Table 4.2b), confirm the association for both T_2 and T_1 lesion volumes. The stronger relationship was with T_2 volume, which gave an r^2 of 0.41 for BPF and 0.30 for GMF suggesting that about a third of the BPF and GMF reduction can be explained by variations in T_2 load. These lesion load effects were confirmed after allowing for disease duration by the model.

There are several potential explanations for this relationship between T_2 lesions, which are virtually all located in white matter, and atrophy located in grey matter. First, the decrease in GMF may reflect both retrograde degeneration to the cell body and Wallerian (predominantly anterograde) degeneration extending along fibre tracts (Simon *et al.*,2000) following axonal transection in white matter lesions (Trapp *et al.*,1998). Secondly, axonal damage without transection but associated with demyelination *per se* (Ferguson *et al.*,1997) may lead to axonal and neuronal atrophy (Yin *et al.*,1998). Thirdly, grey matter lesions, though rarely seen on MRI, are commonly found at post mortem (Bo *et al.*,2000; Brownell and Hughes, 1962; Kidd *et al.*,1999); such lesions are associated with demyelination and possibly with local axonal and neuronal damage, and their total volumes may be correlated with white matter lesion loads. They might also cause subtle changes in signal intensity that

affects segmentation between cortex and CSF such that grey matter volume appears reduced. Finally, both overt lesion genesis and tissue atrophy may be manifestations of some other common pathogenic mechanism that has yet to be elucidated.

The absence of a clear correlation between lesion volumes and WMF, despite the greater extent of WMF reduction when compared with GMF, could be interpreted as an early global WM disease process resulting in atrophy which is at least partly independent of overt lesion genesis. Alternatively, water content changes due to low grade inflammation or oedema, along with glial proliferation in the normal-appearing white matter (Allen and McKeown, 1979; Tourtellotte and Parker, 1968) might alter white matter volumes and obscure a relationship between lesion volume and WMF loss. It is also worth recalling that WMF reproducibility was not quite as good as that for GMF, and this may contribute towards the masking of relationships. Studies making use of a larger sample with greater lesion volume heterogeneity are needed.

The present study indicates a stronger relationship between atrophy and T_2 than T_1 hypo-intense lesion load in a cohort with clinically early MS. It has been suggested that T_1 lesions are associated with greater axonal loss (van Walderveen *et al.*,1998b) when compared with T_2 lesions, and they should therefore correlate more strongly with atrophy if the link mechanism is secondary tract degeneration. However, the T_1 lesion load was relatively small in this early disease cohort and the stronger correlation of grey matter atrophy with T_2 lesion volumes suggests that in early MS, the link between white matter lesions and grey matter atrophy may have additional mechanisms. Relatively few studies have presented data on the association between atrophy and both T_1 and T_2 weighted lesion loads. Paolillo *et al.* (2000)

explored the cross-sectional relationship between atrophy and lesions in a cohort with RRMS and a mean disease duration of 5.6 years. They found a correlation between a regional cerebral hemisphere volume measure and T_1 (r=-0.48, P<0.001), but not T_2 lesion loads, although both T_1 and T_2 lesion loads correlated equally with corpus callosum area (r=-0.53, P<0.001 and r=-0.52, P<0.001 respectively). Similarly, Sailer *et al.* in a mixed cohort of 29 RRMS and SPMS subjects found no association between T_2 lesion load and cerebral atrophy, although they did observe a relationship with T_1 lesion load (Sailer *et al.*,2001). However Zivadinov *et al.* (2003) found nearly equal correlations between both T1 and T2 lesion loads, and BPF (r=-0.54 and r=-0.52 respectively, P<0.005).

Relationship between brain tissue fractions and disease duration

Disease duration was found to have a modest but significant additional effect upon GMF but not WMF. This was detected after allowing for associations between T_2 lesion load and tissue fractional volumes. A possible explanation for this result is that there is on-going grey matter atrophy which was initiated during acute lesion genesis but is not dependent on further lesion activity. The observation that on-going axonal loss occurs in chronically demyelinated plaques may be relevant here (Kornek *et al.*,2000). The disparity between GMF and WMF has been considered above, with all the same reasons applying to these findings as were discussed in relation to lesion volume and tissue fraction correlations. Saindane *et al.* (2000) have also noted an association between disease duration at baseline and fractional brain tissue volume (r_s=-0.64, p<0.001), and Paolillo *et al.* (2000) observed a correlation between disease duration and corpus callosum area (r_s=-0.31, p=0.03).

Atrophy and cell loss

The disease associated volume reduction in our subjects of c. 2.8 % in GMF and c. 4.9% in WMF, compares with a reduction in NAA in the normal appearing GM (mean 5.6%) and WM (mean 4.5%) in subjects from the same cohort (see section 4.3). If we assume that neuronal numbers are directly proportional to both tissue volumes and tNAA concentrations, which they may not be, these results would represent a ~10% reduction in GM and ~11% reduction in WM total neuronal and axonal populations.

Other investigators have reported a proportionately greater reduction in NAA to Cr ratios than brain volumes in relapsing-remitting MS (Collins *et al.*,2000) (a circa -1.1% change in brain normalised to intracranial volume and a circa -8.7% reduction in the NAA to Cr ratio in a large central voxel). These discordant findings could indicate that axonal and neuronal loss is more marked than that indicated by fractional tissue volume loss alone (for reasons already discussed) or that the more marked reduction in NAA may indicate a transient effect of axonal and neuronal dysfunction rather than absolute axonal and neuronal loss on the concentration of this metabolite (Mader *et al.*,2000; Narayana *et al.*,1998).

Study limitations

While this study indicates atrophy can be detected early in the clinical course of MS, it is based upon relatively homogeneous cross-sectional data, and the strength of associations with either lesion loads or disease duration in the MS cohort should be considered in this light. In addition, while age, disease duration and lesion volumes were all found to significantly influence disease related tissue specific

atrophy, the trends detected need to be explored again in more heterogeneous and larger samples. It is important not to extrapolate the results outside of the parameter ranges covered by the present study: while the assumptions of linear relationships between parameters, such as age and tissue fractions, appear satisfactory for the present cohort, this can not be assumed to be true for a greater range of values. In addition, when interpreting the magnitude of disease effects, it should also be remembered that various methods for assessing tissue volumes might yield different absolute values dependent upon both the segmentation methodology and scan acquisition utilised.

It should also be recalled that the data have been explored with multiple statistical tests, and as such there is real potential for results considered significant at a $P<0.05$ level to be spurious. In particular, nearly 40 correlations between brain lesion loads and other parameters have been assessed, and so it may be expected that about two statistically significant results would be seen even if there were no true associations.

Brain tissue segmentation in any disease processes may be complicated by both changes in tissue signal intensity characteristics and, in the case of MS, the presence of lesions. There are a number of further segmentation strategies which could be employed to potentially improve upon that used in this study, although each method will be associated with differing susceptibilities for disease related segmentation bias. In addition, there is no accepted standard technique for measuring brain tissue volumes, thus it is not possible to fully validate and calibrate any segmentation methodology. Given this, it is important that multiple segmentation

methodologies are independently implemented and applied to different scan acquisitions as each will have their own advantages and disadvantages.

While the MS and control subjects were well matched for age, there was some imbalance in genders. However, this should not have markedly impacted upon our results as gender and age effects were allowed for in the models used. Indeed, neither age nor gender effects were detected in the MS cohort, probably because they were obliterated by overlying disease related effects (as seen on inspection of Figure 4.2b).

Conclusions

The present study shows that, after allowing for normal age and gender effects, there is evidence that significant fractional brain volume loss has already occurred early on in the clinical course of relapsing remitting MS and that, unlike age related changes, this is proportionally more evident in white matter. Significant relationships were found between lesion volumes and the degree of tissue atrophy in grey but not white matter. This suggests that white matter, and to a lesser degree grey matter, pathology may occur by mechanisms that are at least partly independent of overt lesion genesis.

Gender	Subject type					
	Normal control			MS		
	BPF	GMF	WMF	BPF	GMF	WMF
Male	0.839, 0.850, 0.784 to 0.868	0.552, 0.550, 0.515 to 0.574	0.288, 0.284, 0.263 to 0.320	0.793, 0.817, 0.717 to 0.820	0.530, 0.544, 0.467 to 0.562	0.263, 0.257, 0.250 to 0.280
Female	0.840, 0.850, 0.782 to 0.871	0.563, 0.570, 0.507 to 0.600	0.277, 0.275, 0.252 to 0.303	0.819, 0.823, 0.773 to 0.852	0.553, 0.551, 0.510 to 0.588	0.266, 0.268, 0.231 to 0.303
Both	0.840, 0.850, 0.782 to 0.871	0.558, 0.560, 0.507 to 0.600	0.282, 0.281, 0.252 to 0.320	0.812, 0.818, 0.717 to 0.852	0.547, 0.551, 0.467 to 0.588	0.265, 0.266, 0.231 to 0.303

Table 4.2a: Mean, median (range) fractional tissue volumes by gender in normal control and MS subjects. Results are from 13 male (mean age at scanning 36.3 years, median 32.3, range 27.2 to 52.7) and 16 female (mean age at scanning 36.8 years, median 33.5, range 23.2 to 55.2) controls subjects; and 7 male (mean age at scanning 33.4 years, median 31.8, range 24.8 to 48.1) and 20 female (mean age at scanning 35.3 years, median 34.5, range 24.1 to 48.4) MS subjects.

Tissue parameter	Lesion parameter		
	T_2 hyper-intense	T_1 hypo-intense	Gd-enhancing
BPF	-0.64, -0.83 to -0.34, <0.001	-0.58, -0.79 to -0.25, 0.001	-0.26, -0.59 to 0.14, 0.189
GMF	-0.55, -0.77 to -0.20, 0.003	-0.57, -0.79 to -0.23, 0.002	-0.18, -0.53 to 0.23, 0.378
WMF	-0.18, -0.53 to 0.23, 0.382	-0.07, -0.45 to 0.33, 0.735	-0.05, -0.43 to 0.35, 0.798

Table 4.2b: Spearman correlations, CI and P-values, of tissue fractions with total lesion volumes in MS subjects.

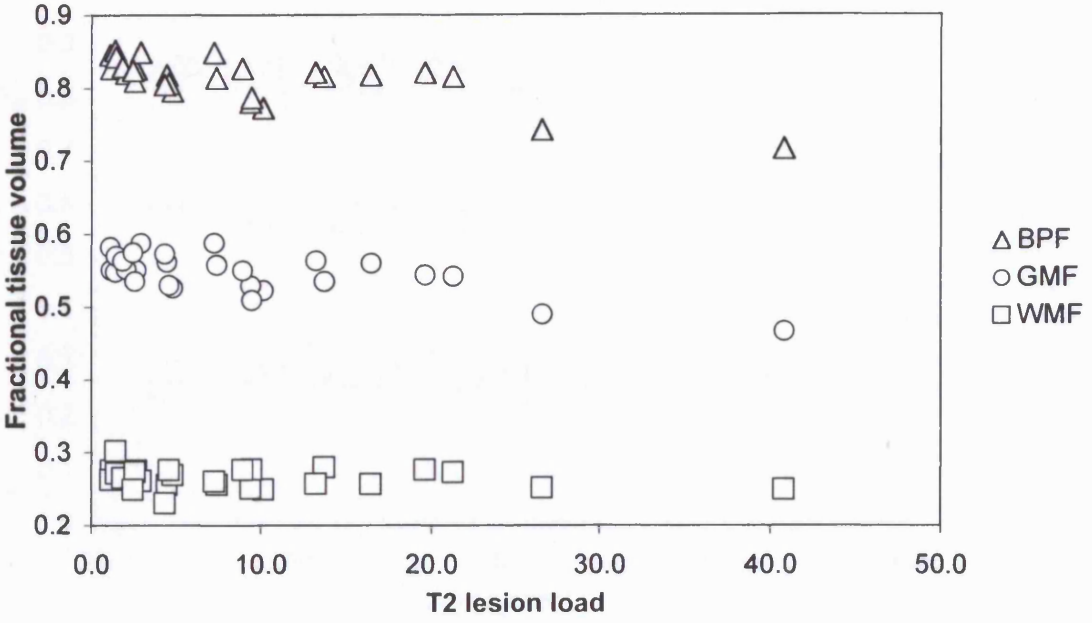

Figure 4.2a: T_2 lesion and fractional brain tissue volumes. Gradients associated with increasing lesion loads can be seen in both the BPF and GMF data, but not the WMF data.

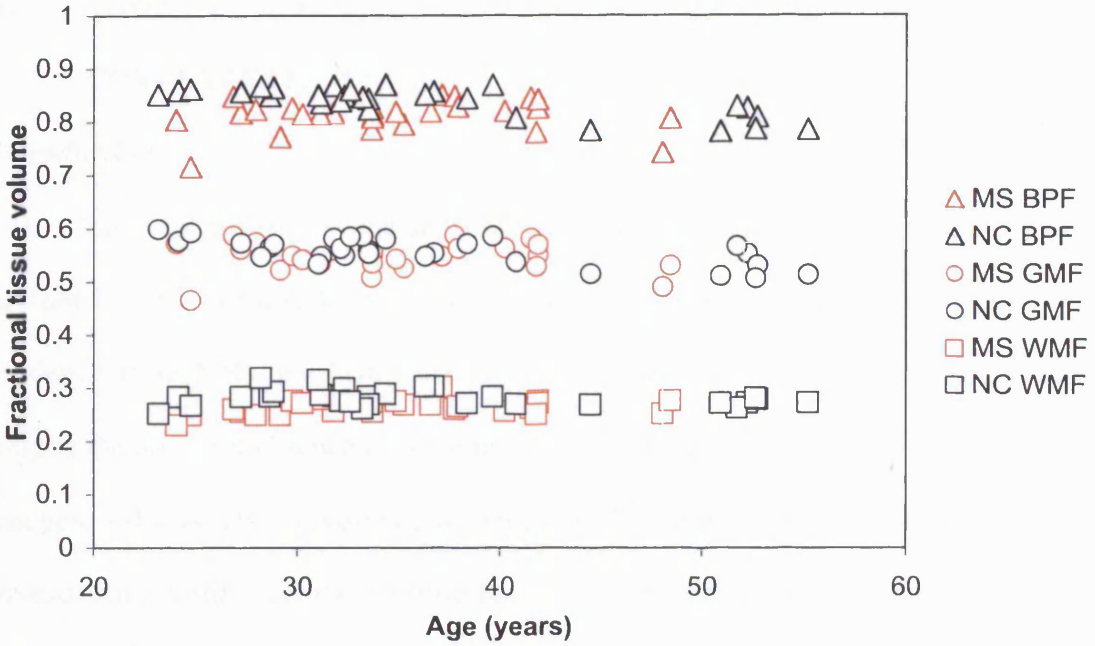

Figure 4.2b: MS disease effects upon fractional brain tissue volumes. Subjects with MS show consistently lower BPF and WMF volumes, and to a lesser degree GMF volumes, when compared with NC subjects, and this effects appears to be greater than age-related trends observable in the NC subjects.

4.3 CROSS-SECTIONAL ESTIMATES OF BRAIN METABOLITE CONCENTRATIONS

Introduction

There is growing evidence to suggest that the effects of MS on brain tissues are not limited to focal WM lesions or even WM *per se*. In the NAWM there is evidence from MRI and histopathology studies indicating extensive involvement despite the apparent absence of overt lesions on conventional T_1 or T_2-weighted MRI images. GM is also involved, although it has not been the focus of much investigation until recently. Despite the considerable volume of GM, its complex anatomy has meant that it has been difficult to study using MRI. The introduction of additional MRI techniques and refinements to conventional imaging methodologies has made the study of this potentially important but under-investigated tissue possible.

This present study investigates clinically early MS disease effects in both NAWM and cortical GM (CGM), using ^{1}H-MRSI to determine tissue specific metabolite concentrations and assessing their relationships with clinical outcome. It builds upon previous preliminary work (Kapeller *et al.*,2001), expanding the MS and NC cohorts; updating the ^{1}H-MRSI processing technique and tissue segmentation methodology (with inclusion of formal lesion quantification); and employing statistical analyses to account for age, gender, tissue type and partial volume effects associated with differences in brain parenchymal volumes.

Methods

Subjects

NC data came from a cohort of 29 subjects (16 females and 13 males, mean age 36.6 years at first scan, median 33.5, range 23.2 to 55.2) with no history of neurological disease or other medical conditions (section 2.1.8).

RRMS data came from a cohort of 27 subjects (20 females and 7 males; mean age 34.9 years when first scanned, median 33.7, range 24.1 to 48.4). The patients were required to have a disease duration of less than 3 years when recruited for the study. At time of scanning, mean delay from first symptom onset was 1.8 years (median 1.7, range 0.5 to 2.8). Their mean EDSS score was 1.2 (median 1.0, range 0.0 to 3.0). None of the MS subjects had received beta-interferon or glatiramer acetate at any stage prior to scanning, nor had they been treated with corticosteroids within the previous month.

Scan acquisition

Volumetric, T1 and T2-weighted, and Gd-enhanced images were acquired as outlined in section 3.1.1.

^{1}H-MRSI data were acquired as outlined in section 3.1.2. The size of PRESS selected volume varied between subjects: in MS subjects the mean anterior to posterior extent was 95 mm (median 97, range 69 to 111 mm) and the mean left to right extent was 66 mm (median 66, range 54 to 74 mm); in NC subjects the mean anterior to posterior extent was 98 mm (median 98, range 77 to 118 mm) and the mean left to right extent was 69 mm (median 69, range 59 to 80 mm). Figure 4.3a shows an axial section through the brain at the level of the spectroscopic slice, with

an overlaid grid of extracted spectra, a selection of which have been enlarged to provide more detailed spectra.

Image processing

^{1}H-MRSI data were processed as outlined in section 3.1.2, yielding tissue specific estimates of metabolite concentrations for a given subject. Brain tissue volumes and lesion loads were determined as described in section 3.1.1.

Clinical Assessments

MS subjects were clinically assessed as outlined in section 4.2.

Statistical analyses

Statistical analyses were performed using SPSS 10.0 (SPSS Inc., Chicago, Illinois, USA). MS disease effects on metabolite concentrations were estimated using multiple (linear) regression models that included gender and disease status (MS or NC) as categorical variables; and age, WM contents of CGM voxels (and *vice versa* for NAWM voxels), voxel CSF contents and BP volume as continuous covariates. This was designed to allow for differences in GM and WM metabolite concentrations; the potential effects of age and gender; and both overt voxel CSF contamination and partial volume effects associated with differences in whole brain volumes.

The relationships between metabolite concentrations and lesion load measures, disease duration, fractional brain tissue measures (BPF, GMF and WMF) and clinical parameters (EDSS, MSFC, HPT, TWT and PASAT) were assessed using Spearman correlations.

Results

Subject demographics, clinical parameters and brain tissue volume measures

CGM data came from 24 of the MS (mean age 35.2 years, median 34.3, range 24.1 to 48.4 years; 19 females and 5 males; mean disease duration (estimated from first symptom onset) 1.7 years, median 1.6, range 0.5 to 2.7 years) and 26 of the NC (mean age 34.8 years, median 33.3, range 23.2 to 55.2 years; 14 females and 12 males) subjects. NAWM data came from 25 of the MS (mean age 35.0 years, median 33.7, range 24.1 to 48.4 years; 19 females and 6 males; mean disease duration 1.7

years, median 1.6, range 0.5 to 2.7 years) and 29 of the NC (mean age 36.6 years, median 33.5, range 23.2 to 55.2 years; 16 females and 13 males) subjects. Clinical, lesion load and tissue volume data for the whole MS cohort are given in section 4.2.

Disease effects upon tissue metabolite concentrations

After allowing for age, gender, voxel tissue contents and brain tissue volumes, significant disease effects (at a $P<0.05$ level) were found in the concentrations of CGM Cho, CGM tNAA, CGM Glx, NAWM tNAA and NAWM Ins (Tables 4.3a, 4.3b and 4.3c).

Relationships between tissue metabolite concentrations and both lesion load and clinical parameters

Spearman correlations between metabolite concentrations and other MRI parameters were significant for T_2 lesion load and NAWM Ins (r_s=0.44, CI 0.04 to 0.71, P=0.030) but not for T_1 hypo-intense or Gd-enhancing lesion loads, or fractional brain tissue volumes. Disease duration did not significantly correlate with any metabolite concentrations.

Correlations between metabolite concentrations and measures of disability were significant for CGM Glx with EDSS (r_s=-0.43, CI -0.72 to -0.02, P=0.035), MSFC (r_s=0.58, CI 0.22 to 0.80, P=0.003), HPT (r_s=-0.42, CI -0.71 to -0.01, P=0.039) and PASAT (r_s=0.54, CI 0.16 to 0.78, P=0.006); NAWM Ins with MSFC (r_s=-0.56, -0.79 to -0.20, P=0.004), HPT (r_s=0.61, CI 0.27 to 0.82, P=0.001), TWT (r_s=0.45, 0.06 to 0.73, P=0.023) and PASAT (r_s=-0.41, CI -0.70 to -0.01, P=0.040); and CGM Cr (noting that a significant overall disease effect was not observed) with MSFC (r_s=0.52, CI 0.14 to 0.77, P=0.009) and HPT (r_s=-0.54, CI -0.78 to -0.16, P=0.007). Figures 4.3b and 4.3c show the relationship between MSFC and both

CGM Glx and NAWM Ins respectively. In those subjects who contributed NAWM voxel data, lesion load measures and disease duration did not correlate significantly with clinical impairment.

Discussion

These results show that in MS compared with NC subjects, tNAA is reduced in both CGM and NAWM; that Ins is elevated in NAWM; and that Cho and Glx are both reduced in CGM. They were obtained allowing for age and gender effects, voxel tissue contents and potential partial volume effects related to brain tissue volumes. Before considering these results further there are some factors that need to be recalled when reviewing them, and some potential pathological interpretations of changes in metabolite concentrations.

Methodological and analytical considerations

Given the volume of ^{1}H-MRSI voxels utilized in this study (2.3 mL), it was not possible to select pure CGM or NAWM voxels. Instead selection criteria were used that would yield voxels with minimal lesion contamination (< 1%); limited CSF and non-brain tissue contents (GM plus NAWM > 80%); and approximately equal proportions of a given tissue type (excluding CSF) to a given voxel type (circa 79% for both CGM and NAWM voxels). Lesion contamination was predominantly an issue with NAWM voxels, whereas brain tissue content was a limiting factor when setting the criteria to yield CGM voxels due to the proximity of CGM to CSF spaces.

In order to assess intrinsic disease effects upon a given tissue type, multiple regression models were used. These allowed for voxel tissue contents and CSF contamination, variability in whole brain volume, age and gender. Previous work has shown tissue specific and regional differences in metabolite concentration, along

with age and gender effects (see section 2.4.4). The inclusion of these factors in the model was designed to ensure the robustness of our overall disease effect conclusions against confounding effects, rather than offer further insight into the role these factors may have in determining metabolite concentrations. These should be explored again in future work.

There are no clearly established methods for constructing appropriate or optimal data models, and there are disadvantages to both under or over-parameterisation (Freund and Wilson, 1998). Erring on the side of caution, all potential confounding factors for which measures were available (age, gender, ^{1}H-MRSI tissue and CSF contents, and BP volume) were included. The relationships between outcome variables and covariates were assumed to be linear and, while this appeared adequate for the present data, this may not be optimal and should be reconsidered in future work. Rather than try to include other disease related parameters such as lesion loads, disease duration and separate brain tissue volume measures in an all-encompassing but potentially markedly over-parameterised model, these were explored separately with Spearman correlations. When considering the results, it should also be recalled that multiple comparisons have been made, and as such some of the results reported to be significant at a $P<0.05$ level may be due to chance alone.

Given that a small amount of brain atrophy has been detected in this MS cohort (see section 4.2), the question arises whether the tissue metabolite changes seen, particularly in CGM, reflect partial volume effects or not. This would appear unlikely for two reasons. Firstly, the reported magnitude of the reduction in the GMF (circa 2.8%) is less than those observed for the significant metabolite decreases in

GM (circa 6.6% to 15.1%). Secondly, the statistical models allowed for ^{1}H-MRSI voxel tissue contents and whole brain volume, yet still identified significant changes in tissue metabolite concentrations.

Cortical grey matter observations

In CGM, Cho, tNAA and Glx were all reduced in MS compared with NC subjects, and this was unrelated to lesion load measures. The marked reduction in Cho may indicate both reduced cellular density and metabolic activity, although subsequent work has not replicated this in deep GM (Inglese *et al.*,2004). The absence of a significant decrease in Ins would suggest that glial loss is not a major contributing factor, assuming that intracellular Ins concentrations remain relatively unchanged in MS. Reductions in tNAA point to more specific neuronal involvement, which may be related to cell loss or metabolic dysfunction or both. Reductions in Glx could mark metabolic dysfunction and loss of neurons and glial cells; once again, the lack of a concurrent significant decrease in Ins favours interpretation of the present results as representing neuronal metabolic dysfunction or loss or both.

Other proton magnetic resonance GM studies in MS had been relatively limited (Kapeller *et al.*,2001; Sharma *et al.*,2001), and had not consistently shown reductions in NAA; subsequent work has detected reductions in NAA in SPMS (but not RRMS, although only five subjects in each MS group) (Adalsteinsson *et al.*,2003), RRMS (Inglese *et al.*,2004), and PPMS (Sastre-Garriga *et al.*,2005b). Histopathology studies have found cortical lesions (Bo *et al.*,2000; Brownell and Hughes, 1962; Kidd *et al.*,1999), with neuronal involvement including axonal and dendritic transection, and neuronal apoptosis (Peterson *et al.*,2001). The present observations appear consistent with these findings.

Normal-appearing white matter observations

Metabolite changes in NAWM were more limited than for CGM. NAWM Ins was significantly elevated and was modestly related to T_2 lesion loads. This may indicate glial proliferation in NAWM and, given that T_2 lesions are to a significant degree associated with previous focal inflammation (Bruck *et al.*,1997; Ciccarelli *et al.*,1999; Katz *et al.*,1993; Lai *et al.*,1996; Miller *et al.*,1988), this would also suggest that focal inflammatory activity is related to a more widespread WM process. The reduction in tNAA in NAWM is compatible with axonal metabolic dysfunction or loss or both.

Pathology studies have shown both gliosis (Allen and McKeown, 1979) and axonal loss (Bjartmar *et al.*,2000; Evangelou *et al.*,2000) in NAWM. Proton spectroscopy studies of NAWM have found reductions in absolute NAA concentrations all clinical subtypes of MS (Adalsteinsson *et al.*,2003; Davie *et al.*,1997; Kapeller *et al.*,2001; Sastre-Garriga *et al.*,2005b; Suhy *et al.*,2000; van Walderveen *et al.*,1999a), although not entirely consistently (Vrenken *et al.*,2005), and also reduced relative (to Cr) (Fu *et al.*,1998; Leary *et al.*,1999a; Tourbah *et al.*,1999), although in the case of ratio analyses this may in part be due to increased Cr concentrations (Rooney *et al.*,1997; Suhy *et al.*,2000; Vrenken *et al.*,2005). Ins concentrations have also been found to be absolutely (Kapeller *et al.*,2001; Sastre-Garriga *et al.*,2005b; Vrenken *et al.*,2005) and relatively (to Cr) (Tourbah *et al.*,1999) elevated. The present findings appear consistent with previous studies and mirror known histopathology.

Clinical outcome and MRI parameters

CGM Glx and NAWM Ins concentrations correlated most consistently with clinical outcome in this clinically early cohort, while tNAA did not correlate with any outcome measure. An overall disease effect on CGM Cr was not found to be significant and caution is needed when interpreting its relationship to clinical parameters. Taken together, the present findings could be interpreted as showing a relationship between neuronal metabolic dysfunction and clinical impairment, hinting that the former may be an important factor in determining clinical status at an early stage in the clinical evolution of relapsing-remitting MS. This may not be the case in the long-term: absolute axonal and neuronal loss may be more important as the disease progresses. This may in part explain the discrepancy between the present results and those from some previous studies that have investigated cohorts with longer disease durations and shown a correlation between disability and reductions in NAA:Cr ratios (De Stefano *et al.*,1998; De Stefano *et al.*,2001; Fu *et al.*,1998; Fu *et al.*,1996; Ruiz-Pena *et al.*,2004). In PPMS subjects, correlations between CGM tNAA, NAWM Glx and Ins have been observed using the same techniques employed in the present work (Sastre-Garriga *et al.*,2005b), although an overall reduction in NAWM Glx was again not observed.

The relationship between clinical impairment and NAWM Ins implies that glial proliferation is associated with a negative effect upon clinical function. While NAWM Ins concentrations appear to be modestly related to T_2 lesion loads ($r_s = 0.44$, P=0.030), only circa 19% ($r_s^2 = 0.19$) of variability can be accounted for by this link, suggesting that glial proliferation is to a large extent independent of focal lesion genesis. Further, clinical status was not related to T_2 lesion load, which would

support the concept that glial proliferation intrinsically, or another pathological process leading to it, has a significant role to play in determining impairment.

Study limitations

In addition to those considerations mentioned at the start of this discussion, there are a number of other limitations that should be noted when comparing results from this present work with others. While the metabolite quantification technique employed yields mmol/L values, it is not possible to calibrate these against actual *in vivo* values. Thus, different metabolite quantification techniques may produce different values and so a direct comparison cannot be made. Further, imperfect ^{1}H-MRSI slice excitation profiles will also influence estimates of metabolite concentrations, although we would anticipate that this would affect MS and NC subjects similarly. Brain tissue volume quantifications also cannot be considered entirely accurate, with scan acquisition and processing methodologies all affecting the apparent tissue volumes, and no definitive gold standard *in vivo* results to calibrate these against. Further, the estimated magnitude of disease effects will, to a degree, be dependent upon the statistical model employed and this must be remembered when looking at the values given in Table 4.3c.

As noted above, cortical lesions are found in MS. Such lesions are visible on MRI scans (Bakshi *et al.*,2001; Boggild *et al.*,1996; Rovaris *et al.*,2000), although this is hampered by the structural complexity of GM and the relatively similar MRI signal intensity characteristics of GM and lesions on some sequences. Further, MRI probably underestimates their extent (Geurts *et al.*,2005). Given this, tissue classified as CGM in the present study is likely to contain some focal lesions and it is not possible to determine whether the observed CGM metabolite changes reflect the

effects of lesions or more diffuse abnormality. The apparent absence of an increase in CGM Ins contrasts with observations made on focal WM lesions (Brex *et al.*,2000b; Davie *et al.*,1994; De Stefano *et al.*,1995; Kapeller *et al.*,2001; Koopmans *et al.*,1993) and may reflect relatively less glial proliferation in GM lesions when compared with those found in WM.

Conclusions

This study provides evidence for neuronal and axonal metabolic dysfunction or loss, or both, in CGM and NAWM, and for glial proliferation in NAWM, early in the clinical course of MS. The results suggest that metabolic dysfunction, particularly evident in CGM, may be more closely related to disability in the early stages of MS than absolute neuronal and axonal loss. Further work is required to clarify the metabolic and structural contributions towards disability throughout the clinical course of MS.

Voxel type	Parameter	Subject type	
		NC	MS
CGM	Cho	1.16, 1.15 (0.78 to 1.59)	1.00, 0.97 (0.74 to 1.36)
	Cr	6.31, 6.26 (5.15 to 7.80)	5.73, 5.81 (3.93 to 6.93)
	Ins	4.51, 4.41 (3.79 to 5.48)	4.29, 4.38 (3.23 to 4.99)
	tNAA	8.93, 8.76 (7.92 to 11.55)	8.21, 8.33 (6.30 to 9.27)
	Glx	12.28, 12.01 (9.86 to 15.46)	10.61, 10.81 (6.88 to 13.46)
	GM%	71.29, 71.02 (65.49 to 77.65)	67.99, 67.87 (61.18 to 76.86)
	WM %	16.19, 16.76 (7.45 to 28.63)	18.07, 18.59 (8.89 to 24.71)
	CSF %	11.93, 12.22 (5.29 to 16.86)	13.25, 13.27 (8.63 to 18.04)
	Lesion %	-	0.04, 0.00 (0.00 to 0.39)

Table 4.3a: Proton magnetic resonance spectroscopic imaging voxel metabolite concentrations (mmol/L) and tissue (percentage of total) contents presented as mean, median (range) values in NC and MS subjects' CGM. Data came from 24 MS and 26 NC subjects.

Voxel type	Parameter	Subject type	
		NC	MS
NAWM	Cho	1.28, 1.23 (1.00 to 1.75)	1.20, 1.17 (0.96 to 1.60)
	Cr	4.87, 4.79 (4.11 to 6.39)	4.86, 4.85 (4.17 to 5.83)
	Ins	3.65, 3.56 (2.99 to 4.66)	3.98, 3.76 (2.93 to 5.45)
	tNAA	8.81, 8.79 (7.61 to 10.28)	8.30, 8.22 (6.84 to 9.92)
	Glx	7.72, 7.86 (6.64 to 8.90)	7.51, 7.73 (5.07 to 9.43)
	GM %	19.07, 19.06 (13.64 to 27.42)	20.53, 21.18 (5.10 to 28.24)
	WM %	79.57, 79.13 (71.09 to 85.58)	77.12, 77.06 (62.75 to 92.94)
	CSF %	0.81, 0.76 (0.08 to 2.09)	1.55, 1.06 (0.36 to 9.02)
	Lesion %	-	0.13, 0.08 (0.00 to 0.78)

Table 4.3b: Proton magnetic resonance spectroscopic imaging voxel metabolite concentrations (mmol/L) and tissue (percentage of total) contents presented as mean, median (range) values in NC and MS subjects' NAWM. Data came from 25 MS and 29 NC subjects.

Metabolite	Adjusted means (SE) (mmol/L)[a]		MS disease effects[b]		
	NC	MS	Mean (SE) (mmol/L)	Percentage effect [c]	P value
CGM Cho	**1.18 (0.04)**	**1.02 (0.05)**	**-0.17 (0.06)**	**-14.0%**	**0.011**
CGM Cr	6.26 (0.12)	5.93 (0.15)	-0.33 (0.20)	-5.2%	0.108
CGM Ins	4.50 (0.10)	4.35 (0.11)	-0.15 (0.15)	-3.2%	0.347
CGM tNAA	**8.85 (0.14)**	**8.37 (0.17)**	**-0.48 (0.23)**	**-5.6%**	**0.041**
CGM Glx	**12.13 (0.29)**	**11.12 (0.34)**	**-1.01 (0.47)**	**-8.3%**	**0.035**
NAWM Cho	1.28 (0.04)	1.22 (0.04)	-0.06 (0.05)	-4.9%	0.243
NAWM Cr	4.92 (0.08)	4.88 (0.09)	-0.04 (0.12)	-0.8%	0.745
NAWM Ins	**3.69 (0.10)**	**4.09 (0.11)**	**+0.40 (0.15)**	**+11.0%**	**0.008**
NAWM tNAA	**8.77 (0.13)**	**8.38 (0.14)**	**-0.39 (0.19)**	**-4.5%**	**0.048**
NAWM Glx	7.75 (0.14)	7.84 (0.16)	+0.09 (0.22)	+1.2%	0.677

Table 4.3c: MS disease effects estimated from multiple regression models. Model R^2: CGM Cho 0.306; CGM Cr 0.426; CGM Ins 0.251; CGM tNAA 0.366; CGM Glx 0.410; NAWM Cho 0.203; NAWM Cr 0.311; NAWM Ins 0.344; NAWM tNAA 0.259; NAWM Glx 0.412. [a] Tissue metabolite concentrations in MS and normal control subjects estimated from multiple regression models, evaluated at the mean

BPV, age, voxel tissue and CSF contents of both MS and NC subjects. [b] MS disease effects estimated from multiple regression models allowing for age, gender, voxel tissue and CSF contents, and BPV. [c] Percentage difference in MS CGM or NAWM voxels compared with adjusted mean values in NC subjects.

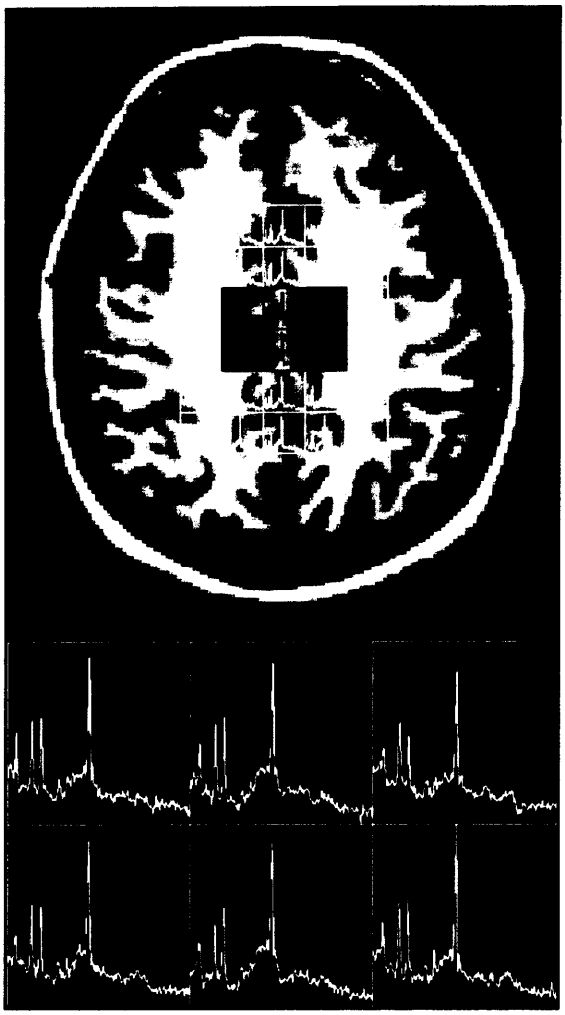

Figure 4.3a: 3D FSPGR (T_1-weighted) structural image overlaid by the proton magnetic resonance spectroscopic imaging grid in a normal control subject. Only those voxels fully within the spectroscopic excitation volume are shown. The inverted-contrast section of the image corresponds to the magnified spectra shown below it. The two central voxels in the magnified grid come from voxel fulfilling the GM classification criteria, while the others fulfil the WM criteria. The main peaks from left to right are: Ins, Cho, Cr and NAA, with smaller Glx peaks to be found between those of Cr and NAA.

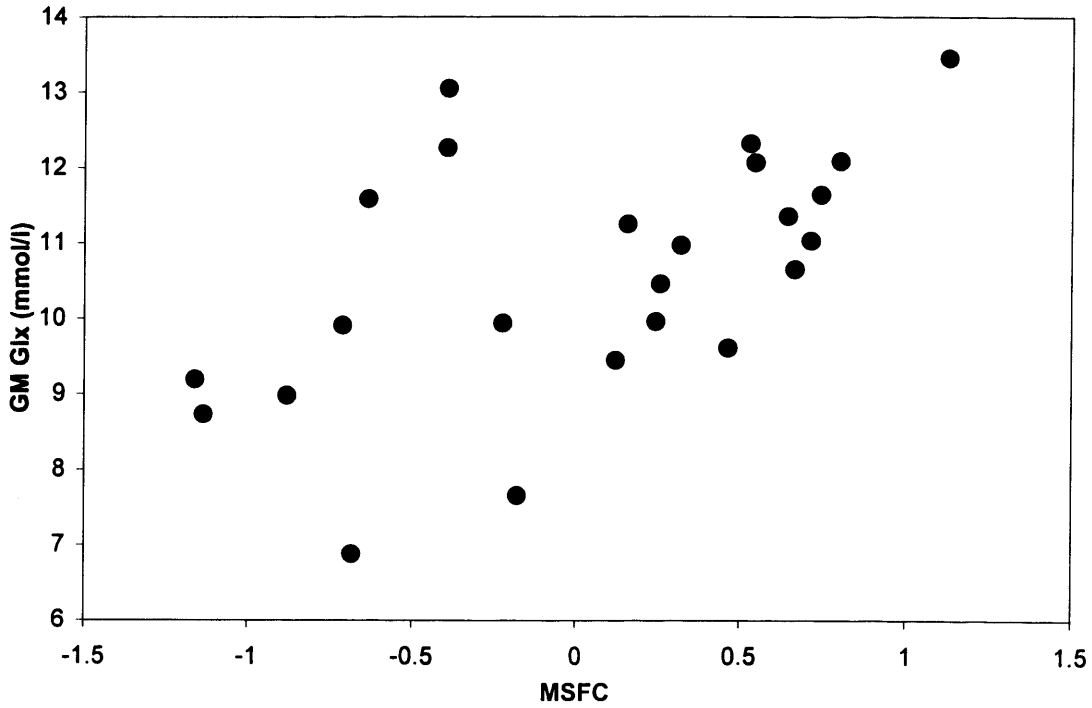

Figure 4.3b: CGM Glx concentrations (mmol/L) against MSFC scores in MS subjects.

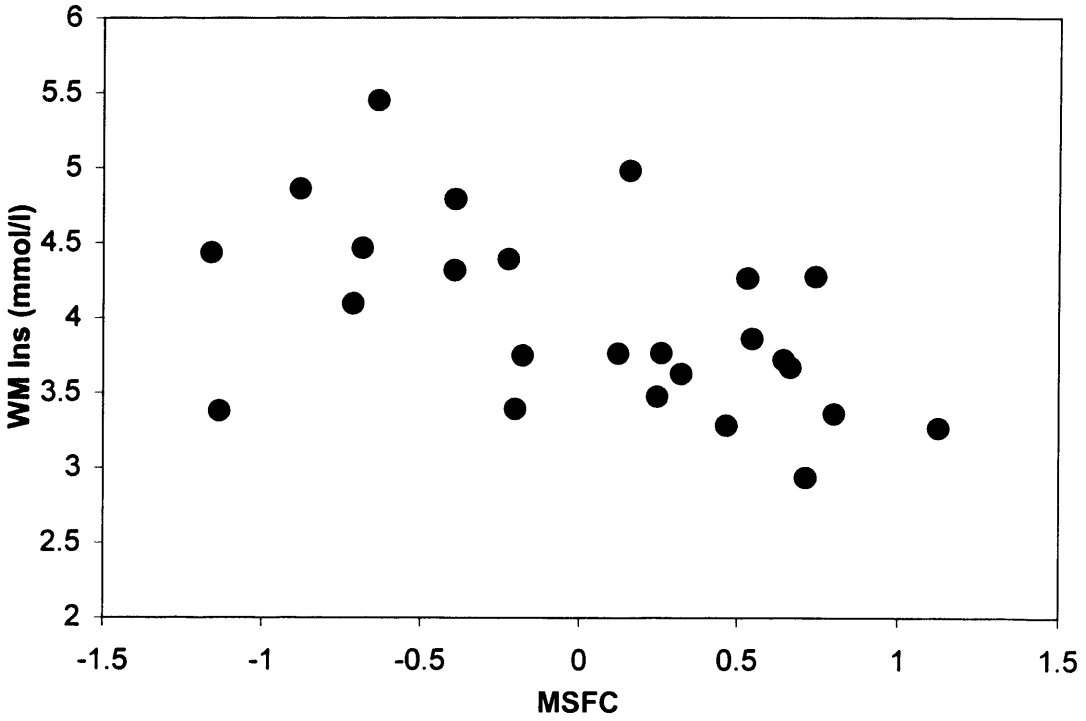

Figure 4.3c: NAWM Ins concentrations (mmol/L) against MSFC scores in MS subjects.

4.4 LONGITUDINAL ESTIMATES OF BRAIN ATROPHY

Introduction

Having previously noted that atrophy may be detected both in GM and WM early in the clinical course of MS, the dynamics of early tissue specific atrophy was, and to a degree remains, unclear. At the time the work presented in this section was undertaken only a limited number of longitudinal studies had been performed (Dalton *et al.*,2002; Luks *et al.*,2000). Noting that previous cross-sectional work in this cohort has observed both WM and GM atrophy, with the former predominating when considered as fractions of intra-cranial volumes (see section 4.2), it would appear that there is potential for rates of atrophy to differ in WM and GM, and for such atrophy to differentially relate to clinically apparent disease progression.

This study addresses such issues in clinically early relapsing-remitting MS subjects followed-up with brain WM and GM volume measurement, and clinical assessments, every 6 months for 18 months.

Methods

Subjects

Data came from 13 patients with clinically definite RRMS (mean age at baseline 36.4 years, median 36.5, range 26.9 to 48.1; 9 females and 4 males; mean disease duration at baseline 1.9 years [estimated from first symptom onset], median 2.1, range 0.5 to 2.7; mean EDSS 1.0, median 1.0, range 0.0 to 2.0); and 9 NC subjects (mean age at baseline 36.7 years, median 33.5, range 31.2 to 52.7; 4 females and 5 males) followed up over 18 months (mean 1.5 and 1.6 years in MS and NC subjects respectively. None of the MS subjects had received beta-interferon or glatiramer acetate at any stage prior to scanning, nor had they been treated with

corticosteroids within the previous month. These subjects represent a subset of those included in the cross-sectional study (section 4.2).

Scan acquisition

Subjects were scanned at six-month intervals as outlined in section 4.1.

Image processing

Image data were processed as outlined in section 3.1.2.

Clinical assessments

Clinical assessments as outlined in section 4.2 were undertaken at six monthly intervals coincident with scanning. The number of relapses during the 18 months prior to baseline assessments and during the 18 months of follow-up was also estimated.

Statistical analyses

In order to minimise the number of statistical tests, gradients over time were examined, after allowing for global inter-subject differences. For MS versus NC comparisons of fractional tissue volumes, the model included subject and subject type (MS or NC) as categorical covariates, time in follow-up as a continuous covariate and subject type × time in follow-up interaction term. Change in lesion load and clinical parameters (except for EDSS) in the MS subjects were assessed using models that included subject as a categorical covariate and time in follow-up as a continuous covariate. Change in EDSS was assessed using the Wilcoxon signed rank test. Associations between changing fractional tissue volumes and lesion loads were assessed using a model that included subject as a categorical variable, and time in follow-up and lesion load as continuous covariates.

Results

While all subjects were scanned at baseline, six and 18 months, one MS and one NC subject was not scanned at 12 months. MS subjects were followed up on average after 191, 373 and 559 days after baseline assessments (medians 193, 377 and 563 respectively); NC subjects were followed up on average after 201, 380 and 581 days after baseline scanning (medians 203, 383 and 565 respectively).

Tissue volume changes over time

The rate of change of BPF was significantly higher in the MS compared with the control subjects (difference P=0.010; -0.002 per year in NC, CI -0.006 to 0.003; -0.010 in MS subjects, CI -0.014 to -0.006; model R^2=0.954). Similarly GMF decreased significantly faster in the MS compared with the NC subjects (difference P=0.013; -0.0022 per year in NC, CI -0.006 to 0.002; -0.009 per year in the MS subjects, CI -0.012 to -0.005; model R^2=0.950). No such significant difference was observed in the WMF. These patterns can be seen in Table 4.4a.

Lesion volume changes over time

There was no evidence of significant change in lesion loads over the 18 months of follow-up for the whole MS sample (Table 4.4b). Estimated mean changes (CI) in lesion loads (ml per year) were for T_1: -0.164 (-0.482 to 0.153), P=0.302; T_2: 0.071 (-0.592 to 0.733), P=0.830; Gd-enhancing: -0.080 (-0.389 to 0.229), P=0.601; 3D FSPGR: 0.200 (-0.188 to 0.587), P=0.303.

Associations between fractional tissue volumes and lesions volumes

3D FSPGR, T2 and T1 lesion loads significantly influenced WMF (0.002 per lesion ml, CI 0.001 to 0.004, P=0.007; 0.001 per lesion ml, CI 0.000 to 0.002,

P=0.010; 0.002 per lesion ml, CI 0.000 to 0.005, P=0.027 respectively), otherwise no associations were observed.

Clinical measures

In the 18 months prior to baseline there was a mean of 1.6 relapses per subject, median 1, range 0 to 3; in the 18 months of follow-up there was a mean of 1.5 relapses per subject, median 1, range 0 to 6.

There was a suggestion that EDSS score at the end of follow-up was higher than at baseline (P=0.053, Wilcoxon Sign Rank test). While there was no clear evidence of change in the overall MSFC scores over follow-up (Table 4.4c) (0.062 per year; CI -0.125 to 0.248; P=0.507), patients appeared to improve on the HPT (average reciprocal value as used to estimate MSFC; 0.003 per year; CI 0.001 to 0.005; P=0.010) and PASAT (4.095 per year; CI 0.783 to 7.406; P=0.017) components, while deteriorating on the TWT component (0.303 per year; CI 0.001 to 0.605; P=0.049).

Discussion

Disease related tissue atrophy

The results of this study suggest that while WM atrophy may be more apparent at baseline, GM changes are more dynamic over the period of observation. These results appear consistent with the previous cross-sectional work on this cohort (section 3.2.1), confirming an association between GM - but not WM - atrophy and disease duration. Further, in subjects with clinically isolated syndromes suggestive of demyelination, WM atrophy has been observed while GM atrophy has not (Traboulsee *et al.*,2002), indicating that WM atrophy may be an early event. Subsequent longitudinal work appears to support these findings, noting progressive

GM volume loss in subjects with CIS (Dalton *et al.*,2004), RRMS (Valsasina *et al.*,2005) and PPMS (Sastre-Garriga *et al.*,2005a). Similarly progressive GM changes have also been observed with DTI (Oreja-Guevara *et al.*,2005).

Considering the WM observations first, these suggest that atrophy in WM is either of earlier onset and a less rapid process than that seen in GM, or that they are non-linear processes that need not occur concurrently. The two may be related, with a variable time delay, or they may be semi-independent. The results raise the question of when, if ever, the WM volume in MS subjects was normal? The rates of change observed in this study, if linear from onset, would suggest that WM abnormalities might have occurred several years in advance of clinical onset of MS. However, atrophy may not be a linear process, and as such we may simply be observing a period of relative WM volume stability, with previously more rapid WM atrophy. This apparent stability may not be matched by pathological quiescence: oedema and cellular infiltration associated with inflammation may mask concurrent axonal degeneration and myelin loss. The present data cannot directly answer these questions but further work focusing on subjects with clinically isolated syndromes and continued follow-up of the present cohort may offer useful insight.

GM atrophy in the MS subjects, while modest at baseline, progressed at a rate in excess of that observed with normal ageing. Backward linear projections would suggest that, in contrast to WM effects, this process began at around the same time as clinical onset of the disease.

Tissue specific atrophy and focal lesions

The MS subjects had a relatively limited range of lesion loads with no readily apparent sustained change in brain lesion loads over the 18 months of follow-up, and

this counsels caution when interpreting results. WMF appeared to be modestly related to lesion 3D FSPGR and T_1 lesion loads, although BPF and GMF were not. Considered overall, these results suggest that GM and WM volumes may be differentially influenced by focal lesion genesis.

The modest correlations also suggest that in general the relationship between focal lesion genesis and atrophy is not strong and that additional factors may have a significant role to play in determining tissue loss.

Pathological basis of atrophy

The apparent dissociation of GM and WM atrophy raises questions as to the pathological interpretation of these changes. With certain caveats, it appears reasonable to assume that neuronal and axonal loss is a significant component of observed atrophy (Miller *et al.*,2002). However, if this equally affected neuronal cell bodies and axonal projections we may expect to observe both GM and WM atrophy in equal proportion. Given this, either the magnitude of axonal loss is greater than neuronal cell body loss in early relapsing-remitting MS or other factors, such as demyelination, contribute directly towards apparent WM atrophy.

Demyelination may lead to axonal atrophy (Yin *et al.*,1998), and increased vulnerability to additional stressors such as nitric oxide (Smith *et al.*,2001). However, this need not immediately lead to axonal (Kornek *et al.*,2000) or neuronal cell body loss. The findings of this study could be interpreted as showing pre-existing WM focal demyelination and axonal damage (decrease in WMF on entry to the study) priming subsequent neuronal cell body atrophy and loss (progressive decrease in GMF during the study). If this were the case then we would anticipate that GM changes would eventually be in proportion to those in WM, although there

may be a substantial delay before parity is reached. An alternative interpretation is that GM and WM atrophy are at least semi-independent, and that mechanisms for neuronal cell body damage may differ from those leading to axonal and myelin loss in white matter.

Clinical features and tissue specific atrophy

The cohort of MS subjects included in this study showed only limited clinical impairment (Table 4.4c), with a modest increase in EDSS concurrent with improvements in scores on HPT and PASAT. These latter observations may represent a learning effect, and as such be biasing the MSFC against detecting progressive neurological impairment. Given this, it was felt inappropriate to explore longitudinal associations, and accordingly the results are not presented. Further work is required to optimise the use of longitudinal clinical data, paying particular attention to the interplay between neurological function and potential learning effects. The inclusion of a greater range of cognitive assessments should also be considered.

Study limitations

There are a number of study limitations that should be recalled when considering the results, as previously outlined in section 4.2. It is reassuring to note that lesion misclassification or associated segmentation bias is unlikely to markedly influence any conclusions drawn from the results presented here: MS associated reductions in WMF volumes are around four times greater than the total observable brain lesion loads (relative to TI volumes), while the rate of change in GMF volumes was about 50 times greater than that of concurrent changes in lesion loads (relative to TI volumes).

Conclusions

In this early relapsing-remitting MS cohort, while WM atrophy was more apparent at baseline, progressive GM atrophy was more noticeable over the 18 months of follow-up. This suggests that factors leading to WM and GM atrophy may be semi-independent of each other or temporally dissociated, or both. The results also indicate that the relationship between focal lesion genesis and both GM and WM atrophy is limited and that other factors may have a significant role to play determining atrophy. Further work is required to confirm the present observations independently (although longer follow up of the same cohort yields concordant results (Tiberio *et al.*,2005)), to explore the dynamics of tissue specific atrophy over greater periods of follow-up, and to address more effectively any potential links between tissue specific atrophy, focal lesion genesis and clinical outcome.

Time-point	Tissue volume					
	BPF		GMF		WMF	
	MS	NC	MS	NC	MS	NC
Baseline	0.82, 0.82, 0.74 to 0.85	0.84, 0.84, 0.78 to 0.87	0.55, 0.55, 0.49 to 0.59	0.55, 0.55, 0.52 to 0.58	0.27, 0.27, 0.25 to 0.30	0.29, 0.29, 0.27 to 0.30
6 months	0.81, 0.81, 0.72 to 0.85	0.83, 0.84, 0.78 to 0.86	0.54, 0.54, 0.47 to 0.58	0.55, 0.55, 0.51 to 0.58	0.27, 0.27, 0.25 to 0.30	0.28, 0.28, 0.27 to 0.30
12 months	0.80, 0.81, 0.72 to 0.84	0.84, 0.84, 0.79 to 0.87	0.54, 0.54, 0.47 to 0.58	0.55, 0.55, 0.52 to 0.58	0.27, 0.27, 0.25 to 0.30	0.29, 0.29, 0.27 to 0.30
18 months	0.80, 0.81, 0.71 to 0.84	0.83, 0.83, 0.77 to 0.87	0.53, 0.54, 0.47 to 0.57	0.55, 0.55, 0.51 to 0.58	0.27, 0.27, 0.24 to 0.31	0.29, 0.29, 0.27 to 0.30

Table 4.4a: Fractional brain tissue volumes (mean, median and range) in MS and NC subjects throughout the 18 months of follow-up MS n=13 except at 12 months when n=12; NC n=9 except at 12 months when n=8.

Time-point	Lesion volume measure			
	3D FSPGR	T_2	T_1	Gd-enhancing
Baseline	6.3, 3.3, 0.5 to 21.0	7.2, 4.5, 1.4 to 26.6	1.5, 0.5, 0.0 to 9.9	0.6, 0.2, 0.0 to 4.3
6 months	6.2, 3.3, 0.6 to 21.0	7.1, 3.8, 1.0 to 29.2	1.1, 0.5, 0.0 to 7.9	0.2, 0.1, 0.0 to 0.9
12 months	6.8, 3.6, 1.0 to 21.5	7.8, 5.0, 2.0 to 28.1	1.4, 0.8, 0.0 to 7.3	0.4, 0.2, 0.0 to 1.3
18 months	6.6, 3.5, 0.4 to 22.4	7.3, 5.0, 0.8 to 26.7	1.2, 0.7, 0.1 to 6.3	0.4, 0.1, 0.0 to 2.5

Table 4.4b: Lesion volumes (mean, median and range) in the MS subjects throughout the 18 months of follow-up; n=13 except at 12 months when n=12.

Time-point	Clinical measure				
	EDSS	MSFC	TWT	HPT	PASAT
Baseline	1.0, 1.0, 0.0 to 2.0	0.0, 0.1, -0.99 to 0.86	4.3, 4.3, 3.8 to 5.5	21.3, 19.7, 16.8 to 29.8	46.5, 52.0, 11.0 to 60.0
6 months	1.6, 2.0, 0.0 to 3.0	0.0, 0.4, -2.0 to 0.9	4.5, 4.1, 3.5 to 7.3	21.0, 19.3, 16.4 to 30.1	50.8, 56.0, 23.0 to 60.0
12 months	1.4, 1.5, 0.0 to 2.5	0.3, 0.4, -1.1 to 1.1	4.5, 4.4, 4.0 to 5.5	19.5, 18.5, 15.0 to 32.5	56.3, 57.0, 51.0 to 60.0
18 months	1.6, 1.5, 0.0 to 3.5	0.1, 0.3, -1.9 to 1.0	4.7, 4.7, 3.7 to 7.3	19.8, 18.7, 15.8 to 31.0	50.0, 55.0, 13.0 to 60.0

Table 4.4c: Clinical measures (mean, median, and range) in MS subjects throughout the 18-month of follow-up; n=13 except at 12 months when n=12.

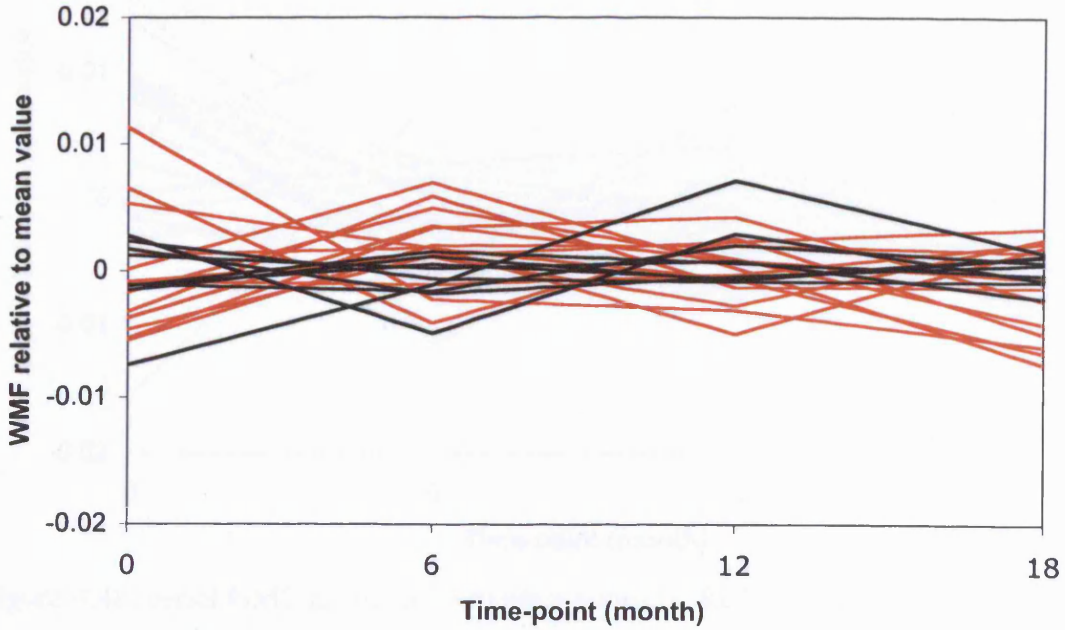

Figure 4.4a: serial WMF results in individual subjects. Red lines indicate data from MS subjects; black lines represent data from NC.

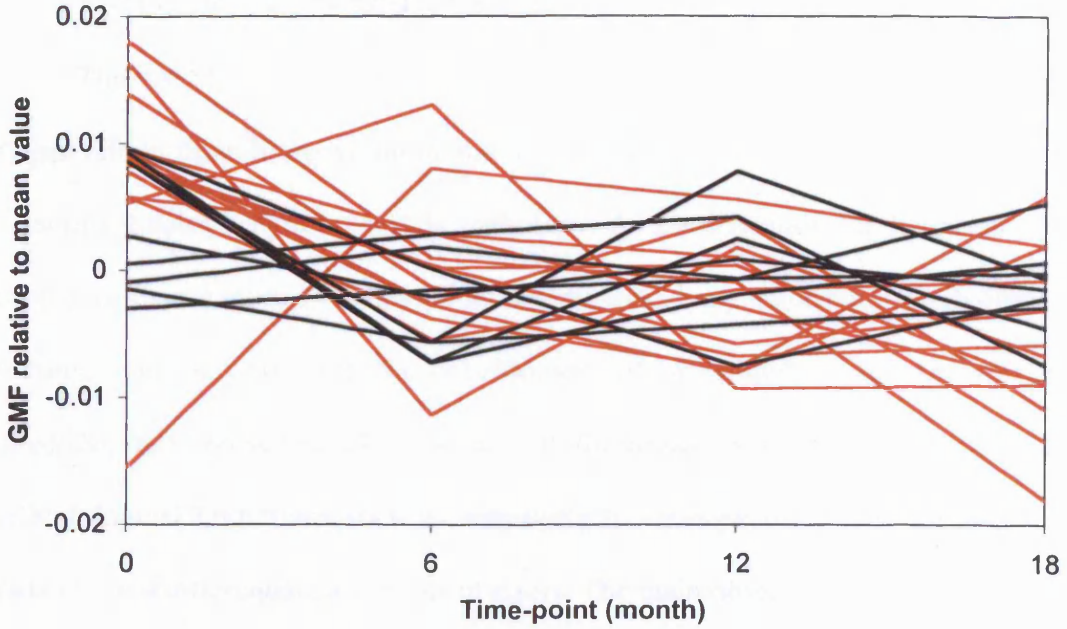

Figure 4.4b: serial GMF results in individual subjects. Red lines indicate data from MS subjects; black lines represent data from NC.

5 SUMMARY AND CONCLUSIONS

The main focus of the work contained in this thesis has been the study of MS disease effects upon tissue volumes and tissue metabolite concentration with a view to gaining greater insight in to early pathology, the inter-relationship between focal lesion genesis and more global tissue involvement, and any associations with clinical outcome. This has required the development of integrated approaches to data collection, data and statistical analyses, with the results being set in the context of methodological limitations such as sensitivity to cross-sectional and longitudinal gradients, and differential measurement errors. The main observations were that:

i. WM atrophy is more prominent than GM atrophy early in the course of the disease;

ii. Despite this, GM atrophy over an 18 month period of observation (covering disease durations from 1.9 to 3.4 years) is more rapid than that of WM;

iii. WM atrophy may precede both clinical onset and GM atrophy;

iv. In contrast, early metabolite alterations appear more prominent in GM compared with WM, with decreases in GM and WM tNAA, GM Glx and GM Cho, and increases in WM Ins;

v. Lesion loads appear to be associated with only a fraction of disease associated atrophy and metabolite concentration changes;

vi. Cross-sectional data suggest that there is a stronger association between GM compared with WM atrophy and lesion loads;

vii. Noting that the cohort studied had only limited clinical impairment; metabolite alterations appear more tightly related to clinical status than atrophy in the early stages of the disease.

Before considering these observations further, it should be noted that, given the number of statistical tests presented in this thesis, there is real potential for some of the results found to be significant at a $P<0.05$ level to be spurious, although it is not possible to definitively determine which without further independent studies being undertaken. In this regard: GM atrophy has been relatively consistently seen in subsequent cross-sectional and longitudinal studies, as has the limited relationship between brain lesion loads and atrophy (reviewed by Bermel & Bakshi, 2006); reduced brain GM and WM NAA levels have also been near constant findings, as noted in a recent meta-analysis by Caramanos *et al.* (2005) of 30 peer-reviewed published studies, along with increased WM Ins concentrations (Sastre-Garriga *et al.*, 2005b; Vrenken *et al.*, 2005; Fernando *et al.*, 2005); while GM Cho and Glx concentration reductions have not been reproduced, and as such should be regarded with due caution.

The results presented in this thesis would appear to suggest that neuronal metabolic dysfunction and loss are early events in the clinical course of MS, as is WM glial proliferation and or activation. It is also interesting to note that while reductions in tNAA are more marked in GM than WM, WM atrophy appears more marked than GM. Assuming that total neuronal and axonal populations may be estimated from tissue volume and tNAA concentrations, this suggests that total disease associated reductions in neuronal cell body (GM) and axonal (WM) populations are similar (~10% in GM and ~11% in WM), a perhaps surprisingly large disease effect to remain apparently clinically silent. Instead, metabolic dysfunction may be more tightly related to clinical status in the early stages of the disease, as indicated by associations between clinical measures, GM Glx and GM Cr.

This should not be taken as suggesting that metabolic dysfunction is more important in determining clinical outcome than neuronal and axonal loss. In the early stages, while not apparently overtly linked to clinical status, such cell loss may serve to magnify the effects of metabolic dysfunction, while later on it may assume a more overt role, as suggested by studies exploring cohorts with longer disease durations (De Stefano *et al.*,1998; De Stefano *et al.*,2001; Fu *et al.*,1998; Fu *et al.*,1996). Further, noting that elevations in WM Ins appear to be related to clinical status early in the clinical course of the disease, the potential importance of glial activiation and or proliferation in determinig longer term clinical outcomes should also not be overlooked. These are matters that the present work is unable to effectively resolve and it will require further longitudinal follow-up to attempt to do so.

It is also somewhat surprising that GM disease effects appear to be quite so extensive and at least as relevant to early clinical outcome as WM effects. Indeed, the limited relationship between WM changes and outcomes, when compared with GM findings, is curious and may in part be explained by the presence of a clinically less relevant process that differentially affects WM and GM. It has previously been noted that inflammation is more marked in WM than in GM lesions (Peterson *et al.*,2001) indicating the potential for such differential tissue effects.

The findings also serve to reiterate that the most obvious disease effect on MRI, the accumulation of focal lesions, need not determine absolutely the course of other more global processes. Global disease effects may be at least as important as focal lesion genesis when determining clinical outcome. This is not surprising when we recall that focal lesions constitute the minority of brain tissue, even in subjects with long-standing and clinically advanced MS. In the present cohort, on average

less than 1% of brain tissue was overtly abnormal on structural images; even if tissue destruction was absolute within such lesion, this would only account for a 1% reduction in axons. In contrast more subtle but global effects may constitute a ~10% reduction in brain neuronal and axonal populations. From the present work it is only possible to comment on the early stages of the disease, but studies looking at longer-term follow-up have similarly suggested a limited role for lesions in the long term (Brex *et al.*,2002; Beck *et al.*,2004; Chard *et al.*,2003; Jasperse *et al.*,2007).

It would be interesting to explore longitudinal changes in metabolite concentrations, but in the cohort available sensitivity to disease effects would be limited (see section 3.1.2). For the most reliable measure, WM tNAA as defined by CV, in 15 subjects changes of ~8% would be detectable, although this figure assumes only two measurements are made, one baseline and one follow-up. Indeed, preliminary analysis of data from 20 of the MS subjects included in the present work appears consistent with this, observing a partial recovery in WM tNAA concentrations, but otherwise no significant change in metabolite profiles (Tiberio *et al.*,2006).

It remains for the prognostic significant of early global changes to be determined and longitudinal studies should be undertaken to explore this along with characterising the dynamics of tissue damage on MS extending through from the earliest stages through to progressive phases of the disease. It may transpire that while lesions offer only limited prognostic information, this may be augmented by assessment of global tissue damage. In subjects with CIS, it would appear that changes in lesion loads in the first five years only partially relates to outcomes 14

years after disease onset, suggesting that early disease effects may have prognostic value (Brex *et al.*,2002).

In conclusion, the work contained in this thesis indicates that MS disease effects occur early; are more extensive than would be suggested if we were to consider focal lesions alone; and include neuronal and axonal damage, and glial activation and or proliferation. GM and WM effects may be either semi-independent of each other or focal lesion genesis, or be temporally separated, or both. Clinical outcome at an early stage of the disease does not appear to be strongly related to irreversible tissue degeneration but may be related to neuronal and axonal metabolic dysfunction, and glial activation or proliferation. Further multiparametric MR and clinical studies are required to confirm and expand upon these observations, hopefully including additional MR measures such as estimates of tissue relaxation, diffusion and magnetisation transfer characteristics; and additional clinical measures including a more complete assessment of cognitive function.

6 REFERENCES

Adalsteinsson E, Langer-Gould A, Homer RJ, Rao A, Sullivan EV, Lima CA, *et al.* Gray matter N-acetyl aspartate deficits in secondary progressive but not relapsing-remitting multiple sclerosis. AJNR Am J Neuroradiol 2003; 24: 1941-5.

Al-Araji AH, Oger J. Reappraisal of Lhermitte's sign in multiple sclerosis. Mult Scler 2005; 11: 398-402.

Alfano B, Brunetti A, Covelli EM, Quarantelli M, Panico MR, Ciarmiello A, *et al.* Unsupervised, automated segmentation of the normal brain using a multispectral relaxometric magnetic resonance approach. Magn Reson Med 1997; 37: 84-93.

Allen IV, McKeown SR. A histological, histochemical and biochemical study of the macroscopically normal white matter in multiple sclerosis. J Neurol Sci 1979; 41: 81-91.

Armstrong BK, White E, Saracci R. Principles of exposure measurement in epidemiology. Oxford: Oxford University Press, 1992.

Arnold JB, Liow JS, Schaper KA, Stern JJ, Sled JG, Shattuck DW, *et al.* Qualitative and quantitative evaluation of six algorithms for correcting intensity nonuniformity effects. Neuroimage 2001; 13: 931-943.

Ashburner J, Friston KJ. Voxel-based morphometry - the methods. Neuroimage 2000; 11: 805-821.

Babbe H, Roers A, Waisman A, Lassmann H, Goebels N, Hohlfeld R, *et al.* Clonal expansions of CD8(+) T cells dominate the T cell infiltrate in active multiple sclerosis lesions as shown by micromanipulation and single cell polymerase chain reaction. J Exp Med 2000; 192: 393-404.

Bakshi R, Ariyaratana S, Benedict RH, Jacobs L. Fluid-attenuated inversion recovery magnetic resonance imaging detects cortical and juxtacortical multiple sclerosis lesions. Arch Neurol 2001; 58: 742-748.

Bakshi R, Shaikh ZA, Janardhan V. MRI T2 shortening ('black T2') in multiple sclerosis: frequency, location, and clinical correlation. Neuroreport 2000; 11: 15-21.

Bammer R, Augustin M, Strasser-Fuchs S, Seifert T, Kapeller P, Stollberger R, *et al.* Magnetic resonance diffusion tensor imaging for characterizing diffuse and focal white matter abnormalities in multiple sclerosis. Magn Reson Med 2000; 44: 583-91.

Barnett MH, Prineas JW. Relapsing and remitting multiple sclerosis: pathology of the newly forming lesion. Ann Neurol 2004; 55: 458-68.

Baslow MH. Functions of N-acetyl-L-aspartate and N-acetyl-L-aspartylglutamate in the vertebrate brain: role in glial cell-specific signaling. J Neurochem 2000; 75: 453-459.

Beck RW, Smith CH, Gal RL, Xing D, Bhatti MT, Brodsky MC, *et al.* Neurologic impairment 10 years after optic neuritis. Arch Neurol 2004; 61: 1386-9.

Benedikz J, Magnusson H, Guthmundsson G. Multiple sclerosis in Iceland, with observations on the alleged epidemic in the Faroe Islands. Ann Neurol 1994; 36 Suppl 2: S175-S179.

Bermel RA, Bakshi R. The measurement and clinical relevnce of brain atrophy in multiple sclerosis. Lancet Neurol 2006; 5(2): 158-170.

Bermel RA, Sharma J, Tjoa CW, Puli SR, Bakshi R. A semiautomated measure of whole-brain atrophy in multiple sclerosis. J Neurol Sci 2003; 208: 57-65.

Bhakoo KK, Pearce D. In vitro expression of N-acetyl aspartate by oligodendrocytes: implications for proton magnetic resonance spectroscopy signal in vivo. J Neurochem 2000; 74: 254-262.

Bitsch A, Bruhn H, Vougioukas V, Stringaris A, Lassmann H, Frahm J, *et al.* Inflammatory CNS demyelination: histopathologic correlation with in vivo quantitative proton MR spectroscopy. AJNR Am J Neuroradiol 1999; 20: 1619-1627.

Bitsch A, Schuchardt J, Bunkowski S, Kuhlmann T, Bruck W. Acute axonal injury in multiple sclerosis. Correlation with demyelination and inflammation. Brain 2000; 123: 1174-1183.

Bjartmar C, Battistuta J, Terada N, Dupree E, Trapp BD. N-acetylaspartate is an axon-specific marker of mature white matter in vivo: A biochemical and immunohistochemical study on the rat optic nerve. Ann Neurol 2002; 51: 51-58.

Bjartmar C, Kidd G, Mork S, Rudick R, Trapp BD. Neurological disability correlates with spinal cord axonal loss and reduced N-acetyl aspartate in chronic multiple sclerosis patients. Ann Neurol 2000; 48: 893-901.

Bjartmar C, Kinkel RP, Kidd G, Rudick RA, Trapp BD. Axonal loss in normal-appearing white matter in a patient with acute MS. Neurology 2001; 57: 1248-1252.

Bland JM, Altman DG. Measurement error and correlation coefficients. BMJ 1996a; 313: 41-42.

Bland JM, Altman DG. Measurement error proportional to the mean [published erratum appears in BMJ 1996 Sep 21;313(7059):744]. BMJ 1996b; 313: 106.

Bland JM, Altman DG. Measurement error [corrected and republished article originally printed in BMJ 1996 Jun 29;312(7047):1654]. BMJ 1996c; 313: 744.

Bland M. Significance tests. An introduction to medical statistics. Oxford: Oxford University Press, 1987: 148-164.

Blatter DD, Bigler ED, Gale SD, Johnson SC, Anderson CV, Burnett BM, *et al.* Quantitative volumetric analysis of brain MR: normative database spanning 5 decades of life. AJNR Am J Neuroradiol 1995; 16: 241-251.

Bluml S, Seymour KJ, Ross BD. Developmental changes in choline- and ethanolamine-containing compounds measured with proton-decoupled (31)P MRS in in vivo human brain. Magn Reson Med 1999; 42: 643-654.

Bo L, Nyland H, Vedeler C, Trapp BD, Mork SJ. Extensive cortical demyelination in multiple sclerosis brains. Rev Neurol 2000; 156 Suppl 3: S25.

Bo L, Vedeler CA, Nyland H, Trapp BD, Mork SJ. Intracortical multiple sclerosis lesions are not associated with increased lymphocyte infiltration. Mult Scler 2003; 9: 323-31.

Boggild MD, Williams R, Haq N, Hawkins CP. Cortical plaques visualised by fluid-attenuated inversion recovery imaging in relapsing multiple sclerosis. Neuroradiology 1996; 38 Suppl 1: S10-S13.

Boulanger Y, Labelle M, Khiat A. Role of phospholipase A(2) on the variations of the choline signal intensity observed by 1H magnetic resonance spectroscopy in brain diseases. Brain Res Rev 2000; 33: 380-389.

Brand A, Richter-Landsberg C, Leibfritz D. Multinuclear NMR studies on the energy metabolism of glial and neuronal cells. Dev Neurosci 1993; 15: 289-298.

Brex PA, Ciccarelli O, O'Riordan JI, Sailer M, Thompson AJ, Miller DH. A longitudinal study of abnormalities on MRI and disability from multiple sclerosis. N Engl J Med 2002; 346: 158-164.

Brex PA, Jenkins R, Fox NC, Crum WR, O'Riordan JI, Plant GT, *et al.* Detection of ventricular enlargement in patients at the earliest clinical stage of MS. Neurology 2000a; 54: 1689-1691.

Brex PA, Leary SM, Plant GT, Thompson AJ, Miller DH. Magnetization transfer imaging in patients with clinically isolated syndromes suggestive of multiple sclerosis. AJNR Am J Neuroradiol 2001; 22: 947-51.

Brex PA, Parker GJ, Leary SM, Molyneux PD, Barker GJ, Davie CA, *et al.* Lesion heterogeneity in multiple sclerosis: a study of the relations between appearances on T1 weighted images, T1 relaxation times, and metabolite concentrations. J Neurol Neurosurg Psychiatry 2000b; 68: 627-632.

Brink BP, Veerhuis R, Breij EC, van der Valk P, Dijkstra CD, Bo L. The pathology of multiple sclerosis is location-dependent: no significant complement activation is detected in purely cortical lesions. J Neuropathol Exp Neurol 2005; 64: 147-55.

Brownell B, Hughes JT. The distribution of plaques in the cerebrum in multiple sclerosis. J Neurol Neurosurg Psychiatry 1962; 25: 315-320.

Bruck W, Bitsch A, Kolenda H, Bruck Y, Stiefel M, Lassmann H. Inflammatory central nervous system demyelination: correlation of magnetic resonance imaging findings with lesion pathology. Ann Neurol 1997; 42: 783-793.

Brunetti A, Postiglione A, Tedeschi E, Ciarmiello A, Quarantelli M, Covelli EM, *et al.* Measurement of global brain atrophy in Alzheimer's disease with unsupervised segmentation of spin-echo MRI studies. J Magn Reson Imaging 2000; 11: 260-266.

Brusa A, Jones SJ, Plant GT. Long-term remyelination after optic neuritis: A 2-year visual evoked potential and psychophysical serial study. Brain 2001; 124: 468-479.

Caramanos Z, Narayanan S, Arnold DL. 1H-MRS quantification of tNA and tCr in patients with multiple sclerosis: a meta-analystic review. Brain 2005; 128: 2483-2506.

Carswell R. Pathological anatomy: illustrations of the elementary forms of disease. London: Longman, 1838.

Cercignani M, Bozzali M, Iannucci G, Comi G, Filippi M. Magnetisation transfer ratio and mean diffusivity of normal appearing white and grey matter from patients with multiple sclerosis. J Neurol Neurosurg Psychiatry 2001; 70: 311-317.

Cercignani M, Iannucci G, Rocca MA, Comi G, Horsfield MA, Filippi M. Pathologic damage in MS assessed by diffusion-weighted and magnetization transfer MRI. Neurology 2000; 54: 1139-1144.

Cermelli C, Jacobson S. Viruses and multiple sclerosis. Viral Immunol 2000; 13: 255-267.

Chakraborty G, Mekala P, Yahya D, Wu G, Ledeen RW. Intraneuronal N-acetylaspartate supplies acetyl groups for myelin lipid synthesis: evidence for myelin-associated aspartoacylase. J Neurochem 2001; 78: 736-745.

Chang A, Tourtellotte WW, Rudick R, Trapp BD. Premyelinating oligodendrocytes in chronic lesions of multiple sclerosis. N Engl J Med 2002; 346: 165-173.

Chang L, Ernst T, Poland RE, Jenden DJ. In vivo proton magnetic resonance spectroscopy of the normal aging human brain. Life Sci 1996; 58: 2049-2056.

Charcot JM. Lectures on the diseases of the nervous system. London: The New Sydenham Society, 1877.

Chard DT, Brex PA, Ciccarelli O, Griffin CM, Parker GJ, Dalton C, *et al.* The longitudinal relation between brain lesion load and atrophy in multiple sclerosis: a 14 year follow up study. J Neurol Neurosurg Psychiatry 2003; 74: 1551-4.

Chari DM, Blakemore WF. New insights into remyelination failure in multiple sclerosis: implications for glial cell transplantation. Mult Scler 2002; 8: 271-277.

Ciccarelli O, Giugni E, Paolillo A, Mainero C, Gasperini C, Bastianello S, *et al.* Magnetic resonance outcome of new enhancing lesions in patients with relapsing-remitting multiple sclerosis. Eur J Neurol 1999; 6: 455-459.

Ciccarelli O, Werring DJ, Wheeler-Kingshott CA, Barker GJ, Parker GJ, Thompson AJ, *et al.* Investigation of MS normal-appearing brain using diffusion tensor MRI with clinical correlations. Neurology 2001; 56: 926-933.

Cifelli A, Arridge M, Jezzard P, Esiri MM, Palace J, Matthews PM. Thalamic neurodegeneration in multiple sclerosis. Ann Neurol 2002; 52: 650-3.

Coffey CE, Lucke JF, Saxton JA, Ratcliff G, Unitas LJ, Billig B, *et al.* Sex differences in brain aging: a quantitative magnetic resonance imaging study [published erratum appears in Arch Neurol 1998;55(5):627]. Arch Neurol 1998; 55: 169-179.

Coffey CE, Wilkinson WE, Parashos IA, Soady SA, Sullivan RJ, Patterson LJ, *et al.* Quantitative cerebral anatomy of the aging human brain: a cross- sectional study using magnetic resonance imaging. Neurology 1992; 42: 527-536.

Coles AJ, Wing MG, Molyneux P, Paolillo A, Davie CM, Hale G, *et al.* Monoclonal antibody treatment exposes three mechanisms underlying the clinical course of multiple sclerosis. Ann Neurol 1999; 46: 296-304.

Collins DJ, Narayanan S, Caramanos Z, De Stefano N, Arnold DL. Relation of Cerebral Atrophy in Multiple Sclerosis to Severity of Disease and Axonal Injury. Neurology 2000; 54: A17.

Compston A. The genetic epidemiology of multiple sclerosis. Philos Trans R Soc Lond B Biol.Sci. 1999; 354: 1623-1634.

Compston A, Coles A. Multiple sclerosis. Lancet 2002; 359: 1221-1231.

Compston DA, Morgan BP, Campbell AK, Wilkins P, Cole G, Thomas ND, *et al.* Immunocytochemical localization of the terminal complement complex in multiple sclerosis. Neuropathol Appl Neurobiol 1989; 15: 307-316.

Confavreux C, Vukusic S, Adeleine P. Early clinical predictors and progression of irreversible disability in multiple sclerosis: an amnesic process. Brain 2003; 126: 770-82.

Confavreux C, Vukusic S, Moreau T, Adeleine P. Relapses and progression of disability in multiple sclerosis. N Engl J Med 2000; 343: 1430-1438.

Corley SM, Ladiwala U, Besson A, Yong VW. Astrocytes attenuate oligodendrocyte death in vitro through an alpha(6) integrin-laminin-dependent mechanism. Glia 2001; 36: 281-294.

Cross AH, Trotter JL, Lyons J. B cells and antibodies in CNS demyelinating disease. J Neuroimmunol 2001; 112: 1-14.

Cruvellhier J. Anatonile pathologique du corps humain. Paris: Bailliere, 1842.

Cutter GR, Baier ML, Rudick RA, Cookfair DL, Fischer JS, Petkau J, *et al.* Development of a multiple sclerosis functional composite as a clinical trial outcome measure. Brain 1999; 122: 871-882.

Dalton CM, Brex PA, Jenkins R, Fox NC, Miszkiel KA, Crum WR, *et al.* Progressive ventricular enlargement in patients with clinically isolated syndromes is associated with the early development of multiple sclerosis. J Neurol Neurosurg Psychiatry 2002; 73: 141-147.

Dalton CM, Chard DT, Davies GR, Miszkiel KA, Altmann DR, Fernando K, *et al.* Early development of multiple sclerosis is associated with progressive grey matter atrophy in patients presenting with clinically isolated syndromes. Brain 2004; 127: 1101-7.

Davie CA, Barker GJ, Thompson AJ, Tofts PS, McDonald WI, Miller DH. 1H magnetic resonance spectroscopy of chronic cerebral white matter lesions and normal appearing white matter in multiple sclerosis. J Neurol Neurosurg Psychiatry 1997; 63: 736-742.

Davie CA, Hawkins CP, Barker GJ, Brennan A, Tofts PS, Miller DH, *et al.* Serial proton magnetic resonance spectroscopy in acute multiple sclerosis lesions. Brain 1994; 117: 49-58.

Davis FA, Bergen D, Schauf C, McDonald I, Deutsch W. Movement phosphenes in optic neuritis: a new clinical sign. Neurology 1976; 26: 1100-1104.

De Groot CJ, Bergers E, Kamphorst W, Ravid R, Polman CH, Barkhof F, *et al.* Post-mortem MRI-guided sampling of multiple sclerosis brain lesions: increased yield of active demyelinating and (p)reactive lesions. Brain 2001; 124: 1635-1645.

De Stefano N, Iannucci G, Sormani MP, Guidi L, Bartolozzi ML, Comi G, *et al.* MR correlates of cerebral atrophy in patients with multiple sclerosis. J Neurol 2002; 249: 1072-7.

De Stefano N, Matthews PM, Antel JP, Preul M, Francis G, Arnold DL. Chemical pathology of acute demyelinating lesions and its correlation with disability. Ann Neurol 1995; 38: 901-909.

De Stefano N, Matthews PM, Filippi M, Agosta F, De Luca M, Bartolozzi ML, *et al.* Evidence of early cortical atrophy in MS: relevance to white matter changes and disability. Neurology 2003; 60: 1157-62.

De Stefano N, Matthews PM, Fu L, Narayanan S, Stanley J, Francis GS, *et al.* Axonal damage correlates with disability in patients with relapsing- remitting multiple sclerosis. Results of a longitudinal magnetic resonance spectroscopy study. Brain 1998; 121: 1469-1477.

De Stefano N, Narayanan S, Francis GS, Arnaoutelis R, Tartaglia MC, Antel JP, *et al.* Evidence of Axonal Damage in the Early Stages of Multiple Sclerosis and Its Relevance to Disability. Arch Neurol 2001; 58: 65-70.

Dehmeshki J, Chard DT, Leary SM, Watt HC, Silver NC, Tofts PS, *et al.* The normal appearing grey matter in primary progressive multiple sclerosis A magnetisation transfer imaging study. J Neurol 2003; 250: 67-74.

Demougeot C, Garnier P, Mossiat C, Bertrand N, Giroud M, Beley A, *et al.* N-Acetylaspartate, a marker of both cellular dysfunction and neuronal loss: its relevance to studies of acute brain injury. J Neurochem 2001; 77: 408-415.

Evangelou N, Esiri MM, Smith S, Palace J, Matthews PM. Quantitative pathological evidence for axonal loss in normal appearing white matter in multiple sclerosis. Ann Neurol 2000; 47: 391-395.

Fawcett JW, Asher RA. The glial scar and central nervous system repair. Brain Res Bull 1999; 49: 377-391.

Felts PA, Baker TA, Smith KJ. Conduction in segmentally demyelinated mammalian central axons. J Neurosci 1997; 17: 7267-7277.

Ferguson B, Matyszak MK, Esiri MM, Perry VH. Axonal damage in acute multiple sclerosis lesions. Brain 1997; 120: 393-399.

Fernando KT, McLean MA, Chard DT, MacManus DG, Dalton CM, Miszkiel KA, *et al.* Elevated white matter myo-inositol in clinically isolated syndromes suggestive of multiple sclerosis. Brain 2004; 127: 1361-9.

Fernando KT, Tozer DJ, Miszkiel KA, Gordon RM, Swanton JK, Dalton CM, *et al.* Magnetization transfer histograms in clinically isolated syndromes suggestive of multiple sclerosis. Brain 2005; 128: 2911-25.

Filippi M, Campi A, Martinelli V, Colombo B, Yousry T, Canal N, *et al.* Comparison of triple dose versus standard dose gadolinium-DTPA for detection of MRI enhancing lesions in patients with primary progressive multiple sclerosis. J Neurol Neurosurg Psychiatry 1995; 59: 540-544.

Filippi M, Gawne-Cain ML, Gasperini C, vanWaesberghe JH, Grimaud J, Barkhof F, *et al.* Effect of training and different measurement strategies on the reproducibility of brain MRI lesion load measurements in multiple sclerosis. Neurology 1998a; 50: 238-244.

Filippi M, Horsfield MA, Rovaris M, Yousry T, Rocca MA, Baratti C, *et al.* Intraobserver and interobserver variability in schemes for estimating volume of brain lesions on MR images in multiple sclerosis. AJNR Am J Neuroradiol 1998b; 19: 239-244.

Filippi M, Iannucci G, Cercignani M, Assunta RM, Pratesi A, Comi G. A quantitative study of water diffusion in multiple sclerosis lesions and normal-appearing white matter using echo-planar imaging. Arch Neurol 2000; 57: 1017-1021.

Filippi M, Marciano N, Capra R, Rocca MA, Prandini F, Gasparotti R, *et al.* The effect of imprecise repositioning on lesion volume measurements in patients with multiple sclerosis. Neurology 1997a; 49: 274-276.

Filippi M, Rocca MA, Horsfield MA, Rovaris M, Pereira C, Yousry TA, *et al.* Increased spatial resolution using a three-dimensional T1-weighted gradient-echo

MR sequence results in greater hypointense lesion volumes in multiple sclerosis. AJNR Am J Neuroradiol 1998c; 19: 235-238.

Filippi M, Rovaris M, Sormani MP, Horsfield MA, Rocca MA, Capra R, *et al.* Intraobserver and interobserver variability in measuring changes in lesion volume on serial brain MR images in multiple sclerosis. AJNR Am J Neuroradiol 1998d; 19: 685-687.

Filippi M, van Waesberghe JH, Horsfield MA, Bressi S, Gasperini C, Yousry TA, *et al.* Interscanner variation in brain MRI lesion load measurements in MS: implications for clinical trials. Neurology 1997b; 49: 371-377.

Fischer JS, Jak AJ, Kniker JE, Rudick RA, Cutter G. Administration and scoring manual for the multiple sclerosis functional composite measure (MSFC). New York: Demos, 1999.

Freund RJ, Wilson WJ. Problems with the model. In: Freund RJ and Wilson WJ, editors. Regression analysis: statistical modeling of a response variable. San Diego: Academic Press, 1998: 229-269.

Fu L, Matthews PM, De Stefano N, Worsley KJ, Narayanan S, Francis GS, *et al.* Imaging axonal damage of normal-appearing white matter in multiple sclerosis. Brain 1998; 121: 103-113.

Fu L, Wolfson C, Worsley KJ, De Stefano N, Collins DL, Narayanan S, *et al.* Statistics for investigation of multimodal MR imaging data and an application to multiple sclerosis patients. NMR Biomed 1996; 9: 339-346.

Garbern JY, Yool DA, Moore GJ, Wilds IB, Faulk MW, Klugmann M, *et al.* Patients lacking the major CNS myelin protein, proteolipid protein 1, develop length-dependent axonal degeneration in the absence of demyelination and inflammation. Brain 2002; 125: 551-561.

Gasperini C, Paolillo A, Giugni E, Galgani S, Bagnato F, Mainero C, *et al.* MRI brain volume changes in relapsing-remitting multiple sclerosis patients treated with interferon beta-1a. Mult Scler 2002; 8: 119-23.

Gay FW, Drye TJ, Dick GW, Esiri MM. The application of multifactorial cluster analysis in the staging of plaques in early multiple sclerosis. Identification and characterization of the primary demyelinating lesion. Brain 1997; 120: 1461-1483.

Ge Y, Grossman RI, Udupa JK, Babb JS, Mannon LJ, McGowan JC. Magnetization transfer ratio histogram analysis of normal-appearing gray matter and normal-appearing white matter in multiple sclerosis. J Comput Assist Tomogr 2002; 26: 62-8.

Ge Y, Grossman RI, Udupa JK, Babb JS, Nyul LG, Kolson DL. Brain atrophy in relapsing-remitting multiple sclerosis: fractional volumetric analysis of gray matter and white matter. Radiology 2001; 220: 606-610.

Ge Y, Grossman RI, Udupa JK, Wei L, Mannon LJ, Polansky M, *et al.* Brain atrophy in relapsing-remitting multiple sclerosis and secondary progressive multiple sclerosis: longitudinal quantitative analysis. Radiology 2000; 214: 665-670.

Geurts JJ, Bo L, Pouwels PJ, Castelijns JA, Polman CH, Barkhof F. Cortical lesions in multiple sclerosis: combined postmortem MR imaging and histopathology. AJNR Am J Neuroradiol 2005; 26: 572-7.

Glanville NT, Byers DM, Cook HW, Spence MW, Palmer FB. Differences in the metabolism of inositol and phosphoinositides by cultured cells of neuronal and glial origin. Biochim Biophys Acta 1989; 1004: 169-179.

Good CD, Johnsrude I, Ashburner J, Henson RN, Friston KJ, Frackowiak RS. Cerebral asymmetry and the effects of sex and handedness on brain structure: a voxel-based morphometric analysis of 465 normal adult human brains. Neuroimage. 2001; 14: 685-700.

Goodkin DE, Hertsgaard D, Seminary J. Upper extremity function in multiple sclerosis: improving assessment sensitivity with Box-and-Block and Nine-Hole Peg Tests. Arch Phys Med Rehabil 1988; 69: 850-854.

Goodkin DE, Rooney WD, Sloan R, Bacchetti P, Gee L, Vermathen M, *et al.* A serial study of new MS lesions and the white matter from which they arise. Neurology 1998; 51: 1689-1697.

Govindaraju V, Young K, Maudsley AA. Proton NMR chemical shifts and coupling constants for brain metabolites. NMR Biomed 2000; 13: 129-153.

Grachev ID, Apkarian AV. Chemical heterogeneity of the living human brain: a proton MR spectroscopy study on the effects of sex, age, and brain region. Neuroimage 2000; 11: 554-563.

Griffin CM, Chard DT, Parker GJ, Barker GJ, Thompson AJ, Miller DH. The relationship between lesion and normal appearing brain tissue abnormalities in early relapsing remitting multiple sclerosis. J Neurol 2002a; 249: 193-199.

Griffin CM, Dehmeshki J, Chard DT, Parker GJ, Barker GJ, Thompson AJ, *et al.* T1 histograms of normal-appearing brain tissue are abnormal in early relapsing-remitting multiple sclerosis. Mult Scler 2002b; 8: 211-6.

Griffin CM, Parker GJ, Barker GJ, Thompson AJ, Miller DH. MTR and T1 provide complementary information in MS NAWM, but not in lesions. Mult Scler 2000; 6: 327-331.

Griffin JL, Bollard M, Nicholson JK, Bhakoo K. Spectral profiles of cultured neuronal and glial cells derived from HRMAS 1H NMR spectroscopy. NMR Biomed 2002c.

Gronwell DMA. Paced auditory serial-addition task: a measure of recovery from concussion. Percept Mot Skills 1977; 44: 367-373.

Guo AC, MacFall JR, Provenzale JM. Multiple sclerosis: diffusion tensor MR imaging for evaluation of normal-appearing white matter. Radiology 2002; 222: 729-36.

Gur RC, Mozley PD, Resnick SM, Gottlieb GL, Kohn M, Zimmerman R, *et al.* Gender differences in age effect on brain atrophy measured by magnetic resonance imaging. Proc Natl Acad Sci U.S.A 1991; 88: 2845-2849.

Gur RC, Turetsky BI, Matsui M, Yan M, Bilker W, Hughett P, *et al.* Sex differences in brain gray and white matter in healthy young adults: correlations with cognitive performance. J Neurosci 1999; 19: 4065-4072.

Guseo A, Jellinger K. The significance of perivascular infiltrations in multiple sclerosis. J Neurol 1975; 211: 51-60.

Guttmann CR, Jolesz FA, Kikinis R, Killiany RJ, Moss MB, Sandor T, *et al.* White matter changes with normal aging. Neurology 1998; 50: 972-978.

Halliday AM, McDonald WI, Mushin J. Delayed visual evoked response in optic neuritis. Lancet 1972; 1: 982-985.

Harris GJ, Barta PE, Peng LW, Lee S, Brettschneider PD, Shah A, *et al.* MR volume segmentation of gray matter and white matter using manual thresholding: dependence on image brightness. AJNR Am J Neuroradiol 1994a; 15: 225-230.

Harris GJ, Schlaepfer TE, Peng LW, Lee S, Federman EB, Pearlson GD. Magnetic resonance imaging evaluation of the effects of ageing on grey- white ratio in the human brain. Neuropathol Appl Neurobiol 1994b; 20: 290-293.

Harris JO, Frank JA, Patronas N, McFarlin DE, McFarland HF. Serial gadolinium-enhanced magnetic resonance imaging scans in patients with early, relapsing-remitting multiple sclerosis: implications for clinical trials and natural history. Ann Neurol 1991; 29: 548-555.

Hobart J, Freeman J, Thompson A. Kurtzke scales revisited: the application of psychometric methods to clinical intuition. Brain 2000; 123: 1027-1040.

Hobart J, Lamping D, Fitzpatrick R, Riazi A, Thompson A. The Multiple Sclerosis Impact Scale (MSIS-29): a new patient-based outcome measure. Brain 2001; 124: 962-973.

Hohlfeld R. Myelin failure in multiple sclerosis: breaking the spell of Notch. Nat Med 2002; 8: 1075-1076.

Hoogervorst EL, van Winsen LM, Eikelenboom MJ, Kalkers NF, Uitdehaag BM, Polman CH. Comparisons of patient self-report, neurologic examination, and functional impairment in MS. Neurology 2001; 56: 934-937.

Inglese M, Liu S, Babb JS, Mannon LJ, Grossman RI, Gonen O. Three-dimensional proton spectroscopy of deep gray matter nuclei in relapsing-remitting MS. Neurology 2004; 63: 170-2.

Jasperse B, Minneboo A, de Groot V, Kalkers NF, van Helden PE, Uitdehaag BM, *et al.* Determinants of cerebral atrophy rate at the time of diagnosis of multiple sclerosis. Arch Neurol 2007; 64: 190-4.

Jenkins R, Fox NC, Rossor AM, Harvey RJ, Rossor MN. Intracranial volume and Alzheimer disease: evidence against the cerebral reserve hypothesis. Arch Neurol 2000; 57: 220-224.

Jernigan TL, Archibald SL, Fennema-Notestine C, Gamst AC, Stout JC, Bonner J, *et al.* Effects of age on tissues and regions of the cerebrum and cerebellum. Neurobiol Aging 2001; 22: 581-594.

Kalkers NF, Bergers L, de G, V, Lazeron RH, van Walderveen MA, Uitdehaag BM, *et al.* Concurrent validity of the MS Functional Composite using MRI as a biological disease marker. Neurology 2001; 56: 215-219.

Kapeller P, McLean MA, Griffin CM, Chard D, Parker GJ, Barker GJ, *et al.* Preliminary evidence for neuronal damage in cortical grey matter and normal appearing white matter in short duration relapsing-remitting multiple sclerosis: a quantitative MR spectroscopic imaging study. J Neurol 2001; 248: 131-138.

Kapoor R, Davies M, Smith KJ. Temporary axonal conduction block and axonal loss in inflammatory neurological disease. A potential role for nitric oxide? Ann NYAcad Sci 1999; 893: 304-308.

Kappos L, Duda P. The Janus face of CNS-directed autoimmune response: a therapeutic challenge. Brain 2002; 125: 2379-80.

Karni A, Bakimer-Kleiner R, Abramsky O, Ben Nun A. Elevated levels of antibody to myelin oligodendrocyte glycoprotein is not specific for patients with multiple sclerosis. Arch Neurol 1999; 56: 311-315.

Katz D, Taubenberger JK, Cannella B, McFarlin DE, Raine CS, McFarland HF. Correlation between magnetic resonance imaging findings and lesion development in chronic, active multiple sclerosis. Ann Neurol 1993; 34: 661-669.

Kidd D, Barkhof F, McConnell R, Algra PR, Allen IV, Revesz T. Cortical lesions in multiple sclerosis. Brain 1999; 122: 17-26.

Koopmans RA, Li DK, Zhu G, Allen PS, Penn A, Paty DW. Magnetic resonance spectroscopy of multiple sclerosis: in-vivo detection of myelin breakdown products. Lancet 1993; 341: 631-632.

Kornek B, Lassmann H. Axonal pathology in multiple sclerosis. A historical note. Brain Pathol 1999; 9: 651-656.

Kornek B, Storch MK, Weissert R, Wallstroem E, Stefferl A, Olsson T, *et al.* Multiple sclerosis and chronic autoimmune encephalomyelitis: a comparative quantitative study of axonal injury in active, inactive, and remyelinated lesions. Am J Pathol 2000; 157: 267-276.

Kreutzberg GW. Microglia: a sensor for pathological events in the CNS. Trends Neurosci 1996; 19: 312-318.

Kuhlmann T, Lingfeld G, Bitsch A, Schuchardt J, Bruck W. Acute axonal damage in multiple sclerosis is most extensive in early disease stages and decreases over time. Brain 2002; 125: 2202-12.

Kurtzke JF. Rating neurologic impairment in multiple sclerosis: an expanded disability status scale (EDSS). Neurology 1983; 33: 1444-1452.

Kurtzke JF. Epidemiologic evidence for multiple sclerosis as an infection. Clin Microbiol Rev 1993; 6: 382-427.

Lai M, Hodgson T, Gawne-Cain M, Webb S, MacManus D, McDonald WI, *et al.* A preliminary study into the sensitivity of disease activity detection by serial weekly

magnetic resonance imaging in multiple sclerosis. J Neurol Neurosurg Psychiatry 1996; 60: 339-341.

Leary SM, Brex PA, MacManus DG, Parker GJ, Barker GJ, Miller DH, *et al.* A (1)H magnetic resonance spectroscopy study of aging in parietal white matter: implications for trials in multiple sclerosis. Magn Reson Imaging 2000; 18: 455-459.

Leary SM, Davie CA, Parker GJ, Stevenson VL, Wang L, Barker GJ, *et al.* 1H magnetic resonance spectroscopy of normal appearing white matter in primary progressive multiple sclerosis. J Neurol 1999a; 246: 1023-1026.

Leary SM, Silver NC, Stevenson VL, Barker GJ, Miller DH, Thompson AJ. Magnetisation transfer of normal appearing white matter in primary progressive multiple sclerosis. Mult Scler 1999b; 5: 313-316.

Lee MA, Smith S, Palace J, Matthews PM. Defining multiple sclerosis disease activity using MRI T2-weighted difference imaging. Brain 1998; 121: 2095-2102.

Lee MA, Smith S, Palace J, Narayanan S, Silver N, Minicucci L, *et al.* Spatial mapping of T2 and gadolinium-enhancing T1 lesion volumes in multiple sclerosis: evidence for distinct mechanisms of lesion genesis? Brain 1999; 122: 1261-1270.

Leigh R, Ostuni J, Pham D, Goldszal A, Lewis BK, Howard T, *et al.* Estimating cerebral atrophy in multiple sclerosis patients from various MR pulse sequences. Mult Scler 2002; 8: 420-429.

Lim KO, Zipursky RB, Watts MC, Pfefferbaum A. Decreased gray matter in normal aging: an in vivo magnetic resonance study. J Gerontol 1992; 47: B26-B30.

Linington C, Lassmann H. Antibody responses in chronic relapsing experimental allergic encephalomyelitis: correlation of serum demyelinating activity with antibody titre to the myelin/oligodendrocyte glycoprotein (MOG). J Neuroimmunol 1987; 17: 61-9.

Liu C, Edwards S, Gong Q, Roberts N, Blumhardt LD. Three dimensional MRI estimates of brain and spinal cord atrophy in multiple sclerosis J Neurol Neurosurg Psychiatry 1999; 66: 323-330.

Losseff NA, Wang L, Lai HM, Yoo DS, Gawne-Cain ML, McDonald WI, *et al.* Progressive cerebral atrophy in multiple sclerosis. A serial MRI study. Brain 1996; 119: 2009-2019.

Lublin FD, Reingold SC. Defining the clinical course of multiple sclerosis: results of an international survey. National Multiple Sclerosis Society (USA) Advisory Committee on Clinical Trials of New Agents in Multiple Sclerosis. Neurology 1996; 46: 907-911.

Lubrich B, Spleiss O, Gebicke-Haerter PJ, van Calker D. Differential expression, activity and regulation of the sodium/myo- inositol cotransporter in astrocyte cultures from different regions of the rat brain. Neuropharmacology 2000; 39: 680-690.

Lucchinetti C, Bruck W, Parisi J, Scheithauer B, Rodriguez M, Lassmann H. Heterogeneity of multiple sclerosis lesions: implications for the pathogenesis of demyelination. Ann Neurol 2000; 47: 707-717.

Luks TL, Goodkin DE, Nelson SJ, Majumdar S, Bacchetti P, Portnoy D, *et al.* A longitudinal study of ventricular volume in early relapsing-remitting multiple sclerosis. Mult Scler 2000; 6: 332-337.

Lumsden CE. The neuropathology of multipe sclerosis. In: P.J. V and G.W. B, editors. Handbook of clinical neurology. Vol 9. Amsterdam: North-Holland, 1970: 217-309.

MacDonald BK, Cockerell OC, Sander JW, Shorvon SD. The incidence and lifetime prevalence of neurological disorders in a prospective community-based study in the UK. Brain 2000; 123: 665-676.

Mader I, Roser W, Kappos L, Hagberg G, Seelig J, Radue EW, *et al.* Serial proton MR spectroscopy of contrast-enhancing multiple sclerosis plaques: absolute metabolic values over 2 years during a clinical pharmacological study. AJNR Am J Neuroradiol 2000; 21: 1220-1227.

Mader I, Seeger U, Weissert R, Klose U, Naegele T, Melms A, *et al.* Proton MR spectroscopy with metabolite-nulling reveals elevated macromolecules in acute multiple sclerosis. Brain 2001; 124: 953-961.

Mancardi G, Hart BA, Capello E, Brok HP, Ben Nun A, Roccatagliata L, *et al.* Restricted immune responses lead to CNS demyelination and axonal damage. J Neuroimmunol. 2000; 107: 178-183.

Martin E, Capone A, Schneider J, Hennig J, Thiel T. Absence of N-acetylaspartate in the human brain: impact on neurospectroscopy? Ann Neurol 2001; 49: 518-521.

Mathalon DH, Sullivan EV, Rawles JM, Pfefferbaum A. Correction for head size in brain-imaging measurements [published erratum appears in Psychiatry Res 1994;55(3):179]. Psychiatry Res 1993; 50: 121-139.

McDonald WI, Compston A, Edan G, Goodkin D, Hartung H-P, Lublin FD, *et al.* Recommended Diagnostic Criteria for Multple Sclerosis: Guidelines from the International Panel on the Diagnosis of Multiple Sclerosis. Ann Neurol 2001; 50: 121-127.

McFarland HF, Barkhof F, Antel J, Miller DH. The role of MRI as a surrogate outcome measure in multiple sclerosis. Mult Scler 2002; 8: 40-51.

McLean MA, Simister RJ, Barker GJ, Duncan JS. Metabolite nulling improves reliability of LCModel analysis of short echo time spectroscopy. Proc Soc Magn Reson Med 2002; 10: 529.

Medana I, Martinic MA, Wekerle H, Neumann H. Transection of major histocompatibility complex class I-induced neurites by cytotoxic T lymphocytes. Am J Pathol 2001; 159: 809-815.

Meier-Ruge W, Ulrich J, Bruhlmann M, Meier E. Age-related white matter atrophy in the human brain. Ann NY Acad Sci 1992; 673: 260-269.

Messert B, Wannamaker BB, Dudley AW, Jr. Reevaluation of the size of the lateral ventricles of the brain. Postmortem study of an adult population. Neurology 1972; 22: 941-951.

Miller AK, Alston RL, Corsellis JA. Variation with age in the volumes of grey and white matter in the cerebral hemispheres of man: measurements with an image analyser. Neuropathol Appl Neurobiol 1980; 6: 119-132.

Miller AK, Corsellis JA. Evidence for a secular increase in human brain weight during the past century. Ann Hum Biol 1977; 4: 253-257.

Miller BL. A review of chemical issues in 1H NMR spectroscopy: N-acetyl-L-aspartate, creatine and choline. NMR Biomed 1991; 4: 47-52.

Miller DH, Barkhof F, Frank JA, Parker GJ, Thompson AJ. Measurement of atrophy in multiple sclerosis: pathological basis, methodological aspects and clinical relevance. Brain 2002; 125: 1676-1695.

Miller DH, Rudge P, Johnson G, Kendall BE, MacManus DG, Moseley IF, *et al.* Serial gadolinium enhanced magnetic resonance imaging in multiple sclerosis. Brain 1988; 111: 927-939.

Minneboo A, Uitdehaag BM, Ader HJ, Barkhof F, Polman CH, Castelijns JA. Patterns of enhancing lesion evolution in multiple sclerosis are uniform within patients. Neurology 2005; 65: 56-61.

Mittal TK, Halpin SF, Bourne MW, Hourihan MD, Perkins T, Sun Y, *et al.* A prospective comparison of brain contrast characteristics and lesion detection using single-shot fast spin-echo and fast spin-echo. Neuroradiology 1999; 41: 480-486.

Mlynarik V, Gruber S, Moser E. Proton T (1) and T (2) relaxation times of human brain metabolites at 3 Tesla. NMR Biomed 2001; 14: 325-31.

Molyneux PD, Tofts PS, Fletcher A, Gunn B, Robinson P, Gallagher H, *et al.* Precision and reliability for measurement of change in MRI lesion volume in multiple sclerosis: a comparison of two computer assisted techniques. J Neurol Neurosurg Psychiatry 1998a; 65: 42-47.

Molyneux PD, Tubridy N, Parker GJ, Barker GJ, MacManus DG, Tofts PS, *et al.* The effect of section thickness on MR lesion detection and quantification in multiple sclerosis. AJNR Am J Neuroradiol 1998b; 19: 1715-1720.

Narayana PA, Doyle TJ, Lai D, Wolinsky JS. Serial proton magnetic resonance spectroscopic imaging, contrast- enhanced magnetic resonance imaging, and quantitative lesion volumetry in multiple sclerosis. Ann Neurol 1998; 43: 56-71.

Neale JH, Bzdega T, Wroblewska B. N-Acetylaspartylglutamate: the most abundant peptide neurotransmitter in the mammalian central nervous system. J Neurochem 2000; 75: 443-452.

Neumann H. Control of glial immune function by neurons. Glia 2001; 36: 191-199.

Oguro H, Okada K, Yamaguchi S, Kobayashi S. Sex differences in morphology of the brain stem and cerebellum with normal ageing. Neuroradiology 1998; 40: 788-792.

Onuki M, Ayers MM, Bernard CC, Orian JM. Axonal degeneration is an early pathological feature in autoimmune- mediated demyelination in mice. Microsc Res Tech 2001; 52: 731-739.

Oreja-Guevara C, Rovaris M, Iannucci G, Valsasina P, Caputo D, Cavarretta R, *et al.* Progressive gray matter damage in patients with relapsing-remitting multiple sclerosis: a longitudinal diffusion tensor magnetic resonance imaging study. Arch Neurol 2005; 62: 578-84.

Pakkenberg B, Gundersen HJ. Neocortical neuron number in humans: effect of sex and age. J Comp Neurol 1997; 384: 312-320.

Paolillo A, Bastianello S, Frontoni M, Gasperini C, Giugni E, Ciccarelli O, *et al.* Magnetic resonance imaging outcome of new enhancing lesions in relapsing-remitting multiple sclerosis patients treated with interferon beta1a. J Neurol 1999; 246: 443-448.

Paolillo A, Pozzilli C, Gasperini C, Giugni E, Mainero C, Giuliani S, *et al.* Brain atrophy in relapsing-remitting multiple sclerosis: relationship with 'black holes', disease duration and clinical disability. J Neurol Sci 2000; 174: 85-91.

Parry A, Clare S, Jenkinson M, Smith S, Palace J, Matthews PM. White matter and lesion T1 relaxation times increase in parallel and correlate with disability in multiple sclerosis. J Neurol 2002; 249: 1279-86.

Passe TJ, Rajagopalan P, Tupler LA, Byrum CE, MacFall JR, Krishnan KR. Age and sex effects on brain morphology. Prog Neuropsychopharmacol Biol Psychiatry 1997; 21: 1231-1237.

Peterson JW, Bo L, Mork S, Chang A, Trapp BD. Transected neurites, apoptotic neurons, and reduced inflammation in cortical multiple sclerosis lesions. Ann Neurol 2001; 50: 389-400.

Petroff OA, Spencer DD, Alger JR, Prichard JW. High-field proton magnetic resonance spectroscopy of human cerebrum obtained during surgery for epilepsy. Neurology 1989; 39: 1197-202.

Pfefferbaum A, Adalsteinsson E, Spielman D, Sullivan EV, Lim KO. In vivo spectroscopic quantification of the N-acetyl moiety, creatine, and choline from large volumes of brain gray and white matter: effects of normal aging. Magn Reson Med 1999; 41: 276-284.

Pfefferbaum A, Mathalon DH, Sullivan EV, Rawles JM, Zipursky RB, Lim KO. A quantitative magnetic resonance imaging study of changes in brain morphology from infancy to late adulthood. Arch Neurol 1994; 51: 874-887.

Plummer DL. Dispimage: a display and analysis tool for medical images. Revista Di Neuroradiologica 1992; 5: 489-495.

Polman CH, Reingold SC, Edan G, Filippi M, Hartung HP, Kappos L, *et al.* Diagnostic criteria for multiple sclerosis: 2005 revisions to the "McDonald Criteria". Ann Neurol 2005; 58: 840-6.

Poser CM, Paty DW, Scheinberg L, McDonald WI, Davis FA, Ebers GC, *et al.* New diagnostic criteria for multiple sclerosis: guidelines for research protocols. Ann Neurol 1983; 13: 227-231.

Prat A, Antel J. Pathogenesis of multiple sclerosis. Curr Opin Neurol 2005; 18: 225-30.

Prineas JW, Connell F. Remyelination in multiple sclerosis. Ann Neurol 1979; 5: 22-31.

Provencher SW. Estimation of metabolite concentrations from localized in vivo proton NMR spectra. Magn Reson Med 1993; 30: 672-679.

Quarantelli M, Ciarmiello A, Morra VB, Orefice G, Larobina M, Lanzillo R, *et al.* Brain tissue volume changes in relapsing-remitting multiple sclerosis: correlation with lesion load. Neuroimage 2003; 18: 360-6.

Rao SM, Leo GJ, Bernardin L, Unverzagt F. Cognitive dysfunction in multiple sclerosis. I. Frequency, patterns, and prediction. Neurology 1991a; 41: 685-691.

Rao SM, Leo GJ, Ellington L, Nauertz T, Bernardin L, Unverzagt F. Cognitive dysfunction in multiple sclerosis. II. Impact on employment and social functioning. Neurology 1991b; 41: 692-696.

Raz N, Gunning FM, Head D, Dupuis JH, McQuain J, Briggs SD, *et al.* Selective aging of the human cerebral cortex observed in vivo: differential vulnerability of the prefrontal gray matter. Cereb Cortex 1997; 7: 268-282.

Redford EJ, Kapoor R, Smith KJ. Nitric oxide donors reversibly block axonal conduction: demyelinated axons are especially susceptible. Brain 1997; 120: 2149-2157.

Reiss AL, Abrams MT, Singer HS, Ross JL, Denckla MB. Brain development, gender and IQ in children. A volumetric imaging study. Brain 1996; 119: 1763-1774.

Resnick SM, Goldszal AF, Davatzikos C, Golski S, Kraut MA, Metter EJ, *et al.* One-year age changes in MRI brain volumes in older adults. Cereb Cortex 2000; 10: 464-472.

Rivera-Quinones C, McGavern D, Schmelzer JD, Hunter SF, Low PA, Rodriguez M. Absence of neurological deficits following extensive demyelination in a class I-deficient murine model of multiple sclerosis. Nat Med 1998; 4: 187-193.

Rodriguez M, Miller DJ, Lennon VA. Immunoglobulins reactive with myelin basic protein promote CNS remyelination. Neurology 1996; 46: 538-545.

Ron MA, Logsdail SJ. Psychiatric morbidity in multiple sclerosis: a clinical and MRI study. Psychol Med 1989; 19: 887-895.

Rooney WD, Goodkin DE, Schuff N, Meyerhoff DJ, Norman D, Weiner MW. 1H MRSI of normal appearing white matter in multiple sclerosis. Mult Scler 1997; 3: 231-237.

Rothman DL, Sibson NR, Hyder F, Shen J, Behar KL, Shulman RG. In vivo nuclear magnetic resonance spectroscopy studies of the relationship between the glutamate-glutamine neurotransmitter cycle and functional neuroenergetics. Philos Trans R Soc Lond B Biol Sci 1999; 354: 1165-1177.

Rovaris M, Bozzali M, Iannucci G, Ghezzi A, Caputo D, Montanari E, *et al.* Assessment of normal-appearing white and gray matter in patients with primary

progressive multiple sclerosis: a diffusion-tensor magnetic resonance imaging study. Arch Neurol 2002; 59: 1406-12.

Rovaris M, Filippi M, Minicucci L, Iannucci G, Santuccio G, Possa F, *et al.* Cortical/subcortical disease burden and cognitive impairment in patients with multiple sclerosis. AJNR Am J Neuroradiol 2000; 21: 402-408.

Rovaris M, Gawne-Cain ML, Sormani MP, Miller DH, Filippi M. The effect of repositioning on brain MRI lesion load assessment in multiple sclerosis: reliability of subjective quality criteria. J Neurol 1998a; 245: 273-275.

Rovaris M, Rocca MA, Capra R, Prandini F, Martinelli V, Comi G, *et al.* A comparison between the sensitivities of 3-mm and 5-mm thick serial brain MRI for detecting lesion volume changes in patients with multiple sclerosis. J Neuroimaging 1998b; 8: 144-147.

Rovaris M, Rocca MA, Sormani MP, Comi G, Filippi M. Reproducibility of brain MRI lesion volume measurements in multiple sclerosis using a local thresholding technique: effects of formal operator training. Eur Neurol 1999; 41: 226-230.

Roxburgh RH, Seaman SR, Masterman T, Hensiek AE, Sawcer SJ, Vukusic S, *et al.* Multiple Sclerosis Severity Score: using disability and disease duration to rate disease severity. Neurology 2005; 64: 1144-51.

Rudick RA, Fisher E, Lee JC, Simon J, Jacobs L. Use of the brain parenchymal fraction to measure whole brain atrophy in relapsing-remitting MS. Multiple Sclerosis Collaborative Research Group. Neurology 1999; 53: 1698-1704.

Ruiz-Pena JL, Pinero P, Sellers G, Argente J, Casado A, Foronda J, *et al.* Magnetic resonance spectroscopy of normal appearing white matter in early relapsing-remitting multiple sclerosis: correlations between disability and spectroscopy. BMC Neurol 2004; 4: 8.

Sailer M, Losseff NA, Wang L, Gawne-Cain ML, Thompson AJ, Miller DH. T1 lesion load and cerebral atrophy as a marker for clinical progression in patients with multiple sclerosis. A prospective 18 months follow-up study. Eur J Neurol 2001; 8: 37-42.

Saindane AM, Ge Y, Udupa JK, Babb JS, Mannon LJ, Grossman RI. The effect of gadolinium-enhancing lesions on whole brain atrophy in relapsing-remitting MS. Neurology 2000; 55: 61-65.

Sanfilipo MP, Benedict RH, Sharma J, Weinstock-Guttman B, Bakshi R. The relationship between whole brain volume and disability in multiple sclerosis: a comparison of normalized gray vs. white matter with misclassification correction. Neuroimage 2005; 26: 1068-77.

Sastre-Garriga J, Ingle GT, Chard DT, Cercignani M, Ramio-Torrenta L, Miller DH, *et al.* Grey and white matter volume changes in early primary progressive multiple sclerosis: a longitudinal study. Brain 2005a; 128: 1454-60.

Sastre-Garriga J, Ingle GT, Chard DT, Ramio-Torrenta L, McLean MA, Miller DH, *et al.* Metabolite changes in normal-appearing gray and white matter are linked with disability in early primary progressive multiple sclerosis. Arch Neurol 2005b; 62: 569-73.

Sastre-Garriga J, Ingle GT, Chard DT, Ramio-Torrenta L, Miller DH, Thompson AJ. Grey and white matter atrophy in early clinical stages of primary progressive multiple sclerosis. Neuroimage 2004; 22: 353-9.

Scheffe H. Random effects models and mixed models. The analysis of variance. New York: John Whiley & Sons, 1959: 221-290.

Schuff N, Ezekiel F, Gamst AC, Amend DL, Capizzano AA, Maudsley AA, *et al.* Region and tissue differences of metabolites in normally aged brain using multislice 1H magnetic resonance spectroscopic imaging. Magn Reson Med 2001; 45: 899-907.

Schwab C, McGeer PL. Complement activated C4d immunoreactive oligodendrocytes delineate small cortical plaques in multiple sclerosis. Exp Neurol 2002; 174: 81-88.

Selhorst JB, Saul RF. Uhthoff and his symptom. J Neuroophthalmol 1995; 15: 63-9.

Shah M, Ross JS, VanDyke C, Rudick RA, Goodkin DE, Obuchowski N, *et al.* Volume T1-weighted gradient echo MRI in multiple sclerosis patients. J Comput Assist Tomogr 1992; 16: 731-736.

Sharma R, Narayana PA, Wolinsky JS. Grey matter abnormalities in multiple sclerosis: proton magnetic resonance spectroscopic imaging. Mult Scler 2001; 7: 221-226.

Shaw PJ, Smith NM, Ince PG, Bates D. Chronic periphlebitis retinae in multiple sclerosis. A histopathological study. J Neurol Sci 1987; 77: 147-152.

Siger-Zajdel M, Selmaj K. Magnetisation transfer ratio analysis of normal appearing white matter in patients with familial and sporadic multiple sclerosis. J Neurol Neurosurg Psychiatry 2001; 71: 752-6.

Silver N, Lai M, Symms M, Barker G, McDonald I, Miller D. Serial gadolinium-enhanced and magnetization transfer imaging to investigate the relationship between the duration of blood-brain barrier disruption and extent of demyelination in new multiple sclerosis lesions. J Neurol 1999; 246: 728-730.

Silver NC, Good CD, Barker GJ, MacManus DG, Thompson AJ, Moseley IF, *et al.* Sensitivity of contrast enhanced MRI in multiple sclerosis. Effects of gadolinium dose, magnetization transfer contrast and delayed imaging. Brain 1997; 120: 1149-1161.

Simmons ML, Frondoza CG, Coyle JT. Immunocytochemical localization of N-acetyl-aspartate with monoclonal antibodies. Neuroscience 1991; 45: 37-45.

Simon JH, Jacobs LD, Campion MK, Rudick RA, Cookfair DL, Herndon RM, *et al.* A longitudinal study of brain atrophy in relapsing multiple sclerosis. The Multiple Sclerosis Collaborative Research Group (MSCRG). Neurology 1999; 53: 139-148.

Simon JH, Kinkel RP, Jacobs L, Bub L, Simonian N. A Wallerian degeneration pattern in patients at risk for MS. Neurology 2000; 54: 1155-1160.

Sled JG, Zijdenbos AP, Evans AC. A nonparametric method for automatic correction of intensity nonuniformity in MRI data. IEEE Trans Med Imaging 1998; 17: 87-97.

Smith KJ, Kapoor R, Hall SM, Davies M. Electrically active axons degenerate when exposed to nitric oxide. Ann Neurol 2001; 49: 470-476.

Smith KJ, McDonald WI. The pathophysiology of multiple sclerosis: the mechanisms underlying the production of symptoms and the natural history of the disease. Philos Trans R Soc Lond B Biol Sci 1999; 354: 1649-1673.

Soher BJ, van Zijl PC, Duyn JH, Barker PB. Quantitative proton MR spectroscopic imaging of the human brain. Magn Reson Med 1996; 35: 356-363.

Solanky M, Maeda Y, Ming X, Husar W, Li W, Cook S, *et al.* Proliferating oligodendrocytes are present in both active and chronic inactive multiple sclerosis plaques. J Neurosci Res. 2001; 65: 308-317.

Suhy J, Rooney WD, Goodkin DE, Capizzano AA, Soher BJ, Maudsley AA, *et al.* 1H MRSI comparison of white matter and lesions in primary progressive and relapsing-remitting MS. Mult Scler 2000; 6: 148-155.

Tedeschi G, Bertolino A, Campbell G, Barnett AS, Duyn JH, Jacob PK, *et al.* Reproducibility of proton MR spectroscopic imaging findings. AJNR Am J Neuroradiol 1996; 17: 1871-1879.

Tedeschi G, Lavorgna L, Russo P, Prinster A, Dinacci D, Savettieri G, *et al.* Brain atrophy and lesion load in a large population of patients with multiple sclerosis. Neurology 2005; 65: 280-5.

Thompson AJ, Kermode AG, Wicks D, MacManus DG, Kendall BE, Kingsley DP, *et al.* Major differences in the dynamics of primary and secondary progressive multiple sclerosis. Ann Neurol 1991; 29: 53-62.

Thompson AJ, Montalban X, Barkhof F, Brochet B, Filippi M, Miller DH, *et al.* Diagnostic criteria for primary progressive multiple sclerosis: a position paper. Ann Neurol 2000; 47: 831-835.

Thompson AJ, Polman CH, Miller DH, McDonald WI, Brochet B, Filippi MM, X, *et al.* Primary progressive multiple sclerosis. Brain 1997; 120 (Pt 6): 1085-1096.

Tiberio M, Chard DT, Altmann DR, Davies G, Griffin CM, McLean MA, *et al.* Metabolite changes in early relapsing-remitting multiple sclerosis. A two year follow-up study. J Neurol 2006; 253: 224-30.

Tiberio M, Chard DT, Altmann DR, Davies G, Griffin CM, Rashid W, *et al.* Gray and white matter volume changes in early RRMS: a 2-year longitudinal study. Neurology 2005; 64: 1001-7.

Tortorella C, Codella M, Rocca MA, Gasperini C, Capra R, Bastianello S, *et al.* Disease activity in multiple sclerosis studied by weekly triple-dose magnetic resonance imaging. J Neurol 1999; 246: 689-692.

Tourbah A, Stievenart JL, Gout O, Fontaine B, Liblau R, Lubetzki C, *et al.* Localized proton magnetic resonance spectroscopy in relapsing remitting versus secondary progressive multiple sclerosis. Neurology 1999; 53: 1091-1097.

Tourtellotte WW, Parker JA. Some spaces and barriers in postmortem multiple sclerosis. Prog Brain Res. 1968; 29: 493-525.

Traboulsee A, Dehmeshki J, Brex PA, Dalton CM, Chard D, Barker GJ, *et al.* Normal-appearing brain tissue MTR histograms in clinically isolated syndromes suggestive of MS. Neurology 2002; 59: 126-128.

Trapp BD, Peterson J, Ransohoff RM, Rudick R, Mork S, Bo L. Axonal transection in the lesions of multiple sclerosis. N Engl J Med 1998; 338: 278-285.

Tsunoda I, Kuang LQ, Libbey JE, Fujinami RS. Axonal injury heralds virus-induced demyelination. Am J Pathol 2003; 162: 1259-69.

Tubridy N, Molyneux PD, Moseley IF, Miller DH. The sensitivity of thin-slice fast spin echo, fast FLAIR and gadolinium- enhanced T1-weighted MRI sequences in detecting new lesion activity in multiple sclerosis. J Neurol 1999; 246: 1181-1185.

Urenjak J, Williams SR, Gadian DG, Noble M. Specific expression of N-acetylaspartate in neurons, oligodendrocyte- type-2 astrocyte progenitors, and immature oligodendrocytes in vitro. J Neurochem 1992; 59: 55-61.

Urenjak J, Williams SR, Gadian DG, Noble M. Proton nuclear magnetic resonance spectroscopy unambiguously identifies different neural cell types. J Neurosci 1993; 13: 981-989.

Valsasina P, Benedetti B, Rovaris M, Sormani MP, Comi G, Filippi M. Evidence for progressive gray matter loss in patients with relapsing-remitting MS. Neurology 2005; 65: 1126-8.

van Waesberghe JH, Kamphorst W, De Groot CJ, van Walderveen MA, Castelijns JA, Ravid R, *et al.* Axonal loss in multiple sclerosis lesions: magnetic resonance imaging insights into substrates of disability. Ann Neurol 1999; 46: 747-754.

van Walderveen MA, Barkhof F, Pouwels PJ, van Schijndel RA, Polman CH, Castelijns JA. Neuronal damage in T1-hypointense multiple sclerosis lesions demonstrated in vivo using proton magnetic resonance spectroscopy. Ann Neurol 1999a; 46: 79-87.

van Walderveen MA, Barkhof F, Tas MW, Polman C, Frequin ST, Hommes OR, *et al.* Patterns of brain magnetic resonance abnormalities on T2-weighted spin echo images in clinical subgroups of multiple sclerosis: a large cross- sectional study. Eur Neurol 1998a; 40: 91-98.

van Walderveen MA, Kamphorst W, Scheltens P, van Waesberghe JH, Ravid R, Valk J, *et al.* Histopathologic correlate of hypointense lesions on T1-weighted spin-echo MRI in multiple sclerosis. Neurology 1998b; 50: 1282-1288.

van Walderveen MA, Truyen L, van Oosten BW, Castelijns JA, Nijeholt GJ, van Waesberghe JH, *et al.* Development of hypointense lesions on T1-weighted spin-echo magnetic resonance images in multiple sclerosis: relation to inflammatory activity. Arch Neurol 1999b; 56: 345-351.

Vanguri P, Koski CL, Silverman B, Shin ML. Complement activation by isolated myelin: activation of the classical pathway in the absence of myelin-specific antibodies. Proc Natl Acad Sci USA 1982; 79: 3290-3294.

Vanhamme L, Sundin T, Van Hecke P, Van Huffel S. MR spectroscopy quantification: a review of time-domain methods. NMR Biomed 2001; 14: 233-246.

Vrenken H, Barkhof F, Uitdehaag BM, Castelijns JA, Polman CH, Pouwels PJ. MR spectroscopic evidence for glial increase but not for neuro-axonal damage in MS normal-appearing white matter. Magn Reson Med 2005; 53: 256-66.

Walters RJ, Fox NC, Crum WR, Taube D, Thomas DJ. Haemodialysis and cerebral oedema. Nephron 2001; 87: 143-147.

Webb PG, Sailasuta N, Kohler SJ, Raidy T, Moats RA, Hurd RE. Automated single-voxel proton MRS: technical development and multisite verification. Magn Reson Med 1994; 31: 365-373.

Werner P, Pitt D, Raine CS. Multiple sclerosis: altered glutamate homeostasis in lesions correlates with oligodendrocyte and axonal damage. Ann Neurol. 2001; 50: 169-180.

Werring DJ, Clark CA, Droogan AG, Barker GJ, Miller DH, Thompson AJ. Water diffusion is elevated in widespread regions of normal-appearing white matter in multiple sclerosis and correlates with diffusion in focal lesions. Mult Scler 2001; 7: 83-9.

Whittall KP, MacKay AL, Li DK, Vavasour IM, Jones CK, Paty DW. Normal-appearing white matter in multiple sclerosis has heterogeneous, diffusely prolonged T(2). Magn Reson Med 2002; 47: 403-8.

Whitwell JL, Crum WR, Watt HC, Fox NC. Normalization of cerebral volumes by use of intracranial volume: implications for longitudinal quantitative MR imaging. AJNR Am J Neuroradiol 2001; 22: 1483-1489.

Wiedermann D, Schuff N, Matson GB, Soher BJ, Du AT, Maudsley AA, *et al.* Short echo time multislice proton magnetic resonance spectroscopic imaging in human brain: metabolite distributions and reliability. Magn Reson.Imaging 2001; 19: 1073-1080.

Wylezinska M, Cifelli A, Jezzard P, Palace J, Alecci M, Matthews PM. Thalamic neurodegeneration in relapsing-remitting multiple sclerosis. Neurology 2003; 60: 1949-54.

Wyss M, Kaddurah-Daouk R. Creatine and creatinine metabolism. Physiol Rev 2000; 80: 1107-1213.

Xu J, Kobayashi S, Yamaguchi S, Iijima K, Okada K, Yamashita K. Gender effects on age-related changes in brain structure. AJNR Am J Neuroradiol 2000; 21: 112-118.

Yates AJ, Thelmo W, Pappius HM. Postmorten changes in the chemistry and histology of normal and edematous brains. Am J Pathol 1975; 79: 555-564.

Yin X, Crawford TO, Griffin JW, Tu P, Lee VM, Li C, *et al.* Myelin-associated glycoprotein is a myelin signal that modulates the caliber of myelinated axons. J Neurosci 1998; 18: 1953-1962.

Zaheer A, Mathur SN, Lim R. Overexpression of glia maturation factor in astrocytes leads to immune activation of microglia through secretion of granulocyte-macrophage- colony stimulating factor. Biochem Biophys Res Commun 2002; 294: 238-244.

Zivadinov R, Locatelli L, Stival B, Bratina A, Grop A, Nasuelli D, *et al.* Normalized regional brain atrophy measurements in multiple sclerosis. Neuroradiology 2003.

Zivadinov R, Sepcic J, Nasuelli D, De Masi R, Bragadin LM, Tommasi MA, *et al.* A longitudinal study of brain atrophy and cognitive disturbances in the early phase of relapsing-remitting multiple sclerosis. J Neurol Neurosurg Psychiatry 2001; 70: 773-780.

Zivadinov R, Zorzon M. Is gadolinium enhancement predictive of the development of brain atrophy in multiple sclerosis? A review of the literature. J Neuroimaging 2002; 12: 302-9.

Zorzon M, De Masi R, Nasuelli D, Ukmar M, Mucelli RP, Cazzato G, *et al.* Depression and anxiety in multiple sclerosis. A clinical and MRI study in 95 subjects. J Neurol 2001; 248: 416-421.

7 APPENDIX

FUNCTIONAL SYSTEM AND EXPANDED DISABILITY STATUS SCALE SCORES

Table A1: functional systems

Pyramidal functions	
0	Normal.
1	Abnormal signs without disability.
2	Minimal disability.
3	Mild or moderate paraparesis or hemiparesis; severe monoparesis.
4	Marked paraparesis or hemiparesis; moderate quadriplegia; or monoplegia.
5	Paraplegia, hemiplegia, or marked quadriparesis.
6	Quadriplegia.

Cerebellar functions	
0	Normal.
1	Abnormal signs without disability.
2	Mild ataxia.
3	Moderate truncal or limb ataxia.
4	Severe ataxia, all limbs.
5	Unable to perform coordinated movements due to ataxia.
X	Is used throughout after each number when weakness (grade 3 or more on pyramidal) interferes with testing.

Brain stem functions	
0	Normal.
1	Signs only.
2	Moderate nystagmus or other mild disability.
3	Severe nystagmus, marked extra-ocular weakness, or moderate disability of other cranial nerves.
4	Marked dysarthria, or other marked disability.
5	Inability to swallow or speak.

Sensory functions	
0	Normal.
1	Vibration or figure-writing decrease only, in one or two limbs.
2	Mild decrease in touch or pain or position sense, and/or moderate decrease in vibration in one or two limbs; or vibratory (c/s figure writing) decrease alone in three or four limbs.
3	Moderate decreases in touch or pain or position sense, and/or essentially lost vibration in one or two limbs; or mild decrease in touch or pain and/or moderate decreases in all proprioceptive tests in three or four limbs.
4	Marked decrease in touch or pain or loss of proprioception, alone or combined, in one or two limbs; or moderate decrease in touch or pain and/or severe proprioceptive decrease in more than two limbs.

5	Loss (essentially) of sensation in one or two limbs; or moderate decrease in touch or pain and/or loss of proprioception for most of the body below the head.
6	Sensation essentially lost below the head.

Bowel and bladder functions	
0	Normal.
1	Mild urinary hesitancy, urgency, or retention.
2	Moderate hesitancy, urgency, retention of bowel or bladder, or rare urinary incontinence.
3	Frequent urinary incontinence.
4	In need of almost constant catheterization.
5	Loss of bladder function.
6	Loss of bowel and bladder function.

Visual (or optic) functions	
0	Normal.
1	Scotoma with visual acuity (corrected) better than 20/30.
2	Worse eye with scotoma with maximal visual acuity (corrected) of 20/30 to 20/59.
3	Worse eye with large scotoma, or moderate decreases in fields, but with maximal visual acuity (corrected) of 20/60 to 20/99.

4	Worse eye with marked decrease of fields and maximal visual acuity (corrected) of 20/100 to 20/200; grade 3 plus maximal acuity of better eye of 20/60 or less.
5	Worse eye with maximal visual acuity (corrected) less than 20/200; grade 4 plus maximal acuity of better eye of 20/60 or less.
6	Grade 5 plus maximal visual acuity of better eye of 20/60 or less.
X	Is added to grades 0 to 6 for presence of temporal pallor.

Cerebral (or mental) functions	
0	Normal.
1	Mood alteration only (does not affect EDSS score).
2	Mild decrease in mentation.
3	Moderate decrease in mentation.
4	Marked decrease in mentation (chronic brain syndrome-moderate).
5	Dementia or chronic brain syndrome-severe or incompetent.

Other functions	
0	None.
1	Any other neurologic findings attributed to MS (specify).

Table A2: The expanded disability status scale

Score	Description
0	Normal neurologic exam (all grade 0 on FS; cerebral grade 1 acceptable).
1.0	No disability, minimal signs in one FS (i.e., grade 1 excluding cerebral grade 1).
1.5	No disability, minimal signs in more than one FS (more than one grade 1 excluding cerebral grade 1).
2.0	Minimal disability in one FS (one FS grade 2, others 0 or 1).
2.5	Minimal disability in two FS (two FS grade 2, others 0 or 1).
3.0	Moderate disability in one FS (one FS grade 3, others 0 or 1), or mild disability in three or four FS (three/four FS grade 2, others 0 or 1) though fully ambulatory.
3.5	Fully ambulatory but with moderate disability in one FS (one grade 3) and one or two FS grade 2; or two FS grade 3; or five FS grade 2 (others 0 or 1).
4.0	Fully ambulatory without aid, self-sufficient, up and about some 12 hours a day despite relatively sever disability consisting of one FS grade 4 (others 0 or 1), or combinations of lesser grades exceeding limits of previous steps. Able to walk without aid or rest some 500 metres.

4.5	Fully ambulatory without ad, up and about much of the day, able to work a full day, may otherwise have some limitation of full activity or require minimal assistance; characterized by relatively severe disability; usually consisting of one FS grade 4 (others 0 or 1) or combinations of lesser grades exceeding limits of previous steps. Able to walk without aid or rest for some 300 metres.
5.0	Ambulatory without aid or rest for about 200 metres; disability severe enough to impair full daily activities (e.g., to work a full day without special provisions). (Usual FS equivalents are one grade 5 alone, others 0 or 1; or combinations of lesser grades usually exceeding specifications for step 4.0).
5.5	Ambulatory without aid or rest for about 100 metres; disability severe enough to preclude full daily activities. (Usual FS equivalents are one grade 5 alone, others 0 or 1; or combinations of lesser grades usually exceeding those for step 4.0).
6.0	Intermittent or unilateral constant assistance (cane, crutch, or brace) required to walk about 100 metres with or without resting. (Usual FS equivalents are combinations with more than two FS grade 3+).
6.5	Constant bilateral assistance (canes, crutches, or braces) required to walk about 20 metres without resting. (Usual Fs equivalents are combinations with more than two FS grade 3+).

7.0	Unable to walk beyond about 5 metres even with aid, essentially restricted to wheelchair; wheels self in standard wheelchair and transfers alone; up and about in w/c some 12 hours a day. (Usual FS equivalents are combinations with more than one FS grade 4+; very rarely, pyramidal grade 5 alone).
7.5	Unable to take more than a few steps; restricted to wheelchair; may need aid in transfer; wheels self but cannot carry on in standard wheelchair a full day; may require motorized wheelchair. (Usual FS equivalents are combinations with more than one FS grade 4+).
8.0	Essentially restricted to bed or chair or perambulated in wheelchair, but may be out of bed itself for much of the day; retains many self-care functions; generally has effective use of arms. (Usual FS equivalents are combinations, generally grade 4+ in several systems).
8.5	Essentially restricted to bed much of the day; has some effective use of arm(s); retains some self-care functions. (Usual FS equivalents are combinations, generally 4+ in several systems).
9.0	Helpless bed patient; can communicate and eat. (Usual FS equivalents are combinations, mostly grade 4+).
9.5	Totally helpless bed patient; unable to communicate effectively or eat/swallow. (Usual FS equivalents are combinations, almost all grade 4+).
10	Death due to MS.